Title

Models of Five Climatically Sensitive Taxa in Central and Northwestern Mexico During the Present, the mid-Holocene and the Last Glacial Maximum

Author

Sengupta, Dyuti

Publication Date

2012

Peer reviewed|Thesis/dissertation

Models of Five Climatically Sensitive Taxa in Central and Northwestern Mexico During the Present, the mid-Holocene and the Last Glacial Maximum

By

Dyuti Sengupta

A dissertation submitted in partial satisfaction of the

requirements for the degree of

Doctor of Philosophy

in

Geography

in the

Graduate Division

of the

University of California at Berkeley

Committee in charge:

Professor Roger Byrne, Chair
Professor Richard Dodd
Professor John Chiang

Fall 2012

Abstract

Models of Five Climatically Sensitive Taxa in Central and Northwestern Mexico During the Present, the mid-Holocene and the Last Glacial Maximum

By
Dyuti Sengupta
Doctor of Philosophy in Geography
University of California, Berkeley
Professor Roger A. Byrne, Chair

This dissertation focuses on the spatial distribution of five climatically sensitive plant taxa in central and northwestern Mexico during three time periods: the present, the mid-Holocene and the Last Glacial Maximum (LGM). The results presented here are rooted in recent methods of bioclimatic envelope modeling that incorporate high-resolution paleoclimate model data, GIS, online herbaria data, and cartography. Although the paleoclimate model data and computer methods used in this work are crucial to its outcome, the validation of the model results for the mid-Holocene and LGM rests largely on paleoecological evidence from Mexican fossil pollen sites. In this dissertation, I have devoted much of the discussion to how well the modeled results agree with the paleoecological records and interpretations.

The majority of fossil pollen sites spanning both the mid-Holocene and Last Glacial Maximum occurs in the northwest and central regions of Mexico. The concentration of these sites led to the narrowing of what spatial distribution to consider in the modeling efforts. In both central and northwestern Mexico, there are plant taxa that appear today whose presence has varied over time as environmental conditions fluctuated. The five plant taxa modeled here are *Abies, Artemisia, Liquidambar, Picea,* and *Taxodium*, all significant taxa in the pollen record as indicators of temperature and moisture change. In the cases of *Abies, Picea* and *Artemisia*, multiple species occur throughout Mexico, which complicates the construction of a climate envelope. In these instances, only one species was modeled in an effort to minimize conflation in the results, which may have happened if multiple species were considered.

The first segment of the work focused on constructing and validating one model for each taxon in the present. The most realistic models from the effort were those for *Abies religiosa, Picea chihuahuana* and *Liquidambar styraciflua*, each having very narrow climatic requirements, and occurring in definable biogeographic regions of Mexico. The success also speaks to the appropriateness of species choice, the accuracy of the climate model data as well as the performance of the bioclimatic envelope model.

The two models that performed less desirably were those of *Taxodium mucronatum* and *Artemisia ludoviciana*. The broad distribution of *Artemisia* presented challenges in pinpointing an appropriate set of climate parameters for the envelope construction. *T. mucronatum* is dependent upon flooded riparian pathways for reproduction, an aspect of the environment that was not included in the model construction. Since only bioclimatic parameters were included, the resulting model

reflects a clear lack of agreement between the predicted and actual distribution. These results illustrate the importance of selecting an appropriate species for envelope modeling methods.

The second segment of the work was that of projecting the present-day models into the past. Predictably, the three accurate present-day models also performed well when projected into past climate data while the other two models did not agree well with paleoproxy data. However, *Picea's* mid-Holocene model did generate surprising results by appearing in the central Mexican region. Pollen evidence of *Picea* in central Mexico during the mid-Holocene is extremely rare and unlikely. Also, some disagreement did appear between the fossil record and the modeled distribution for *Liquidambar*. According to the fossil record, *Liquidambar* did appear in the Mexican Basin during the mid-Holocene, but the model does not reflect that finding. The reasons for the disagreement may lie in the variable selection for the envelope, the climate model data, or more likely, the inability of this broad scale technique to model local conditions that may have influenced *Liquidambar's* distribution.

Finally, the last portion of the work was an experiment comparing species distribution models produced using different climate models modified using EOF analysis. The goal was to determine how, if at all, the ecological models differed from one another. The results indicate some effect, though not particularly significant ones at the broad scale of this work.

In summary, the main finding of the research is that modern bioclimatic modeling techniques with high-resolution climate data are useful in generating paleoecological distributions, but with the following constraints, 1) an appropriate taxon with an easily-defined climatic envelope is modeled, 2) researchers complete a thorough comparison between the model results and palynological records to confirm or refute a models' validity.

TABLE OF CONTENTS

LIST OF TABLES

LIST OF FIGURES

CHAPTER 1

CHAPTER 2

Acknowledgements

I'd like to thank Professors Byrne, Chiang and Dodd for being on my committee. I am grateful for all the knowledge imparted and patience shown as I attempted to complete this very difficult task. Also special thanks also to Professor Cuffey and Marjorie Ensor for being so understanding. My paleoecology lab friends: Liam, Alicia, Tripti. And also to my family, without whom I never would have thought to attempt a PhD. Finally, my daughter, who is the most understanding small child on earth.

1. CHAPTER ONE

Future changes in the global climate are expected to affect plant and animal distributions considerably, yet exactly how these effects will play out remains to be seen. Over the past 30 years, researchers have modeled and predicted future climate changes based on changing conditions in the atmosphere and oceans (CLIMAP Project Members, 1981; Braconnot *et al,* 2007). These models, which depict future climate changes, are combined with ecological models in an effort to predict overall changes in biogeographic distributions of plant or animal species. These modeled distributions are in many ways interesting but at the present time, inherently untestable. In contrast, reconstructions of past species distributions using climate envelope modeling and paleoclimate data are testable insofar as they can be compared with the fossil evidence of the distribution of the taxa in question. This is the approach taken in this dissertation. Reconstructions of past species distributions will be compared with fossil pollen evidence and packrat middens of several Mexican plant taxa and species. Interpretations of diatom studies will also be included when possible. While the idea of using paleoecological proxies as a test for climate models and climate change is not new (Overpeck *et al.*, 1990), such comparisons are to date, relatively rare in the literature.

The emphasis of this dissertation is on the distribution of individual plant taxa, such as a species and genera. This approach differs from more traditional research in biogeography, where the emphasis is more often on constructs such as plant communities, formations or biomes. It seems appropriate therefore in this introductory chapter to briefly review the history of these two different approaches, and to indicate why the individual approach is preferable.

APPROACHES TO THE STUDY OF VEGETATION AND VEGETATION CHANGE

Alexander von Humboldt, the "father of biogeography", introduced the early idea that climate was a primary control on vegetation distribution (Humboldt, 1805) after extensive travel and observation in Latin America. Humboldt's observations contributed to the early idea of an "ecological community." Throughout the 1800's, several other biologists contributed to a more formal concept describing multiple organisms living together in a specific habitat, or *oecologie*, which was essentially the ecological community concept (Schimper, 1898; Haeckel, 1866; Grisebach, 1872).

Following the early observations of vegetation distribution, Braun-Blanquet (1932) outlined another idea whereby several characteristics of plant behavior, especially the nature of associations among species constituted a "community." The work of Braun-Blanquet focused heavily upon the construction of a system to define plant communities. The community approach gained traction in Europe, where it originated. However, in North America, ideas of classification took on a new form.

In the western United States, Clinton Hart Merriam conducted extensive field studies that led to his proposal that climatic gradients, especially temperature, dictated the plant coverage for a given location. Merriam referred to the distinct vegetation patterns as "life zones" (Merriam 1898).

Frederic Clements (1916), an American plant ecologist, suggested a process rather than a classification system. He suggested that vegetation progressed through distinct stages, reaching a final "climax community." Clements focused his work on the degree to which observations in nature deviated from each predefined stage.

Clements' theoretical structure was rather rigid, and relied heavily upon plant and tree "associations" (e.g. an oak-pine association). This rigidity ultimately led to some controversy, slowly building as he published his ideas. Arthur Tansley (1935) had reservations about many terms and definitions that Clements used, while Henry Gleason asserted the importance of a species individual response rather than a collective "community" response to changes in the environment (Gleason, 1926). Initially Gleason had few supporters, and Clements' community approach was the widely held view of ecological processes. However, several years later, another study of the geographic variation of the Wisconsin prairie-forest confirmed Gleason's ideas (Curtis & Macintosh, 1951).

The community, or *synecological*, approach has gained a strong following, as it has a long and well-documented history in the ecological sciences. As already stated, this approach is also typically more common amongst biogeographers. However, under scrutiny, as was the case in Gleason's work, an individual species response is actually a more plausible explanation of how plants respond to changes in the environment, and the climate in particular.

Keeping in line with the ecological norms, Holdridge (1947) reiterated the concept of a biome, which had been initially introduced by Shelford (1945). Holdridge referred to his classification scheme as "life zones". Life zones take more into account the environmental conditions that define regions of temperature and precipitation from which predictable soil and "climax" vegetation emerge. As was the case with Shelford's biomes, life zones include animals and vegetation. While Holdridge defined 38 life zones across the land regions of earth, the system falls short because it cannot account for individual species response or plant succession. It should be pointed out that this shortcoming is a problem with any approach that classifies multiple species into a single group.

More recently, Woodward (1997), following Holdridge's approach, insisted that for the construction of a plant distribution model, dynamic biological interactions and vegetation structure are more important than climatic factors.

Defining communities of vegetation is arbitrary because responses to climate change vary by species and intrinsically alter the composition of any perceived community, as well as "associations" among species. Zimmerman and Kienast (1999) describe the community approach as "a practical reasoning" and "having no formal logic". Paleoecologists also criticize the community approach because pollen evidence indicates that plant species respond individualistically to climate change (Davis 1989; Graham and Grimm 1990; Webb 1986).

Thus far, it was pointed out that Gleason's approaches to ecology and species distribution was instrumental in exposing flaws in the community approach. The competing approach, the autecological approach, rests on the idea that biotic interactions and community dynamics among species are not integral to describing the response of species to broad scale climate changes.

The autecological approach is supported by several independent research findings (Davis *et al.,* 1990, Williams, *et al.,* 2007, Byrne 1982). Each study reports or provides

examples of species assemblages that simply do not exist today. These types of assemblages are referred to as "non-analog."

In terms of seminal works in computerized species distribution modeling, E.O. Box (1981) tested the synecological approach through early computer modeling methods, intending to demonstrate that plant functional types (PFT's) could be predicted using climate data. Plant functional types are essentially a group of plants that respond to similar environmental variables, analogous to plant communities. In testing the two approaches, Box found that the autecological approach was more accurate in reflecting present plant distributions (Box 1981). Box's environmental envelope approach demonstrated that individual species were modeled more accurately than vegetation structure involving complex interactions.

Huntley (1991) offered further support for the autecological approach, stating that the idea of a vegetation community is simply a temporary assemblage of species that change and re-assemble due to individual species responses, an idea that is supported by pollen and midden evidence. However, despite the fact that it is not supported by paleoecological evidence, the synecological approach does have legitimate applications, especially in applications that require broad scale estimates of forest respiration (e.g. carbon cycling).

Palynologists led much of the early work in the area of individual species modeling. Webb *et al.* (1981) demonstrated the use of individual species pollen data to estimate plant abundance using regression techniques. Later, Bartlein *et al.* (1986) extended the idea to the construction of pollen "surfaces" to determine taxa distributions of eastern North American trees. The same approach was implemented for sites throughout North America and Europe (Huntley *et al.,* 1989). The use of ecological response surfaces relies on the selection of climatically sensitive taxa commonly found in pollen studies. Bartlein *et al.* chose several important eastern North American tree genera for his initial study. These included *Fagus, Pinus, Carya, Quercus, Tsuga, Betula,* and *Picea* - all common in classic pollen studies from the region. Huntley*, et al.* (1989) modeled beech *(Fagus)* in both eastern North America and Europe, going on to use the surfaces to explain that the species is in climatic equilibrium in both places, even with different migration histories.

BIOCLIMATIC MODELS

Although modern species distribution models are generated using computer programs and specialized software, the principles of ecology on which they are based date back into the early 20th century to the idea of an *ecological niche.* Grinnell described he *niche* concept as spaces with specific environmental characteristics that enable a species to persist and reproduce (Grinnell, 1917). Charles Elton (1927) also proposed the *niche* concept, but focused on the interactions of a species with other species, more in line with the synecological approach. Other important researchers who further developed the idea of an *ecological niche* included Hutchinson (1957) and MacArthur (1972), both focusing on biotic and abiotic factors in defining a *niche*.

The concept of the *ecological niche* (also sometimes referred to as the *environmental envelope*) is put into practice in one of two ways. One approach is to consider the inherent properties of a species such as life-history and genetic traits to define the *niche* space. Because this approach depends so much on species type, it is less

prevalent, and also more difficult to apply. The alternative approach involves the use of environmental data, usually based on general circulation models (GCM) of the climate, to correlate species locations with environmental variables. This method, the *correlative* approach, is more commonly implemented.

Pearson & Dawson (2003) demonstrate the usefulness of modern bioclimate envelopes by forecasting the distribution of a sedge species (*Carex bigelowii)* under a future climate scenario, yet in the same discussion they illustrate the difficulties of modeling a tree species *(Taxus baccata)* successfully. The inability to model *T. baccata* rests on the fact that not all species reflect distribution due to climate, but to other less obvious variables, such as environmental disturbance or hydrology. Several authors have presented distribution models emphasizing the present climate (e.g. Pearson & Dawson, 2003; Anderson Gomez-Laverde & Peterson, 2002) and others have developed climate change scenarios that have been published (Gomez-Mendoza & Arriaga 2003; Ledig, Rehfeldt, 2010), however a gap remains in the application of climate envelope modeling in the realm of paleoclimates using the most recent GCM data.

Before continuing onto the various applications of envelope modeling in the paleoecological realm, it is important to present basic assumptions made when modeling a paleoecological plant distribution. Briefly, they are: 1) that the species being modeled have fairly well understood environmental predictor variables, 2) the temporal stability of the climatic niche for a single species, and 3) species-climate equilibrium exists. Each of these assumptions is addressed in more detail in the following chapter.

Recent modeling approaches to paleoecological hindcasting have incorporated both machine learning algorithms with newly available high-resolution climate data for the Last Glacial Maximum (21,000 BP) and mid-Holocene (6,000 BP) time periods (Lyons, 2003; Carnaval & Moritz, 2008; Walker, Stockman, Marek & Bond*,* 2009; Roberts & Harmann, 2012). With the exception of Walker et al, these hindcasts explain their results using the community approach. Walker et al combine phylogenetic and phylogeographic approaches with a niche-based ecological model for *Narceus sp.,* a millipede. Lyons (2003) considers range shifts of mammals during the Pleistocene in an effort to quantify the extent of range shifts in terms of communities.

Carnaval & Moritz (2008) speak to the problem exclusively in terms of communities (i.e. forest types), and Roberts & Harmann (2012) take advantage of multiple data sets of individual species, ultimately describing the resulting distribution models in terms of a "class variable" representing a region with a "known species composition". Although Roberts & Harmann do enumerate several points in support of the ecosystems approach (and also emphasize the paleorecord as a valid test data set), independent work (Balselga & Araújo 2009) has shown through comparison of methods that the ecosystem approach to modeling is generally inferior to the species approach.

Finally, in addition to fossil evidence, advances in phylogenetic methods have also enhanced the testing of paleoecological models (Walker *et al*. 2009). While paleoecological modeling provides a powerful set of tools, proxy evidence and phylogenetic methods offer a means of independently testing model output.

CENTRAL AND NORTHWESTERN MEXICO

Thus far, I have presented a brief history of ecological ideas, the concept of a bioclimatic envelope, and a short literature review of different plant distribution models.

In an effort to demonstrate the usefulness of the bioclimatic envelope method in paleoecology, I have selected two study regions that present interesting challenges from a climate science standpoint. Both central and northwestern Mexico have had complicated paleoclimatic histories since at least the Last Glacial Maximum (LGM). The majority of the fossil pollen and packrat midden records are limited to central and northwestern Mexico, which helps to focus this study.

Central Mexico's climate response remains a question for a few reasons, including the obscuring of the proxy records due to volcanism and anthropogenic disturbance since the mid-Holocene (6K BP). Northwestern Mexico's climate response is slightly clearer, owing largely to laminated deep-sea ocean core records. The effort here is to use the latest high-resolution climate model simulations to model individual species distribution, then compare the results to the existing paleoproxy records of the same taxa.

In this dissertation, I have worked out distribution models for five species at three different time periods using bioclimatic envelopes. The time periods are the present, the mid-Holocene and the LGM. Each taxon has been chosen based on its prevalence in central or northwestern Mexican fossil pollen records and sensitivity to climate (*Picea chihuahuana, Abies religiosa, Taxodium mucronatum, Liquidambar styraciflua, Artemisia ludoviciana)*. The bioclimatic models are based in the autecological approach, and take advantage of recent high-resolution climate model output, as well as recently digitized herbaria collections, both of which are integral to the construction of an environmental envelope for each species.

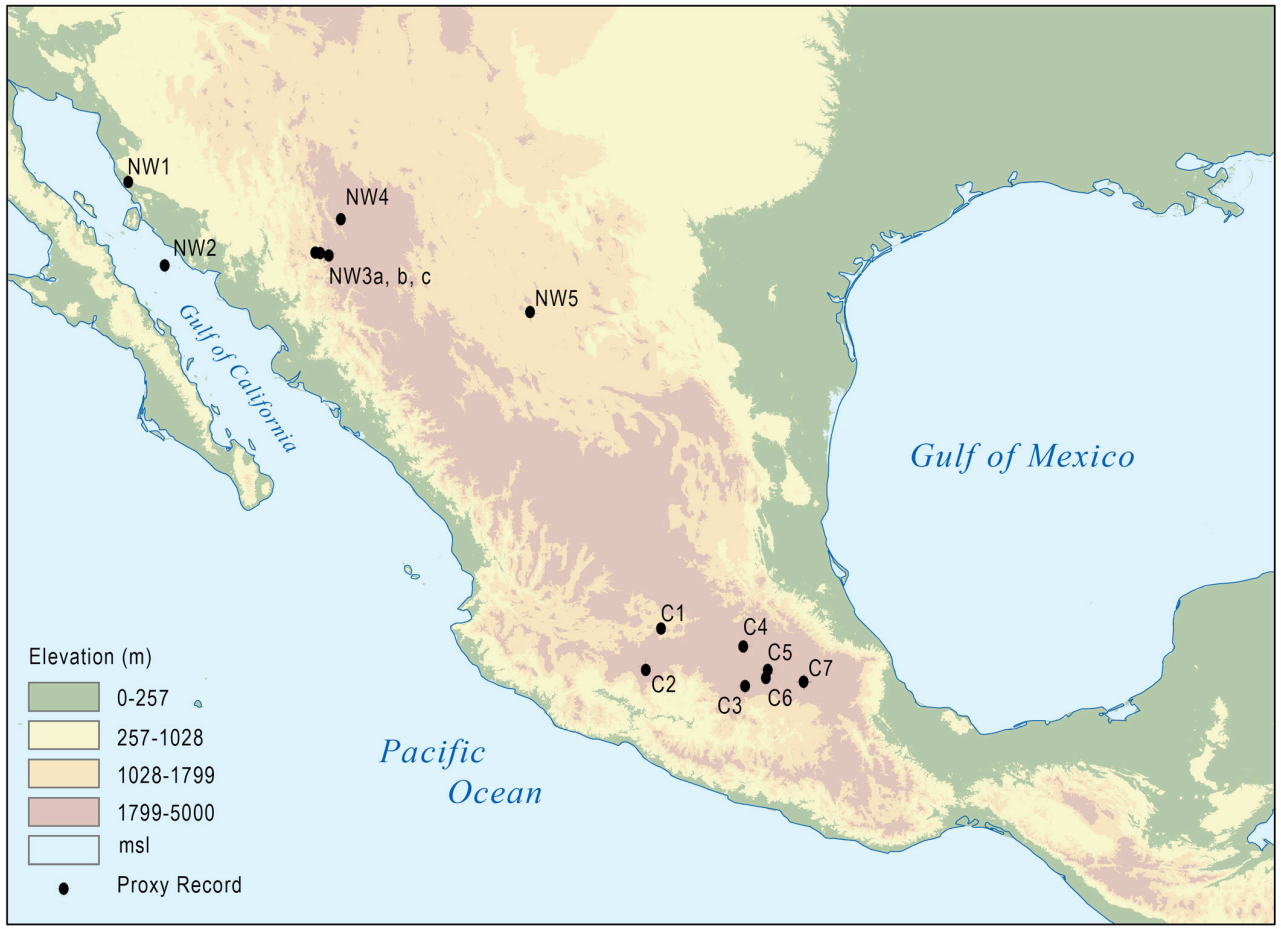

Figure 1.1: Mexican proxy sites discussed in Chapter 1.

REFERENCES

Anderson, R.P., Gomez-Laverde, M. & Peterson, A.T. (2002) Geographical distributions of spiny pocket mice in South America: insights from predictive models. *Global Ecology and Biogeography*, **11,** 131–141.

Bartlein, P.J., I. Prentice, C. & Webb, T. III (1986) Climatic response surfaces from pollen data for some eastern North American taxa. *Journal of Biogeography*, **13**. 35-57.

Bartlein, P. J., K. H. Anderson, P. M. Anderson, M. E. Edwards, C. J. Mock, R. S. Thompson, R. S. Webb, T. Webb III, C. Whitlock (1998) Paleoclimate simulations for North America over the past 21,000 years: features of the simulated climate and comparisons with paleoenvironmental data. *Quaternary Science Reviews*, **17**, 549-585.

Baselga, A., Araújo, M.B. (2009) Individualistic vs community modeling of species distributions under climate change. *Ecography*, **32**, 55-65.

Box, E.O. (1981) Predicting physiognomic vegetation types with climate variables. *Plant Ecology,* **45**, 127-139.

Braconnot, P., Otto-Bliesner, B., Harrison, S., Joussaume, S., Peterchmitt, J.-Y., Abe-Ouchi, A., Crucifix, M., Driesschaert, E., Fichefet, Th., Hewitt, C. D., Kageyama, M., Kitoh, A., Laîné, A., Loutre, M.-F., Marti, O., Merkel, U., Ramstein, G., Valdes, P., Weber, S. L., Yu, Y., and Zhao, Y., 2007. Results of PMIP2 coupled simulations of the Mid-Holocene and Last Glacial Maximum – Part 1: experiments and large-scale features. *Climate of the Past,* **3**, 261-277.

Byrne, R. (1982) Preliminary pollen analysis of Deep Sea Drilling Project Leg 64, Hole 480, cores 1-11. In: R. Curray and D.G. Moore, Editors, *Initial Reports of the Deep Sea Drilling Project*. **64** U.S. Govt. Printing Office, Washington. 1225–1237 Pt. 2.

Carnaval, A. C. & C. Moritz (2008). Historical climate modeling predicts patterns of current biodiversity in the Brazilian Atlantic forest. *Journal of Biogeography,* **35**, 1187-1201.

Clements, F.E. (1916) *Plant succession: an analysis of the development of vegetation*, The Carnegie Institute of Washington

CLIMAP Project Members (1981) Seasonal reconstruction of the earth's surface at the last glacial maximum. *Geological Society of America, Map and Chart Series*, **36**.

Curtis, J.T., & McIntosh, R.P. (1951) An upland forest continuum in the prairie-forest border region of Wisconsin. *Ecology,* **32**, 476-496.

Davis, M.B. (1989) Lags in vegetation response to greenhouse warming. *Climatic Change,* **15**, 75-82.

Davis, M.B., Shaw, R.G. (2001) Range Shifts and Adaptive Responses to Quarternary Climate Change. *Science*, **292,** 673-679.

Davis, A.J., Jenkinson, L.S., Lawton, J.L., Shorrocks, B. & Wood, S. (1998) Making mistakes when predicting shifts in species range in response to global warming. *Nature,* **391**, 783–786.

Elton C. (1927) *Animal Ecology* (Sedgwick and Jackson, London).

Ferrier, S. & Guisan, A. (2006) Spatial modeling of biodiversity at the community level. *Journal of Applied Ecology*, **43,** 393–404.

Gleason, H. (1926) The individualistic concept of plant association, *Bulletin of Torrey Botanical Club,* **53**, 7-26.

Gomez-Mendoza, L., Arriaga, L. (2007). Modeling the effect of climate change on the Distribution of Oak and Pine Species in Mexico. *Conservation Biology*, **21**, 1545-1555.

Graham, R.W., Grimm, E.C. (1990) Effects of global climate change on the patterns of terrestrial biological communities. TREE, **5**, 289-292.

Grinnell, J. (1917) The niche-relationships of the California Thrasher. *The Auk,* **34**, 427–434.

Grisebach, A. (1872) *Der Vegetation der Erde*. Leipzig, Germany.

Haeckel E. (1866*). Generelle Morphologie der Organismen*. Georg Reimer, Berlin, 1, 237.

Holdridge, L. R. (1947) Determination of world plant formations from simple climatic data, *Science.* **105**: 267-268.

Humboldt A von (1805) *Essai sur la géographie des plantes, accompagné d'un tableau physique des régions équinoxiales.* Paris: Schoell.

Huntley, B. (1991) How plants respond to climate change: migration rates, individualism and the consequences for plant communities *Annals of Botany,* **67** 15-22.

Huntley, B., Bartlein, P.J. & Prentice, I.C. (1989) Climatic Control of the Distribution and Abundance of Beech (Fagus L.) in Europe and North America. *Journal of Biogeography,* **16**, 551-560.

Hutchinson G.E. (1957) Concluding remarks. *Cold Spring Harbor Symposium of Quantitative Biology,* **22**, 415–427.

Ledig, T.L, Rehfeldt, G.E., Sáenz-Romero, C. & Flores-López, C. (2010) Projections of suitable habitat for rare species under global warming scenarios. *Americal Journal of Botany* **97**, 970–987.

Lyons, S.K. (2003) A quantitative assessment of the range shifts of Pleistocene mammals. *Journal of Mammalogy*, **84,** 385-40

MacArthur R.H. (1972) *Geographical Ecology* Harper & Row, New York.

Mather, J.R. and Yoshioka, G. (1968) The Role of Climate in Vegetation Distribution. *Annals of the Association of American Geographers*, 1467-8306, **58**, 29 – 41.

Merriam, C.H. (1898) Life zones and crop zones of the United States, *US Department of Agriculture Division Biological Survey Bulletin*, **10,** 1-79.

Pearson, R.G. & Dawson, T.P. (2003). Predicting the impacts of climate change on the distribution of species: are bioclimate envelope models useful? *Global Ecology and Biogeography*, **12**, 361-371.

Overpeck, J. Rind, D. & Goldberg, R. (1990). Climate induced change in forest disturbance and vegetation, *Nature,* **343,** 51-53.

Poore, M.E.D. 1955. The use of phytosociological methods and ecological investigations: I. The Braun-Blanquet System. *Journal of Ecology,* **43,** 226-244.

Roberts, D. R. & Hamann, A. (2012) Predicting potential climate change impacts with bioclimate envelope models: a palaeoecological perspective. *Global Ecology and Biogeography*, **21,** 121–133.

Schimper, A. F. W. (1898) *Pflanzengeographie auf physiologischer Grundlage*. Gustav-Fischer-Verlag, Jena.

Shelford, V.E. (1945). The relative merits of the life zone and biome concepts. *Wilson Bulletin*, **57**, 248-252.

Tansley, A.G. (1935) The Use and Abuse of Vegetational Concepts and Terms *Ecology,* **16,** 284-307.

Walker, M. J., Stockman, A. K., Marek, P. E. & Bond, J. E. (2009) Pleistocene glacial refugia across the Appalachian Mountains and coastal plain in the millipede genus *Narceus*: Evidence from population genetic, phylogeographic, and paleoclimatic data. *BMC Evolutionary Biology,* **9**.

Webb T. III, Howe, S.E., Bradshaw, R.E. & Heide, K.M. (1981) Estimating plant abundances from pollen percentages: the use of regression analysis. *Review of Paleobotany and Palynology,* **34**, 269-300.

Zimmerman, N & Keinast, F.(1999) Predictive mapping of alpine grasslands in Switzerland; Species versus community approach. *Journal of Vegetation Science,* **10**, 469-482.

Williams J.W., Jackson S.T. ,Kutzbach J.E. (2007) Projected distributions of novel and disappearing climates by 2100 AD. *Proceedings of the National Academy of Sciences,* **104,** 5738-5472.

Woodward, F.I. & Beerling, D.J. (1997) The dynamics of vegetation change: health warnings for equilibrium 'dodo' models. *Global Ecology and Biogeography Letters*, **6**, 413-418.

2. CHAPTER TWO

Present-day distribution of five climatically sensitive plant species in central and northwestern Mexico

INTRODUCTION

In this chapter use MaxEnt to model the current distributions of five paleoclimatically important species encountered in Mexican palynological studies, and thereby set. By doing this, I set the stage for their modeling distributions during the mid-Holocene and the Last Glacial Maximum (LGM). The taxa were chosen for three reasons: 1) they show significant changes in the fossil pollen record: 2) they have modern distributions that can be reasonably explained by present-day climate: 3) present-day distributional data are available.

In spite of a significant research effort during the past 50 years, the history of late Quaternary climate change in Mexico is still not well understood. In particular, the relationship between climate change and its effects on plant species distribution is poorly known. The fossil pollen record, though it suffers from several limitations (Watts & Bradbury 1982; Lozano-Garcia *et al,* 1993; González-Quintero, 1986), is still the main source of information regarding the effects of climate change on plant species distribution during the late Pleistocene and Holocene.

Next I discuss the present climate of Mexico, and then introduce plant species I used for the distribution models.

Atmospheric Circulation and Precipitation Patterns in Mexico

Mexico is situated between the tropics and subtropics, falling approximately within 15˚ N and 32˚ N. The landscape can simply be divided into the lowlands and the highlands. Separating the two are mountain ranges -- to the east, the Sierra Madre Oriental, and in the west, the Sierra Madre Occidental. Around 20˚ N, the Trans-Mexican Volcanic Belt (TMVB) bounds the altiplano. One more major range, the Sierra Madre del Sur, connects to the TMVB in northern Oaxaca. Major influences on Mexican precipitation include the Gulf of Mexico, which influences the TMVB, and the Mexican Monsoon in the northwest.

During the boreal summer, between approximately May and September, the Bermuda-Azores high-pressu latitude. The low-pressure regions make way for ascending air, eventually leading to storm activity. The resulting tropical storms are the primary source of precipitation during the summer months, particularly along the eastern Mexican coast (Cavazos & Hastenrath, 1990).

In winter, as the ITCZ moves south, and Mexico comes under the influence of the westerlies and the subtropical high-pressure belt again, generally dry conditions prevail. However occasional incursions of mid-latitude cold air, or *Nortes*, bring cool air to the Mexican coastal regions and highlands. Whether or not the *Nortes* bring precipitation along with cool temperatures depends on the origin of the cold air mass and the positioning of the mass above the Gulf of Mexico. Schultz *et al* (1998) imply that cold air masses originating in the north Pacific are less likely to bring precipitation than air

masses coming from east of the Canadian Rockies. In northwestern Mexico, the influence of the mid-latitude westerlies and associated cold masses produces occasional precipitation.

In northwestern Mexico, precipitation associated with the Mexican monsoon begins as the prevailing winds shift from westerlies to easterlies and begin the cool the rapidly warming land mass. High-level moisture from the Gulf of Mexico and low-level moisture from the eastern Pacific and the Gulf of Mexico both contribute to heavy summer precipitation. This is especially prevalent in the Sierra Madre Occidental foothills (Douglas *et al* 1993). Mosiño & García (1974) emphasize the importance of orographic effects in Mexico, stating that topography has a profound influence on both surface weather and upper air patterns, which in turn affect the synoptic weather patterns throughout Mexico.

SPECIES INCLUDED IN THE ANALYSIS

Initially, I selected five taxa that are considered important climate indicators in the Mexican fossil pollen record: *Abies, Picea, Artemisia, Liquidambar, Taxodium*. However, it became apparent during the research process that working at the species level lent itself better to the modeling process (discussed later). In the following sections, I outline the important climatic and bioclimatic features of the species that are relevant to the construction of envelope models.

SPECIES

Fir (*Abies religiosa)*

Abies is distributed widely in the temperate regions of the northern hemisphere. Although the genus is thought to be characteristic of boreal environments, several species of *Abies* are found at high elevations throughout both northwestern and central Mexico. *Abies'* discontinuous distribution throughout Mexico is suggestive of relict populations. However, the exact evolutionary history, including rates of speciation (assessed using diversification rates) and biogeography are not clearly understood (Aguirre-Planter *et al.,* 2000). Xiang *et al.* (2009) point out the possibility that *Abies* radiated quickly in Mesoamerica upon arrival there.

Phylogenetic studies point to two possible initial southward migrations of *Abies* into Mexico. One scenario places the initial migration at approximately 23 Mya, while the other possibility suggests 5 Mya (Aguirre-Planter *et al.,* 2011). Pollen evidence supports both these possibilities, but in the case of an earlier migration, the pollen can only be interpreted that of a temperate conifer, while the other is definitively *Abies* pollen (Graham, 1999).

According to Farjon (1990) there are seven species of *Abies* in Mexico. Phylogenetic relationships among the species have been examined at the molecular level in an effort to better understand *Abies'* geographic distribution (Aguirre-Planter *et al.,* 2000; Jaramillo-Correa *et al.,* 2008, Xiang *et al.,* 2009; Aguirre-Planter *et al,* 2011). The results of these studies suggest that geographical differentiation exists among *Abies*. Generally, *A. flinckii* occurs in northern Mexico while *A. guatemalensis, A. religiosa,* and *A. hickeli* are more likely to occur in southern and central Mexico. Another species, *A. durangensis,* inhabits the Sierra Madre Occidental in the northwestern part of Mexico.

Xiang *et al.* (2009) place *A. flinckii and A. guatemalensis* in one section, while *A. religiosa and A. hickeli* are in a sister section. Aguirre-Planter *et al.* (2011) point out two important divergences for *Abies, A. flinckii* and *A. concolor.* Of these, *A. flinckii* is thought to have diverged in the first migratory wave, while *A. concolor* may have diverged from *A. concolor* much later, during the LGM, and hybridized with *A. durangensis.*

Modern *Abies* in Mexico experience climate conditions quite different from *Abies* found in North America. Specific climatic factors that differ between the two include more intense insolation, less annual variation in day-length, higher annual average temperatures, greater diurnal variation in temperature extremes, and longer gaps between rainfall. According to Rzedowski, these differences have caused the phenological characteristics of *Abies* in Mexico to be different from other areas in North America (Rzedowski, 1975).

Spruce (*Picea chihuahuana.)*

While most species of *Picea* occur in northern latitudes (e.g. boreal, temperate climates), three distinct spruce species (*Picea mexicana, P. chihuahuana,* and *P. martinezii)* are found in both the Sierra Madre Occidental and Oriental (Ledig *et al.,* 2004). According to Ledig, *P. martinezii* and *P. mexicana* both diverged from *P. chihuahuana* much before the LGM, according to Ledig *et al.* (2004). *Picea mexicana* has been a species since approximately the mid-Pleistocene (ca 725,000 BP) and *P. martinenzii* slightly longer (ca 1-2 Myr BP). All the populations of *Picea* appear to be refugial populations, located in steep, shaded canyons called *barrancas*. According to Gordon (1968), all year-round moisture availability and cool summer temperatures are also crucial to *Picea's* survival. In general, *Picea's* presence in Mexico is highly specialized in terms of environmental conditions and so it lends itself well to the bioclimatic modeling method.

Genetic evidence (Jaramillo-Correa *et al.*, 2006) suggests range shifts for *P. chihuahuana*, *P. mexicana* and *P. martinenzii* in the Sierra Oriental, all occurring in the early to mid Holocene. The phylogenetic study is important in that it illustrates that the changes in species distribution have not been linked to a single climatic event, but are the result of cyclical glacial events.

Sage *(Artemisia ludoviciana)*

According to herbaria records, there are at least 11 species of *Artemisia* present in Mexico today (http://www.gbif.org). The most widespread of these is *A. ludoviciana*, which has at least four subspecies.

Artemisia, or sagebrush (sage), has a range limited in part by summer moisture stress – the genus generally occurs in cool desert steppe settings. *Artemisia* species are unable to survive in very moist environments, and palynologists consider *Artemisia* a sign of dry and cool environments although exceptions exist (Subally & Quezel, 2002). In cross-referencing the herbaria database (GBIF), with Leopold's map of Mexican

vegetation (Leopold, 1950), I found that *Artemisia* is present in the high central chaparral regions in the Mexican Bajio, as well as small areas of thorn and savannah in the Gulf lowlands. In the Valley of Mexico, *A. ludovicana ssp mexicana* is predominant, while in the northwestern regions, *A. ludoviciana ssp sulcata* is common. Garcia *et al.* (2011) recently considered the phylogentic history of North American species of *Artemisia*, finding that *A. ludoviciana's* subspecies*, A. mexicana* Willd and *A. michauxiana* Besser are related to the Siberian species of *Artemisia*. The authors also state that relationships among the many species of *Artemisia* are difficult to discern, even at the genetic scale.

Sweetgum (*Liquidambar styraciflua)*

In Mexico, sweetgum (*Liquidambar)* exists as a single species, *L. styraciflua*. The Mexican populations of *L. styraciflua* occur exclusively in the cloud forests of the Sierra Madre Oriental between 600 and 3000 m. Mexican cloud forests are influenced by fog throughout the year in addition to summer and winter precipitation. These conditions create a unique ecological setting where many temperate hardwoods mix with evergreen conifers and some tropical-. The mild temperatures provide hospitable conditions for cool climate taxa, yet the abundance of moisture and infrequency of frost allows for a presence of tropical taxa. The cloud forests of present-day Mexico are distributed in fragmented patterns, resembling an archipelago (Luna-Vega, *et al.,* 1999).

Specific temperature and precipitation ranges are available for *L. styraciflua* in Mexico and the United States(Macmillan, 1974). Minimum annual temperatures for *L. styraciflua* range from -21˚ C from its northern limit (37˚ N) and -4˚ C to the south (20˚ N). There are approximately 320 frost-free days in Mexico, in contrast to the higher latitude populations where *L. styraciflua* grows, which average 180 days without frost. *L. styraciflua's* upper temperature limit is around 38˚ C (100˚ F). The annual precipitation throughout the range is 1020 mm to 1520 mm with a growing season rainfall between 510 and 610 mm. Mexican populations of *L. styraciflua* bud in late February, slightly earlier than more northern populations (with the exception of Texan populations). Ecological studies suggest that in Mexico, *L. styraciflua* is less sensitive to daily photoperiod and temperature than in more northern latitudes (MacMillan, 1974).

Bald Cypress *(Taxodium mucronatum)*

Taxodium mucronatum is a riparian species that ranges from Durango (Mexico) as far south as Guatemala. It also (though less commonly) is present in marshes and landscapes with springs, though less commonly. The ecological characteristics of *Taxodium mucronatum* are similar to those of *Taxodium distichum* is present in the southeastern United States (Macmillan, 1974). However, morphological differences exist between the two species. Additionally, there are two important physiological differences, *Taxodium mucronatum* is not resistant to frost, and in general is more drought resistant. The ability to manage droughts is explained by *Taxodium mucronatum's* root system, which is capable of securing perennial water sources. Germination is most successful in moisture-laden soils and fails in well-drained soils (McMillan, 1974). Based on *Taxodium* fossil findings at Tlapacoya, Quintero-González (1986) estimated a mean temperature in the Valley of Mexico to be 20˚ C and yearly average precipitation around

1400 mm slightly before the Last Glacial Maximum (ca 23,000 BP).

MATERIALS & METHODS

MaxEnt (Phillips, 2004) is a computer program that has shown considerable success in estimating the likelihood of species distribution, particularly for modern-day distributions (Elith *et al*., 2006). The principle of Maxent is based on the idea of using incomplete data collections (e.g. opportunistically sampled data) to formulate predictions about species distribution. MaxEnt's goal is to estimate a target probability distribution by finding the probability distribution of *maximum entropy* (i.e., the distribution that is the most spread out). This distribution is constrained by the set of climatic variables available.

In some sense, MaxEnt's model is similar to a regression model, which takes in several variables (covariants) and determines the contribution of each variable to the model. In a standard regression model, non-linear data relationships are often put through transformations as a means of "making sense" of the data. MaxEnt takes in variables as a regression model does and also transforms many of the covariant relationships. These transformations are called features, as in the nomenclature used in machine learning algorithms.

MaxEnt is based on Bayesian probability concepts, and more specifically, a postulate stating that the most probable distribution is that with the highest (maximum) degree of entropy. MaxEnt has three important strengths, 1) it requires only presence data, which, unlike absence data, are easy to define unambiguously with field and herbaria records 2) it accepts any environmental data (e.g. climate, soil type) in simple ASCII format 3) it is able to project a present-day climate envelope into past conditions that fall into the present-day range and is also able to avoid novel or non-analog regions. Elith *et al.* (2011) have produced a generalized description of the statistical basis of MaxEnt and its application in ecological problems. The key points of which are summarized in Appendix 1.

Herbaria data were obtained from the Global Bioinformatics Information Facility, or GBIF, (http://www.gbif.org) for each taxon of interest. All duplicate values were removed. The remaining coordinates were mapped using GIS software (ESRI ArcMap 10.0). For *Picea chihuahuana, Artemisia ludoviciana, Liquidambar styraciflua* and *Taxodium mucronatum,* USGS distributions in digital format (Little, 1971) were also mapped in an effort to compare the broad distribution to the data retrieved from the Global Bioinformatics Information Facility. When possible, coordinates and elevation were compared to specimens in the University of California Herbarium, Berkeley, specifically for *Liquidambar styraciflua, Taxodium mucronatum* and *Abies religiosa*. However, for older influenced by topography and elevation.

In the cases of *Taxodium* and *Liquidambar*, each is represented by one species in Mexico, making the herbaria data easy to use. However with *Artemisia, Picea* and *Abies*, this is not true. As I already discussed, there are seven different species of *Abies*, 11 species of *Artemisia*, and at least three species of *Picea* in Mexico. For *Picea* and *Abies*, some inference of their phylogenetic history (discussed earlier) helped to narrow the species that I decided to use in this modeling effort. However, *Artemisia* is problematic,

since there are several species and widely dispersed subspecies. *Artemisia ludoviciana,* the species of interest here, has several subspecies.

For *Abies*, I decided to model *A. religiosa,* since this is the most commonly found fir species in central Mexico. *A. religiosa* is also widely studied because it is habitat for the monarch butterfly and thus an important conservation species (Aguirre-Planter *et al.,* 2012). The species also has the most digitized herbarium records.

Only one species of spruce was included in the modeling analysis, *P. chihuahuana.* The choice here was based on the availability of good ecological and phylogenetic data (Gordon, 1968; Ledig *et al.,* 2010). However, for *Artemisia*, no detailed phylogenetic studies are available. For this reason, I limited the analysis to *A. ludoviciana*, since two of its subspecies appear in both central Mexico and northwestern Mexico.

The present-day bioclimatic envelopes for each taxon were constructed using selected variables from the present day WorldClim Dataset (Hijmans *et al*., 2005). Following a basic approach similar to Thompson *et al.* (2008), I reduced the WorldClim data set to a small subset of four variables for each species modeled. The choice of variables was based on the ecological characteristics. Table 2.2 contains the references and details regarding the choice of variables.

I used existing high-resolution climate model data sets derived from GCM model data (See Appendix 2 for details regarding GCM data manipulation). The WorldClim data set is a high-resolution data product comprised of variables relevant to ecological phenomena (Hijmans *et al.*, 2005). The data set is based on the interpolation of modern instrumental data, mainly precipitation and temperature. For my present-day distribution models, I selected predictor variables for each taxon using WorldClim present-day data (Table 2.1).

The selection of variables is based on my interpretation of several key references for each taxon and their correspondence to available WorldClim variables. A summary of the references and the corresponding WorldClim variables are in Table 2.2. It should be noted that one goal was to use fewer than the total 19 WorldClim variables, and in particular, to focus on the most important ecological variables for each individual taxon, based on available literature whenever possible.

To generate each taxon's realized or potential present-day distribution, I ran MaxEnt with 10-fold cross-validation, a random seed, and clamping with fade. Specific details regarding these settings and others used in the model runs are in Appendix 3. Based on the probability predictions generated by MaxEnt, I converted the results to a raster format compatible using ESRI's ArcGIS program (version 10.0) and created the distribution maps in Figures 2.1a to 2.5a. Because MaxEnt produces a range of probabilities between 0 and 1, I established a threshold level (cutoff) for the final distribution. Liu, Berry, Dawson & Pearson (2005) evaluated several approaches to threshold selection in ecological modeling, and offered at least five simple methods that are superior to the traditional fixed threshold approach, in which the model results are defined by a single value, often 0.5 and above being species presence. I chose the method of approximating the shortest distance from the ROC plot-based approach, originally proposed by Cantor *et al.* (1999 as cited by Liu, 2005).

To generate bivariate graphical representations of the relationship between the most relevant WorldClim variables for each taxon, I used ESRI's ArcGIS 10.0 program to extract climate characteristics for 1) each presence point for each taxon and 2) the range

of predicted locations for each taxon.

RESULTS

The variable contributions from MaxEnt for the five species are summarized in Tables 2.1a to 2.1e. Also in Tables 2.1a to 2.1e is the "permutation importance", a secondary measure of variable contribution reported in MaxEnt's results. The threshold levels selected for this study are summarized in Table 2.3. Figures 2.1a to 2.5c illustrate the herbaria data distributions and the MaxEnt results for the present.

Figures 2.6a to 2.11b illustrate the relationships between the two leading temperature and precipitation variables contributing to the MaxEnt model and are compared to the same two variables based on the herbaria data.

Figure 2.16 depicts a hypothetical transect through the present day modeled distribution in an effort to illustrate the changes in species as elevation varies. The transect traverses approximately 240 km from the eastern coast of Mexico to the Valley of Mexico. Several key pollen diagrams come from this area in Mexico.

In a general sense, the modeled populations of *Abies* and *Picea* follow elevation and climate as expected. More specifically, the relationship between *Abies'* modeled distribution and volcanic regions and *Liquidambar's* occupation of mesic environments is pronounced. The modeled current distribution of *Taxodium* and *Artemisia* are less closely related to their actual distributions. I discuss each taxon's response individually below.

DISCUSSION

The hypothesis is straightforward: that the modeled distribution maps will agree with the known current distributions for each species. If there is agreement, it suggests that the MaxEnt model for the given species is worthy of projection into the past, more specifically, the mid-Holocene and LGM. Furthermore, the current distribution model is crucial to backward projection of the model, because its success implies that the bioclimatic variables I used are important in determining the range of the species.

"Agreement" is assessed not only using the built-in cross-validation technique in MaxEnt (AUC values), but also when possible, using herbaria data or other resources such as reference maps to support the modeled distribution.

Before discussing the details of the model results, I review several important assumptions that must hold in order for the MaxEnt model to be valid. Several of the assumptions are based on critical reviews of the MaxEnt (and other) models in the literature. These assumptions hold true for the present-day distributions and for projections into other time periods that are covered in the subsequent chapters.

Constructing a niche model assumes that the environmental variables chosen for the model are important in limiting the distribution. In this dissertation, I have assumed in the current distribution models that climatic variables are more important than other factors, namely evolutionary processes and non-evolutionary processes such as lag effects. This assumption is important in bioclimatic envelope modeling, whose validity rests on the premise that plant and tree distributions are determined primarily by climate, at least on continental scales (Woodward, 1997; Huntley, 1991).

Another important assumption I make here is that of the climatic niche for a single

species, or "niche stability". The niche stability concept is important because invoking it here means that I have assumed that no shifts in the ecological niche have occurred recently. However, niche shifts are not impossible, and so it is important to pay attention to which species are included in a model. Pearman *et al.* (2008) studied "niche shifting" by comparing species distribution models for the mid-Holocene to pollen records in Europe, where the post-glacial pollen records are well documented. Their work suggested niche shifts are species dependent, and that at a broad scale (e.g. continental) the effects of a niche shift is insignificant.

Finally, species-climate equilibrium is another assumption that must be held when using climate envelope models. Species-climate equilibrium implies that if a species is not present in an area where it is predicted to be, it is because of barriers to dispersal or lag effects. In the distribution models used here, I have assumed equilibrium between climate and the species distribution. I have made the same assumption when constructing the mid-Holocene and LGM scenarios. This is a broad and relevant assumption because human impact in Mexico's environment, as for example with agriculture in some areas, has altered the landscape considerably. Very large population centers are also reminders that any taxon's dispersal and establishment may be impeded resulting in disagreement with a predicted distribution. However, as with niche stability, the scale of the study may be broad enough that human populations are not significant sources of error. In subsequent chapters, I will return to the relevance of species-climate equilibrium as it pertains to past climates.

I will discuss the model results for each taxon, and how well the results agree with field studies, independent of the herbaria data.

Abies religiosa

In general, *A.religiosa's* MaxEnt distribution matches the major areas where *A. religiosa* actually exists.

Despite a lack of herbaria specimens around the volcanic area of Nevado de Toluca, the MaxEnt modeled distribution in Figure 2.1b suggests a high likelihood of *A. religiosa*'s presence. This is actually confirmed by Villers-Ruiz, Rojas-Garcia, & Tenorio-Lezama's (2006) report that *A. religiosa* does occupy several regions around Nevado de Toluca. Further east in the TMVB *A. religiosa* is present between 2100 m and 4100 m on the volcanoes of Popocatépetl and Iztaccíhuatl (Lauer 1973; Muñoz-Jiménez, Rangel-Rios & Garcia, 2005; Bobbink, Heil & Verduyn, 2003). The MaxEnt model additionally suggests suitable conditions for *A.religiosa* in the vicinity of La Malinche, a volcano further east, in Puebla. Ohngemach & Straka's (1983) extensive work near La Malinche confirms the model results. Another study by Alvarado (1983) points out a population of *A. religiosa* to the south-southwest of Mexico City at higher elevations (2700 m - 2800 m). Finally, MaxEnt predicts *A. religiosa* near Pico de Orizaba in the eastern regions of the TMVB. Lauer's (1978) work at Pico de Orizaba confirms that between 2700 and 3200 m, *A. religiosa* is present.

MaxEnt results also suggest a high likelihood of *A. religiosa* in the northwestern corner of the state of Mexico, eastern and central Michoacan, as well as in high altitude regions of Hildalg. Bernal-Salazar & Salgado (2000) confirm *A. religiosa* occurs in western Michohacán. Finally, I find overall excellent agreement between several of the

high altitude MaxEnt-generated results in the Valley of Mexico and a land-use and vegetation map (Figure 2.1c) produced by Calvert & Brower (1986).

While the MaxEnt results for *A. religiosa* represent a very good broad scale present-day distribution, there are some important discrepancies. Firstly, the model results point to a rather wide and uniform distribution of *A. religiosa* around La Malinche. However, Lauer (1978) presents an important observation regarding occurrences of *A. religiosa* and its relationship to aspect. Lauer states that on La Malinche, a distinct asymmetry in the distribution of *A. religiosa*. The species comprises a dense forest on the western side of the mountain, but occurs only on valley slopes on the eastern side. On initial analysis, one might guess that the obvious variable to consider is aspect, but Lauer points out that in the nearby Valley of Mexico, *A. religiosa* appears on the eastern slopes rather than the western slopes, contradicting the aspect hypothesis. Lauer then suggests that the asymmetry phenomenon is not due to aspect, or even insolation differences but rather, tied to the moisture capacity of different soils.

The issue of soil type in this example raises a second, broader point. As pointed out in the discussion of necessary assumptions for climate envelope models, enough attention is not always given to the physiological factors influencing plant species distribution (Woodward & Beerling 1997). In Lauer's observation of *A. religiosa*, we see that the concerns are legitimate if the goal of a model is to reproduce fine scale processes across the landscape. However it is not possible to work at such a fine scale in a paleoecological reconstruction since fine scale data (e.g soil data) are not available.

Ultimately, what I find in the MaxEnt result for *A.religiosa* is excellent agreement with documented present-day field studies, independent of the herbaria data used in the model.

Picea chihuahuana

Picea chihuahuana was chosen for two reasons. First, the presence of *Picea* at low latitudes is unusual, and in the case of Mexico existing populations are most likely refugial wider distributions during glacial periods. Secondly, in the Sierra Madre Occidental, refugial populations occur exclusively in cool, moist canyons called "barrancas" (Gordon, 1968). Because of restrictions to moist and cool climates, it has a narrow climatic envelope.

The resulting distribution of *P. chihuahuana* (Figure 2.2b) compared to field sightings (Figure 2.2a) shows good agreement, especially in the southern regions of the Sierra Madre Occidental. However, there is possible over-prediction in the northern and eastern reaches of the range. One cannot rule out the possibility that there are populations of *Picea* that have not yet been found. Finally, in the southern region of the range, the MaxEnt does capture several of the actual *Picea* stands that occupy the cool canyons (barrancas) at lower elevations.

At a threshold level of 0.8, as per Liu et al. (2005), MaxEnt predicted appropriate conditions for *Picea* in at altitudes between 2000 and 3000 m in the Sierra Madre Occidental and within the eastern TMVB, for example near Pico de Orizaba and La Malinche. Although the climatic conditions may be appropriate for *Picea* in these areas, its absence may reflect the difficulty in dispersal from cool climate areas to the north.

This interesting point, that *Picea* may have been present in these areas during the mid-Holocene, will be discussed later.

Artemisia ludoviciana

The species found throughout Mexico is *Artemisia ludoviciana,* a species with four subspecies. In central Mexico, the dominant subspecies is *A. ludoviciana ssp. mexicana*, while *A. ludoviciana ssp. sulcata* is more prevalent in the northwest. Although these are both the same species, it is possible that their range of tolerance differs, depending on the regional conditions. Because of the broad range, the climate envelope constructed here for the species as a whole may not capture the full extent of the present-day distribution.

The MaxEnt current-day predicted distribution for *A. ludoviciana* is in Figure 2.3b. The predicted area includes the Valley of Mexico throughout the states of Mexico and Puebla and some parts of Michoacan and Guanajuato. However, very little *A. ludoviciana* is projected for more northern regions despite a documented presence from herbaria specimens (Figure 2.3a). Only a small population appears in to the north in Nuevo Leon and San Luis Potosí, and a small area is also projected near the northwestern border of Durango. In general, the model predicts the main area to be in the southeastern central highlands, and area with cool, dry winters and warm summers with moderate precipitation. In the northern states, where the climate is more arid, no *A. ludoviciana* appears in the modeled results. Interestingly, MaxEnt does not predict *A. ludoviciana* to be present in the northern part of central Mexico.

Liquidambar styraciflua

As already pointed out earlier, *L. styraciflua's* distribution in Mexico is fragmented, attributable to either refugial pockets or the result of limited dispersal capacity. The MaxEnt results for the present-day distribution of *L. styraciflua* (Figure 2.4) show the highest likelihood of *L. styraciflua* occurring in the southeast as a narrow strip around 1800 m that coincides with the "cloud forest" zone. The altitudinal range of *L. styraciflua* in the cloud forest is approximately 1200-2000 m (Newton *et al.,* 2009). This region is typified by a cool climate and year-round moisture availability, largely due to persistent foggy conditions that inhibit evapotranspiration. Martin & Harrell's (1957) map of *L. styraciflua* shows a similar distribution, but also illustrates additional refugial populations further south, and another in the southwestern region. MaxEnt depicts the broad scale pattern of the cloud forest where one would expect most sweetgum in Mexico to be found. The results are also roughly in agreement with Little's map of *Liquidambar* distribution (Little, 1971).

Taxodium mucronatum

MaxEnt's present-day predicted distribution for *Taxodium mucronatum* is shown in Figure 2.5b. One interesting outcome is the projected absence of *T. mucronatum* from the Valley of Mexico, where *T. mucronatum* grows (Figure 2.5a). However, many of the modeled regions are in agreement with the field data. Furthermore, sections of the results demonstrate linear patterning along hydrological features (Figure 2.5c) of modern-day Mexico.

In the northwestern part of Mexico, MaxEnt found several areas where *T. mucronatum* might occur. In the arid northern reaches of Chihuahua for example, *T. mucronatum* does grow along rivers, a result that MaxEnt generated. While some of the

results are along riverine channels, MaxEnt, for this species did not predict the distribution as well as it did for *Picea, Abies,* and *Liquidambar.* The failure to accurately model *Artemisia* and *Taxodium* may be due to 1) the climate envelope I defined, 2) the omission of hydrological data in the model, 3) the lack of regional microclimates and conditions in the environmental layers, or 4) MaxEnt may not be the right way to approach this problem. Also, the inaccuracies of this present-day model will impact any projections of the model into past climate data.

Bivariate Graphs

Figures 2.6 through 2.10 illustrate the range of temperature and precipitation values (see exact variables per taxon) for the herbaria specimen locations as compared to the distribution locations. One obvious difference between the two graphs for each taxon is the fact that the herbaria specimens are much fewer in number compared to the modeled distribution. However, it is clear that the modeled distributions have much narrower ranges of values than the herbaria specimen ranges have.

CONCLUSIONS

In this chapter, I present modern-day distribution maps of five climatically significant species in Mexico. These species are key indicators of climate change in Mexican pollen diagrams according to palynological records collected in central and northwestern Mexico.

The MaxEnt models of *Picea, Abies* and *Liquidambar* have excellent correspondence with field data and published maps. However, *Artemisia* and *Taxodium*'s modeled distributions are not optimal representations of the present-day distributions. In the case of *Taxodium*, the lack of agreement may be due to a poor choice of predictor variables, but more likely, the lack of hydrological data as an input variable hampered the model's success. For *Artemisia*, using two subspecies of *A. ludoviciana* may have resulted in too broad a climate envelope and may have contributed to lack of correlation between known locations and modeled predictions. This finding stresses the fact that the selection of a taxon with clearly defined ecological tolerances contributes to success in species distribution modeling.

The MaxEnt predicted distributions here lay the groundwork for the subsequent chapters, where I project the distribution for each taxon during the mid-Holocene and LGM. Both these time periods are significant in that the Earth's orbital characteristics are well understood, and typically used to calibrate modern-day climate models, thus the data are readily available for use in envelope models.

Table 2.1a: Variables used in climate envelope for *Abies religiosa*

Variable	Description	Percent contribution	Permutation importance
bioclim_1	Mean annual precipitation	93.2%	91.3%
bioclim_18	Min Temperature of Coldest Month	2.6%	0.9%
bioclim_2	Mean Diurnal Range (Mean of monthly (max temp - min temp))	2.2%	0.3%
bioclim_6	Mean Temperature of the Coldest Quarter	2.0%	7.5%

Table 2.1b: Variables used in the climate envelope for *Picea chihuahuana*

Variable	Description	Percent Contribution	Permutation importance
bioclim_10	Mean Temperature of Warmest Quarter	74.7%	50%
bioclim_18	Precipitation of Warmest Quarter	12.1%	19.7%
bioclim_6	Min Temperature of Coldest Month	9.8%	0.2%
bioclim_16	Precipitation of Wettest Quarter	3.5%	30.5%

Table 2.1c: Variables used in the climate envelope for *Artemisia ludoviciana*

Variable	Description	Percent contribution	Permutation importance
bio_10	Mean Temperature of Warmest Quarter	73.40%	69.70%
bio_11	Mean Temperature of the Coldest Quarter	9.90%	14.40%
bio_15	Precipitation Seasonality (Coefficient of Variation)	9.80%	9.0%
bio_2	Mean Diurnal Range (Mean of monthly (max temp - min temp))	7.0%	6.90%

Table 2.1d: Variables used in the climate envelope for *Liquidambar styraciflua*

Variable	Description	Percent contribution	Permutation importance
bio_12	Annual precipitation	41.30%	43.60%
bio_15	Precipitation Seasonality (Coefficient of Variation)	25.10%	32.00%
bio_6	Min Temperature of Coldest Month	23.00%	23.50%
bio_5	Max temperature of the Warmest Month	10.60%	0.90%

Table 2.1e: Variables used in the climate envelope for *Taxodium mucronatum*

Variable	Description	Percent contribution	Permutation importance
bio_15	Precipitation Seasonality (Coefficient of Variation)	44.90%	18.50%
bio_11	Mean Temperature of Coldest Quarter	32.20%	42.20%

bio_6	Min Temperature of Coldest Month	14.40%	35.20%
bio_18	Precipitation of Warmest Quarter	8.50%	4.10%

Table 2.2: Variable selection guide for each species, based on inferred ecological characteristics in the research literature.

Taxon	**Reference(s)**	**Corresponding WorldClim variable**
Abies religiosa	Rzedowski (1978)	Annual Mean Temperature
A. religiosa	Rzedowski (1978)	Mean Diurnal Range (Mean of monthly (max temp - min temp))
A. religiosa	Rzedowski (1978)	Precipitation of Warmest Quarter
A. religiosa	None	Min Temperature of Coldest Month
Picea chihuahuana	Gordon (1968)	Mean Temperature of Warmest Quarter
P. chihuahuana	Gordon (1968)	Precipitation of Warmest Quarter
P. chihuahuana	None	Min Temperature of Coldest Month
P. chihuahuana	Gordon (1968)	Precipitation of Wettest Quarter
Artemisia ludoviciana	El-Moslimany (1990)	Mean Temperature of Warmest Quarter
A. ludoviciana	El-Moslimany (1990)	Mean Temperature of the Coldest Quarter
A. ludoviciana	El-Moslimany (1990)	Precipitation Seasonality (Coefficient of Variation)
A. ludoviciana	None	Mean Diurnal Range (Mean of monthly (max temp - min temp))
Liquidambar styraciflua	McMillan (1974)	Annual precipitation
L. styraciflua	McMillan (1974)	Precipitation Seasonality (Coefficient of Variation)
L. styraciflua	McMillan (1974)	Min Temperature of Coldest Month
L. styraciflua	McMillan (1974)	Max temperature of the Warmest Month
Taxodium mucronatum	McMillan (1974) González -Quintero (1986)	Precipitation Seasonality (Coefficient of Variation)
T. mucronatum	McMillan (1974) González-Quintero (1986)	Mean Temperature of Coldest Quarter
T. mucronatum	McMillan (1974)	Min Temperature of Coldest Month
T. mucronatum	McMillan (1974) González-Quintero (1986)	Precipitation of Warmest Quarter

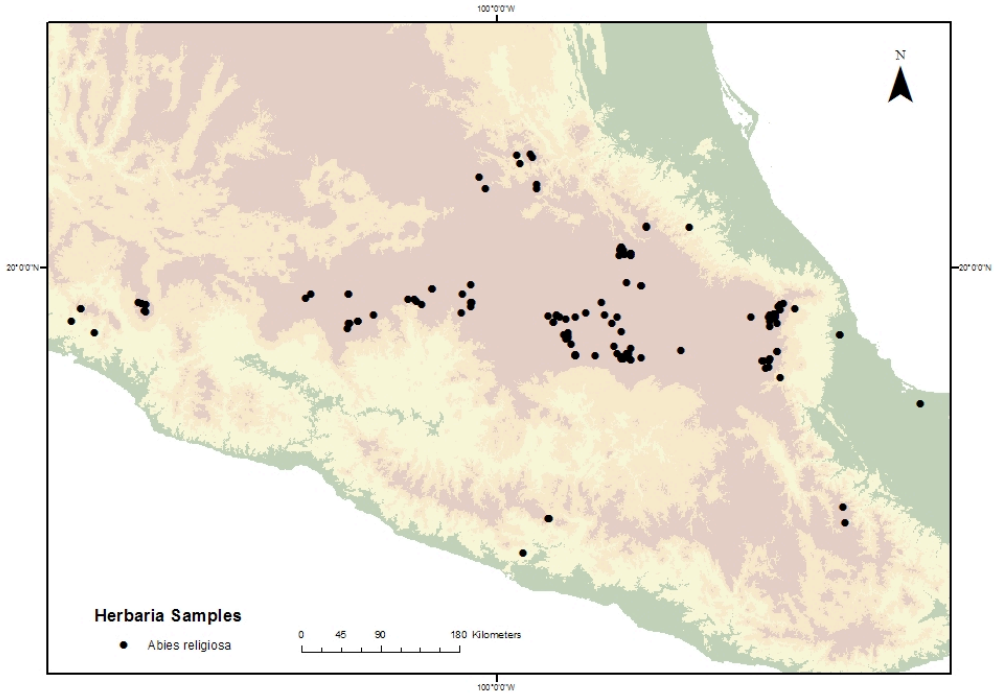

Figure 2.1a: Herbarium specimens: *Abies religiosa*

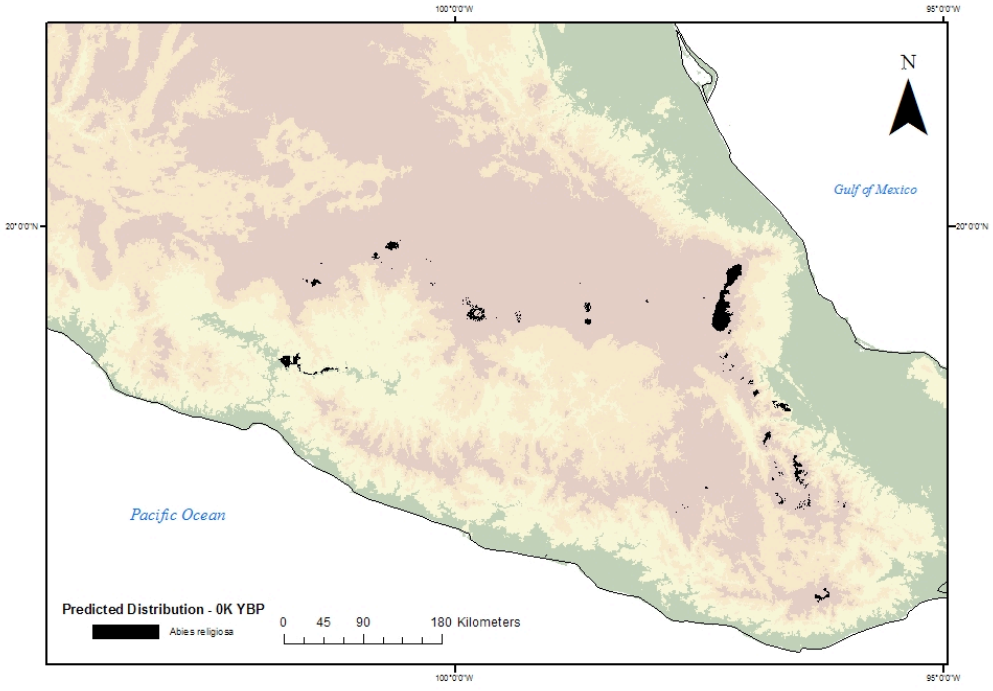

Figure 2.1b: Present *A.religiosa* distribution based on MaxEnt model

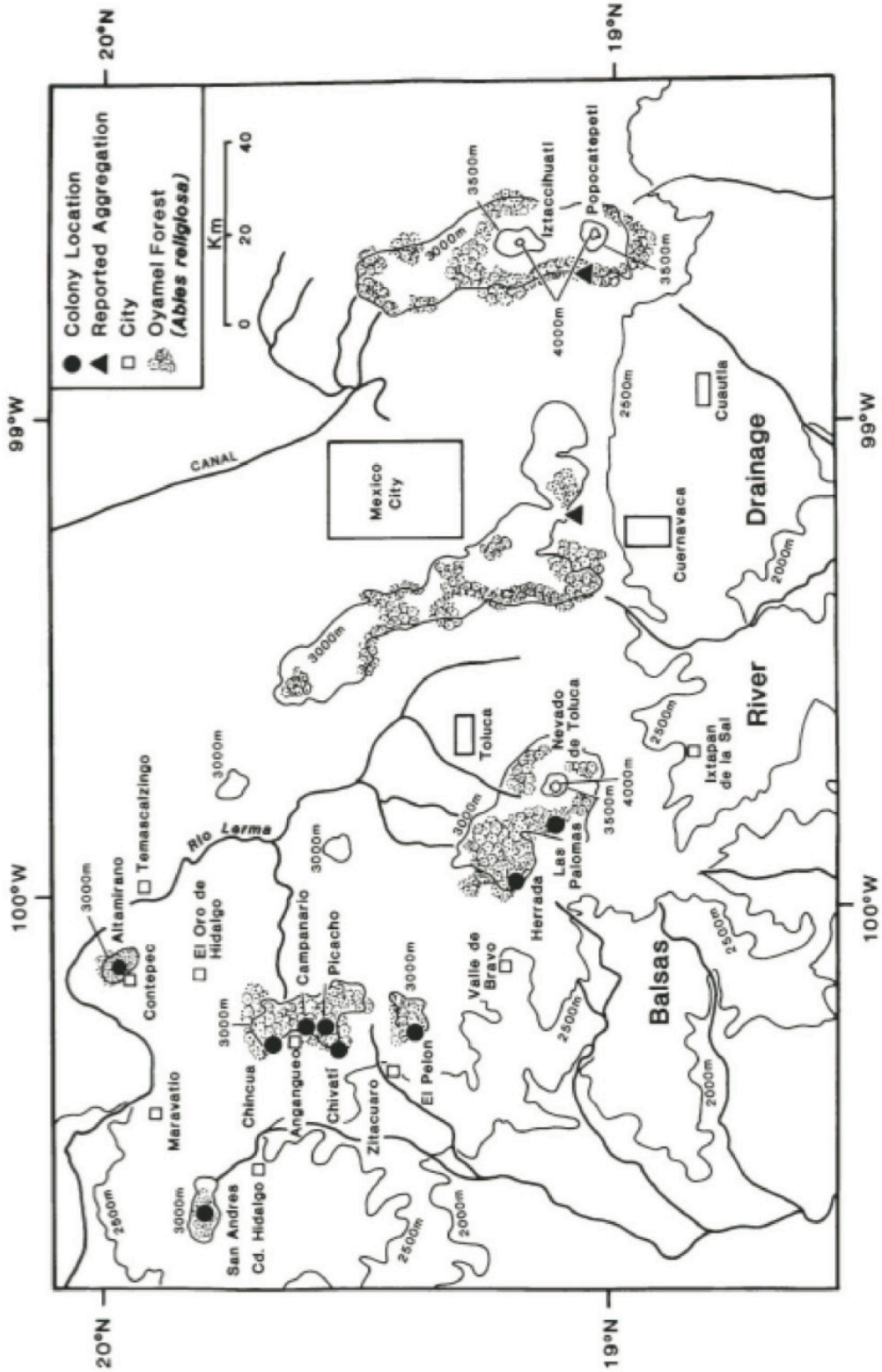

Figure 2.1c: *Abies religiosa* in the Valley of Mexico (Calvert & Brower, 1986)

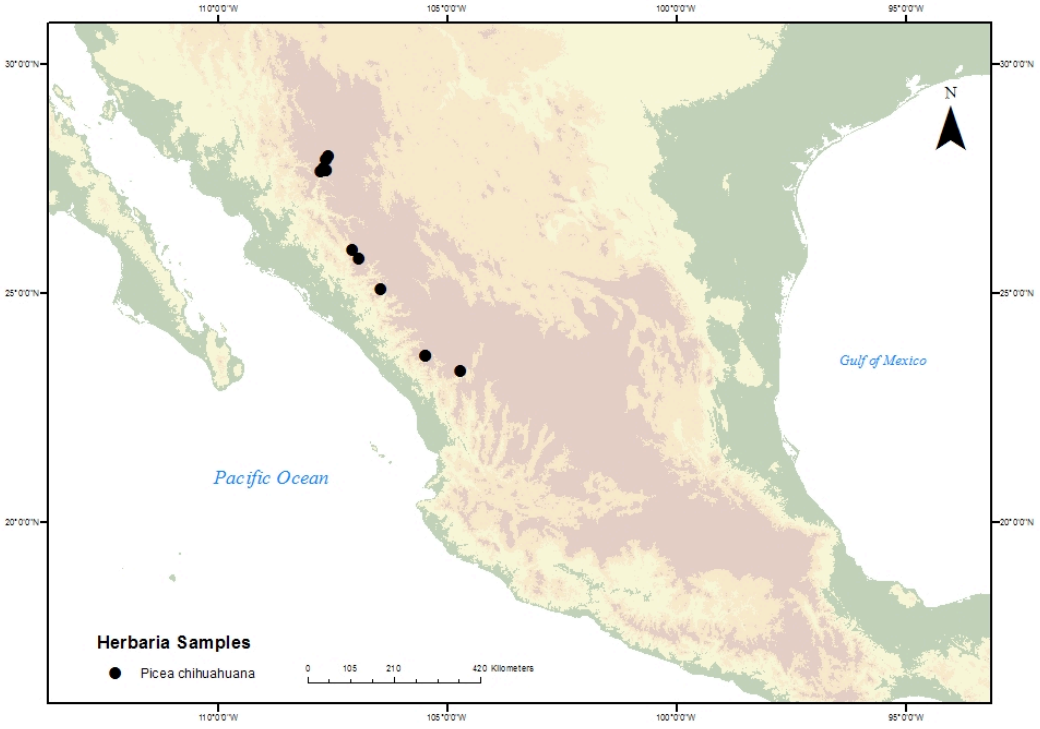

Figure 2.2a: Herbarium specimens: *Picea chihuahuana*

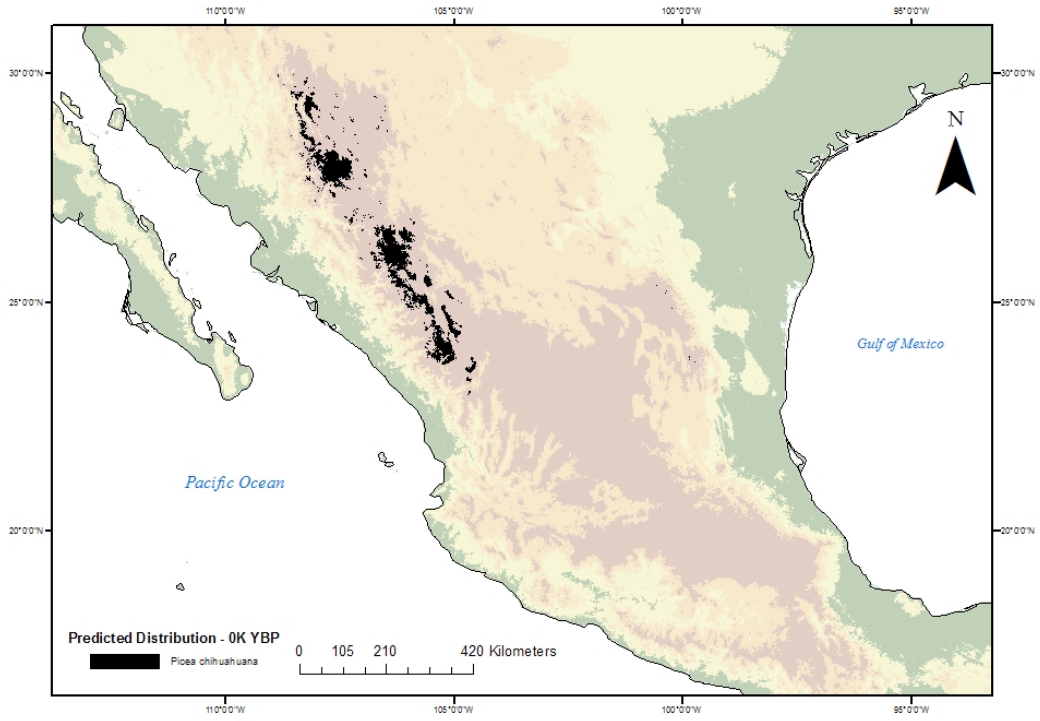

Figure 2.2b: Present *P. chihuahuana* distribution based on MaxEnt model

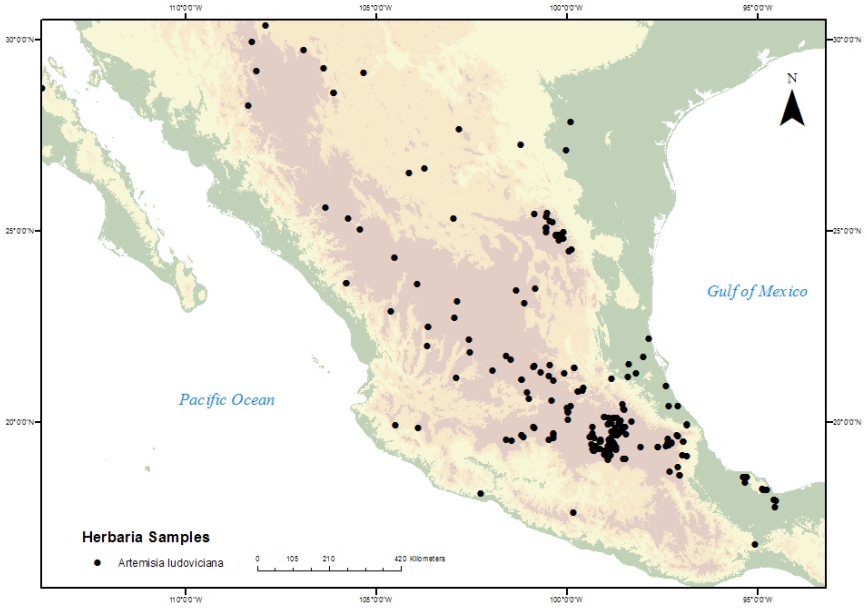

Figure 2.3a: Herbarium specimens: *Artemisia ludoviciana*

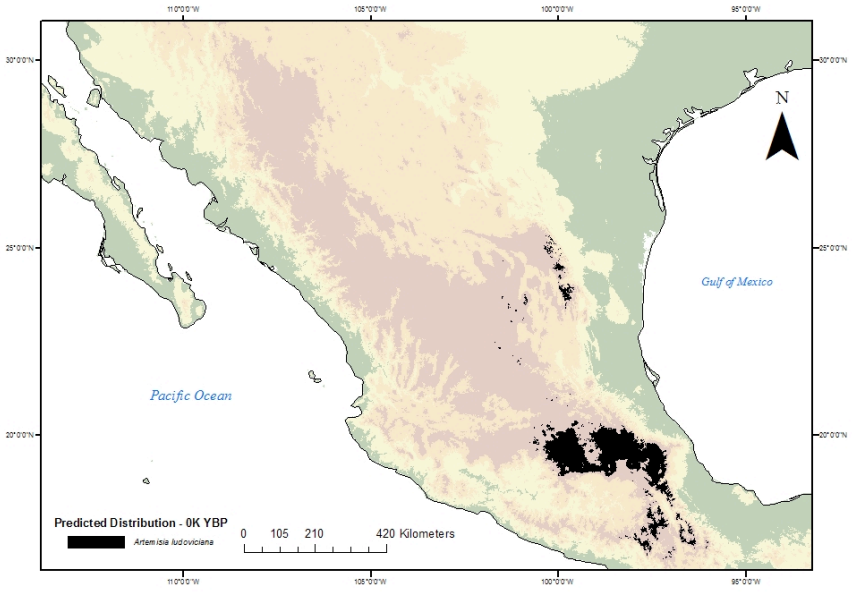

Figure 2.3b: Present distribution of *A. ludoviciana* based on MaxEnt model

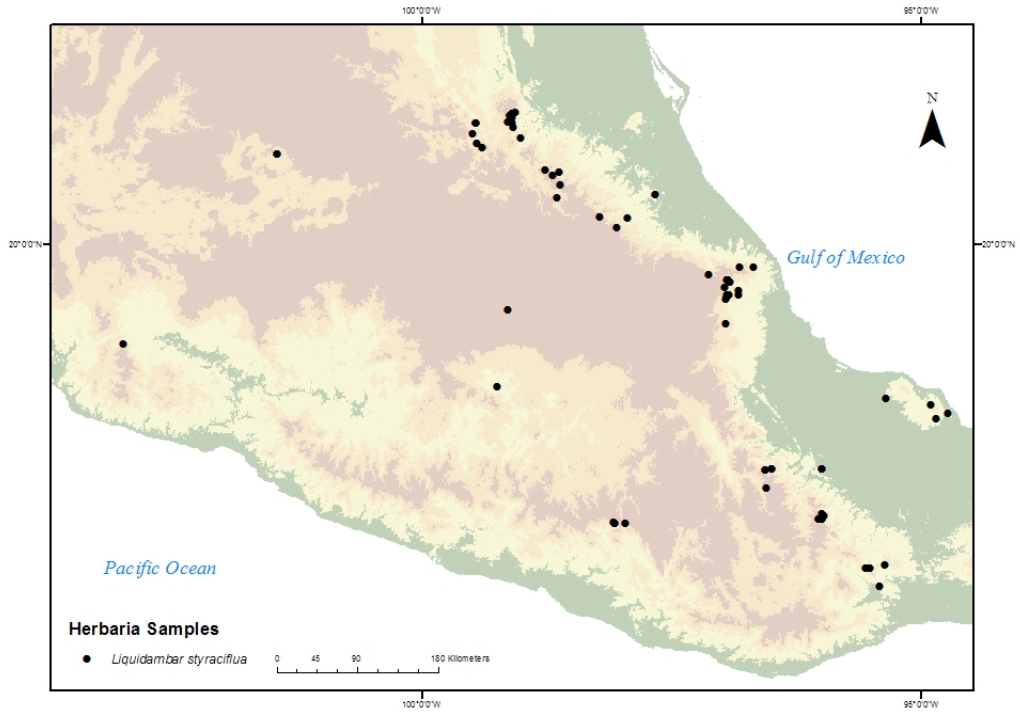

Figure 2.4a: Herbarium specimens: *Liquidambar styraciflua*

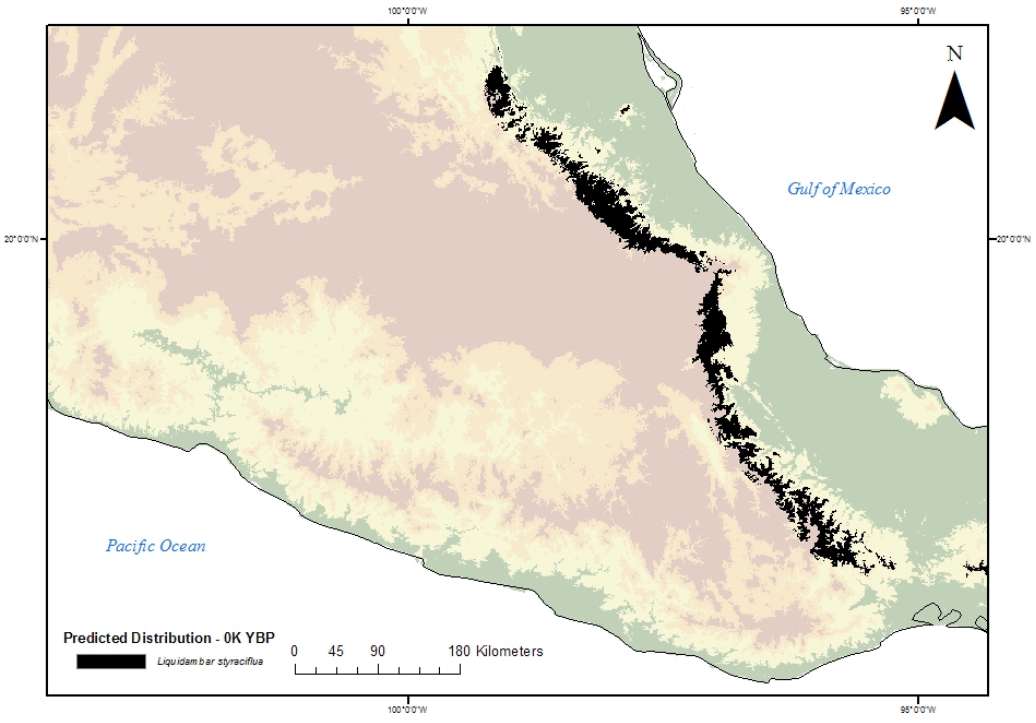

Figure 2.4b: Present distribution of *L. styraciflua* based on MaxEnt model

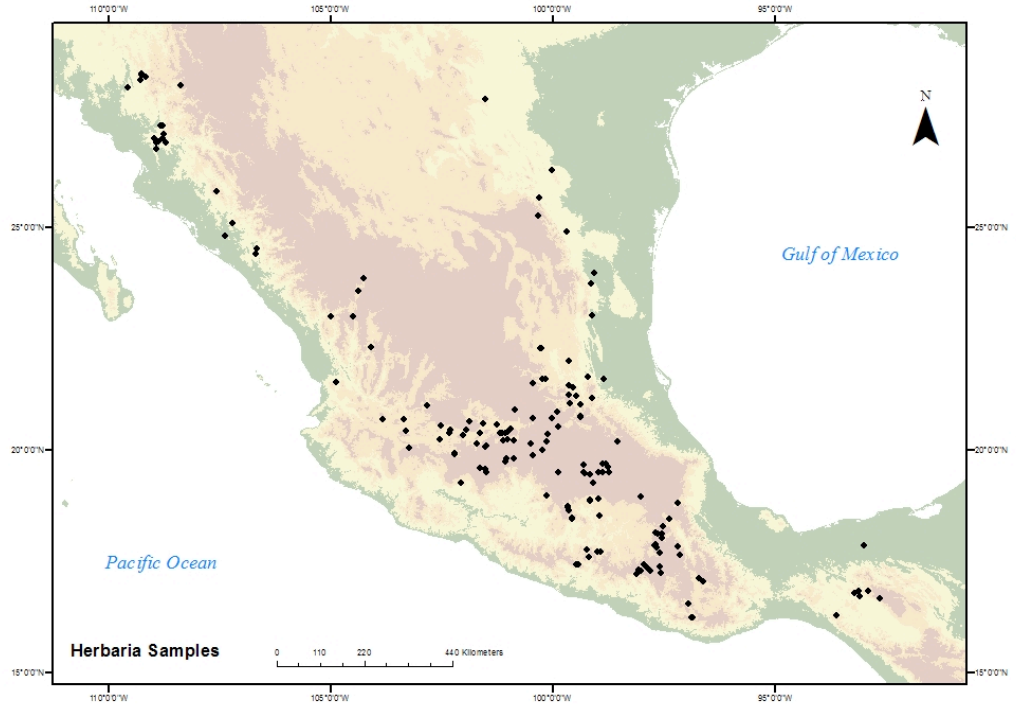

Figure 2.5a: Herbarium samples: *Taxodium mucronatum*

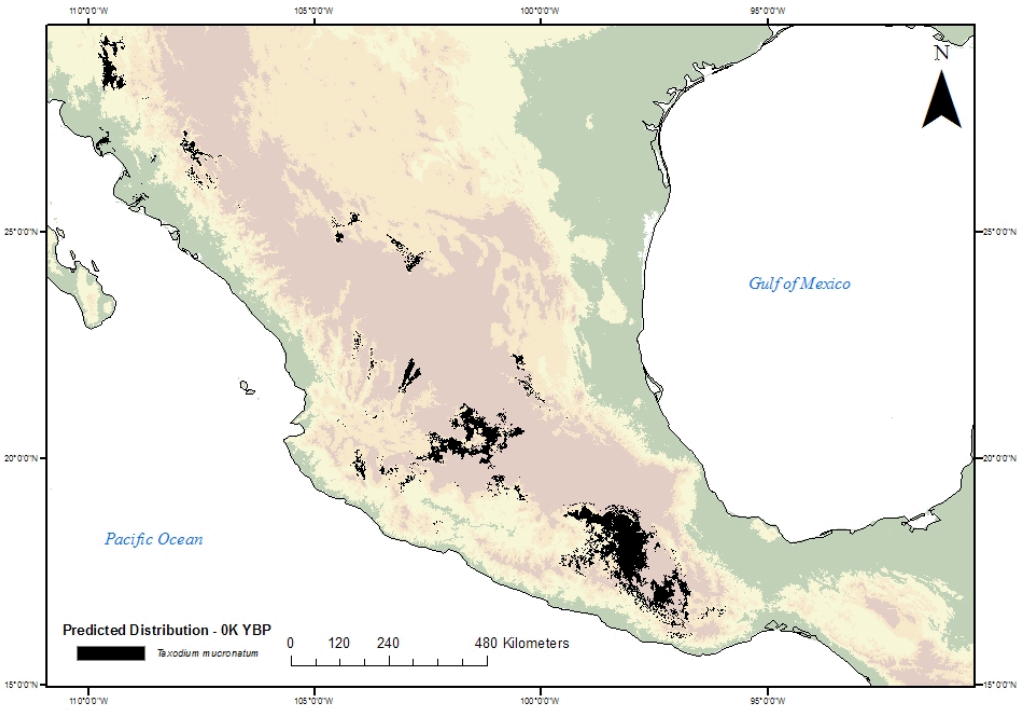

Figure 2.4b: Present distribution of *T. mucronatum* based on MaxEnt model

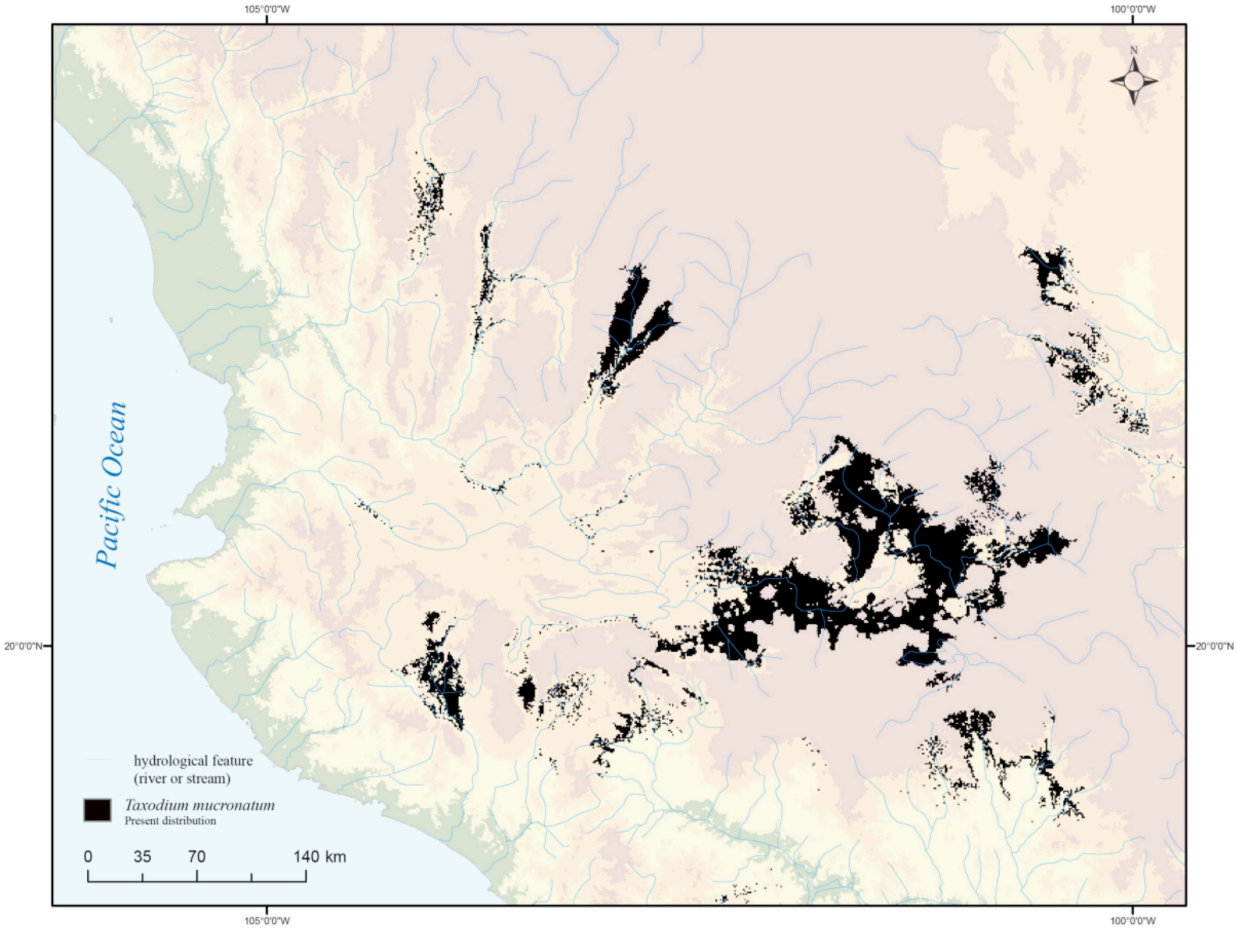

Figure 2.5c: Present distribution of *T. mucronatum* illustrating riparian features.

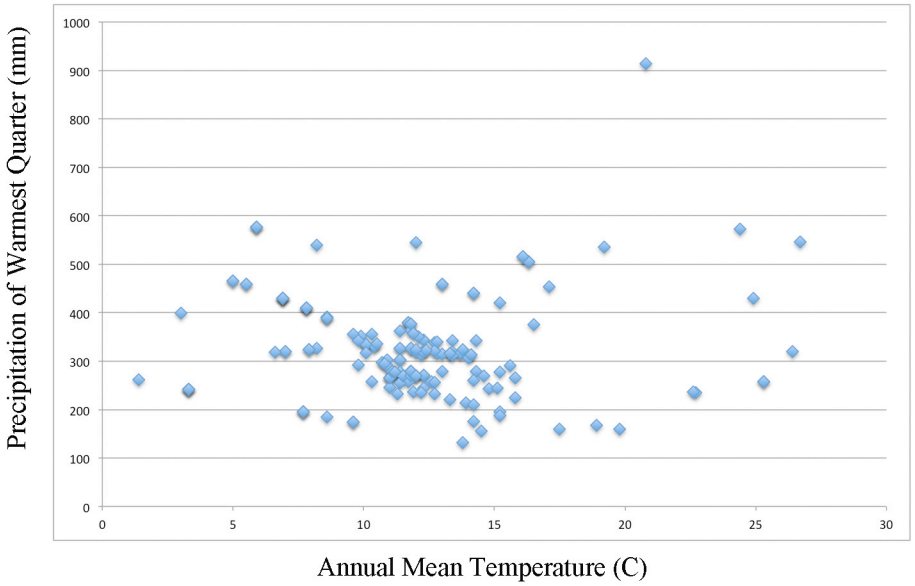

Figure 2.6a Precipitation vs. Temperature relationship for *Abies religiosa* herbaria data

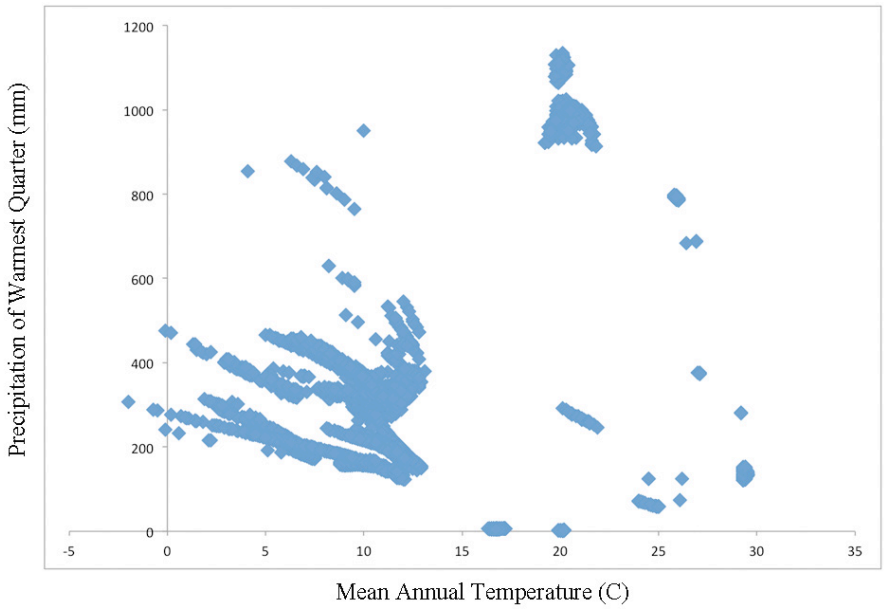

Figure 2.6b Precipitation vs. Temperature relationship for *Abies religiosa* MaxEnt model

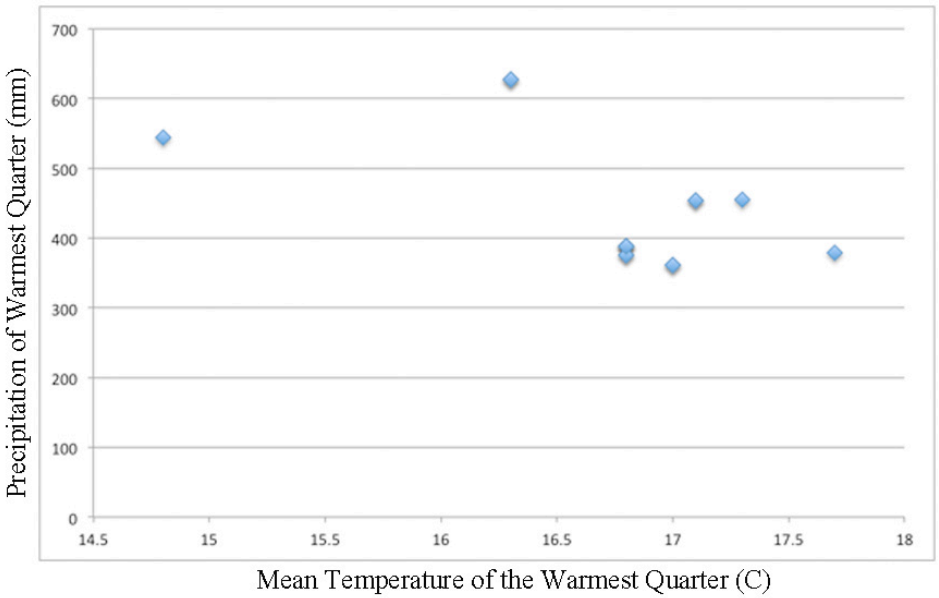

Figure 2.7a: Precipitation vs. Temperature relationship for *Picea chihuahuana* herbaria data

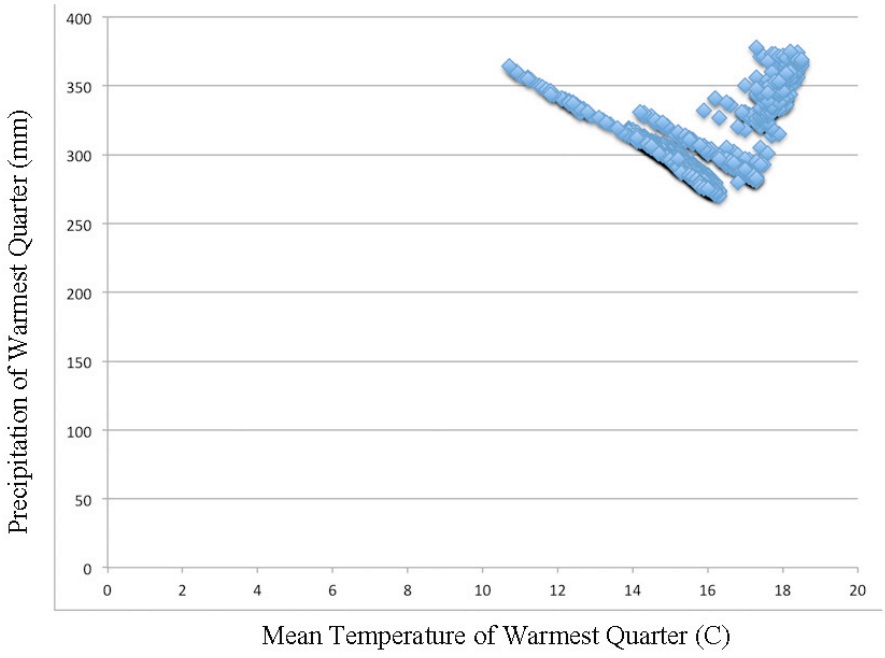

Fig

Figure 2.7b: Precipitation vs. Temperature relationship for *Picea chihuahuana* MaxEnt model

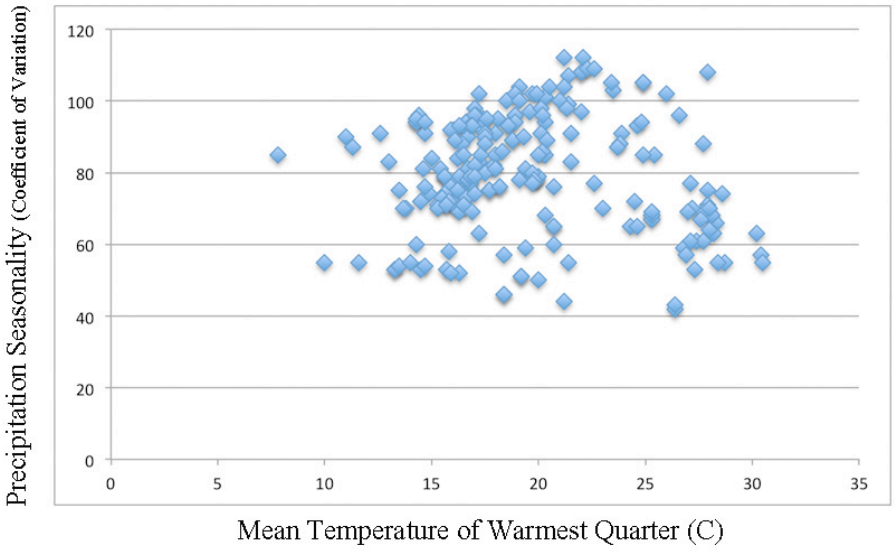

Figure 2.8a: Precipitation vs. Temperature relationship for *Artemisia ludoviciana* herbaria data.

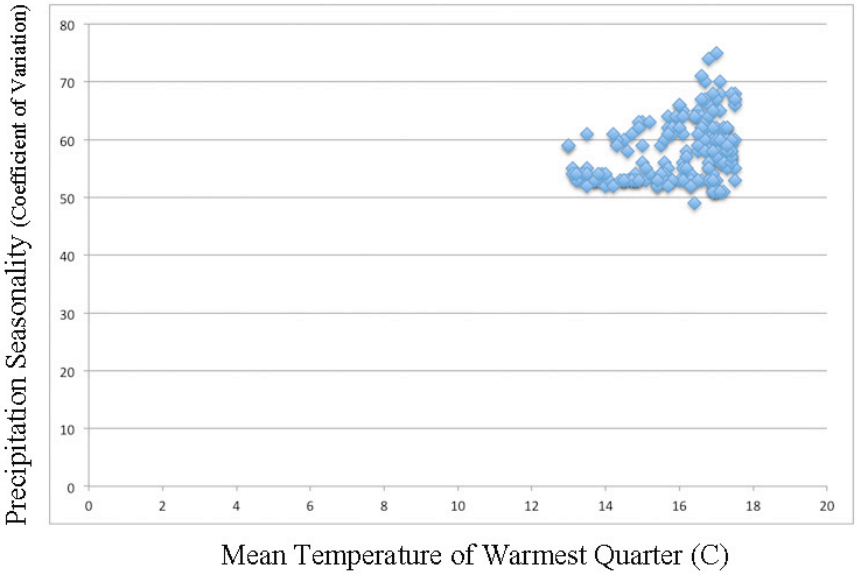

Figure 2.8b: Precipitation vs. Temperature relationship for *Artemisia ludoviciana* MaxEnt model

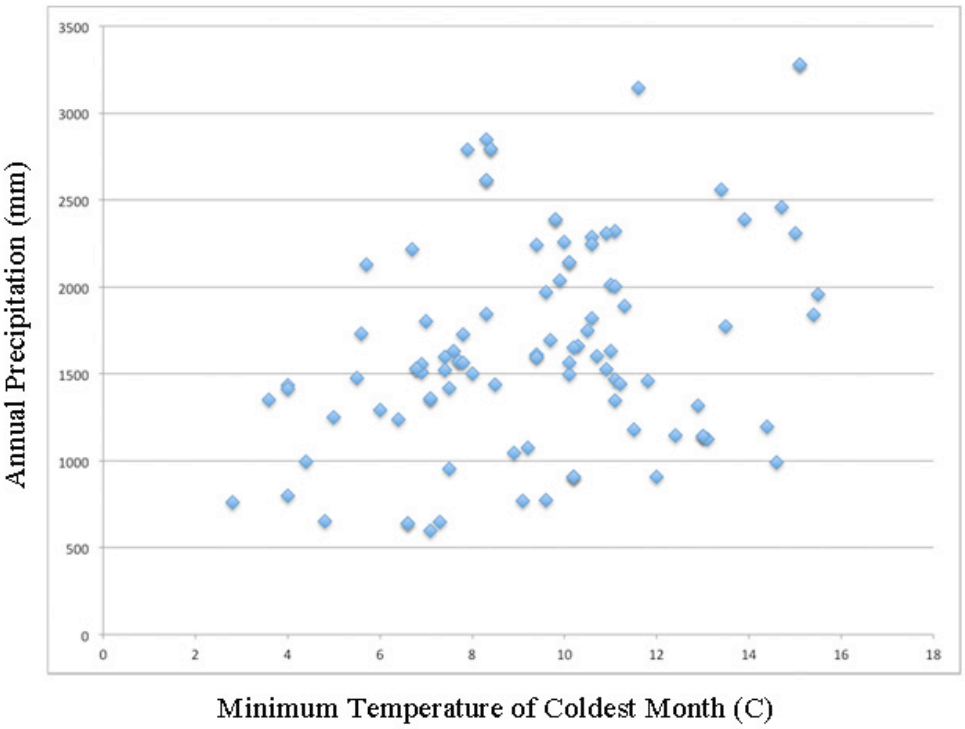

Figure 2.9a: Precipitation vs. Temperature relationship for *Liquidambar styraciflua* herbaria data

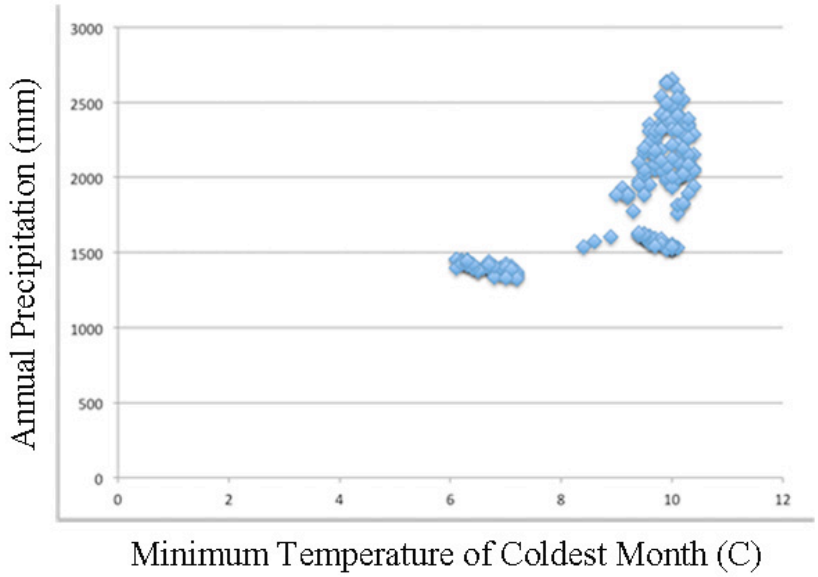

Figure 2.9b: Precipitation vs. Temperature relationship for *Liquidambar styraciflua* MaxEnt model

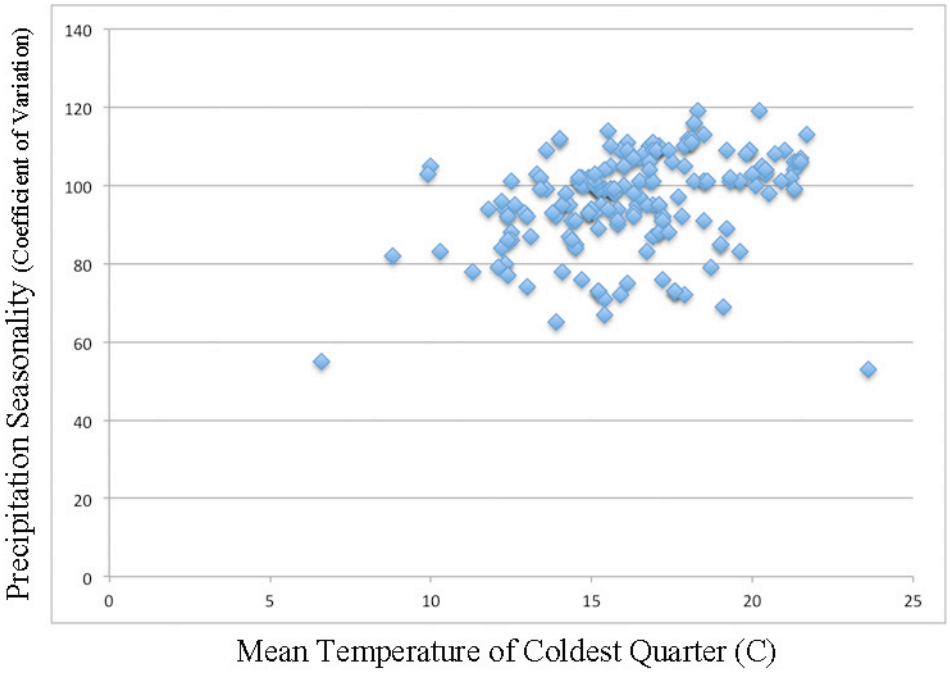

Figure 2.10a: Precipitation vs. Temperature relationship for *Taxodium mucronatum* herbaria data

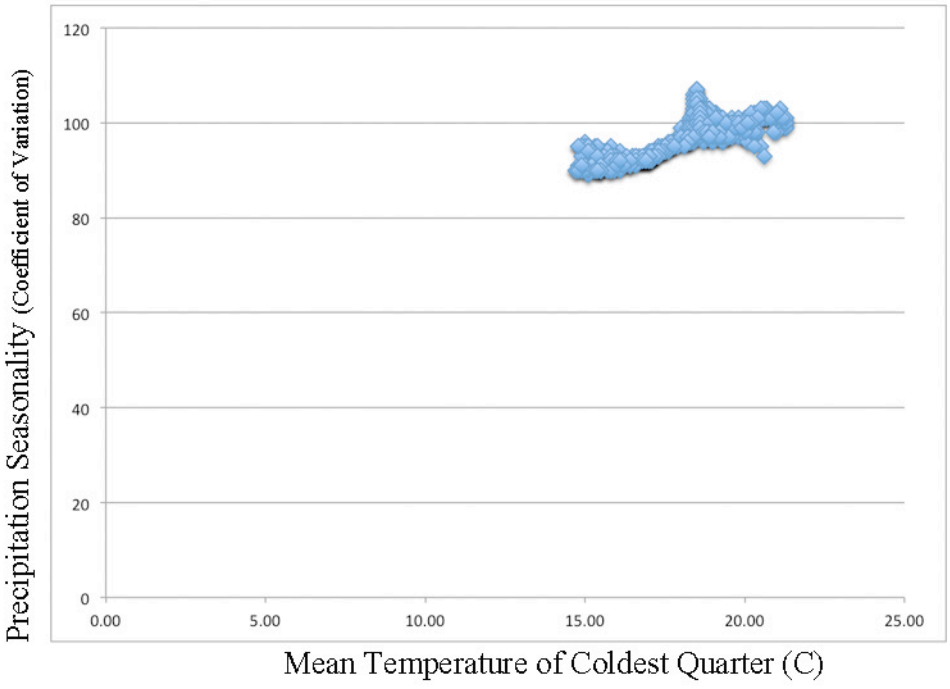

Figure 2.10b: Precipitation vs. Temperature relationship for *Taxodium mucronatum* MaxEnt model

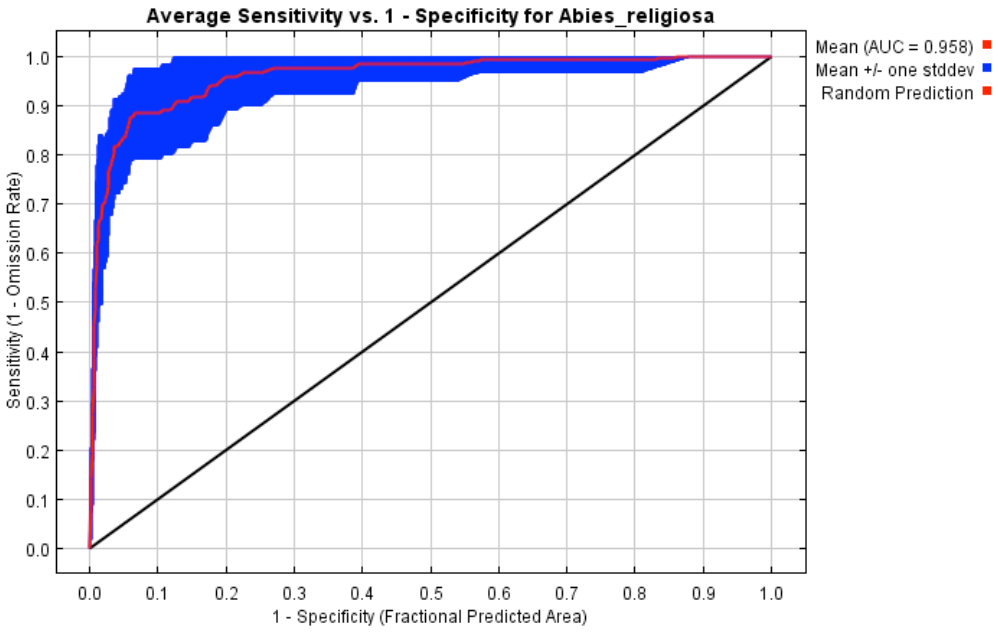

Figure 2.11: Sensitivity vs Specificity – 1 (ROC curve) for *Abies religiosa*

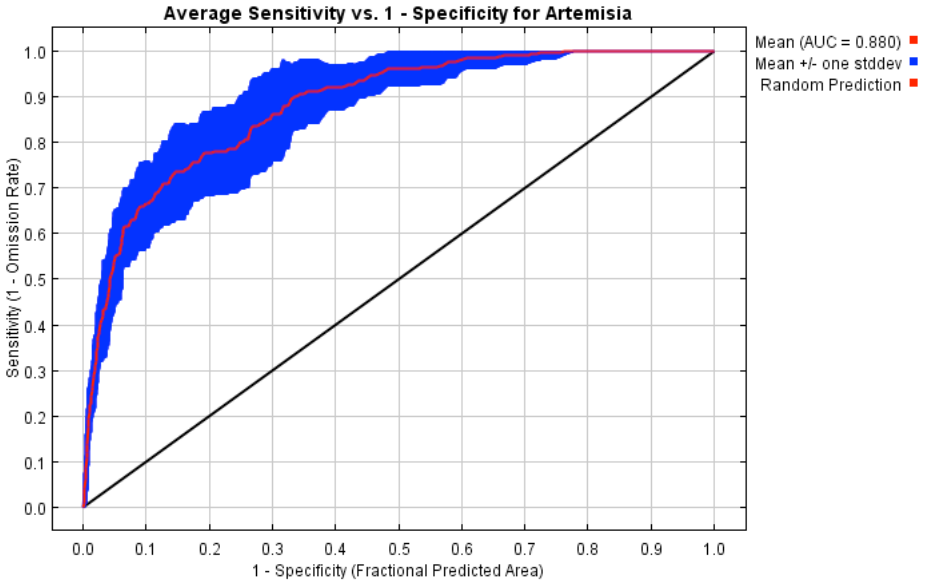

Figure 2.12: Sensitivity vs Specificity – 1 (ROC curve) for *Artemisia ludoviciana*

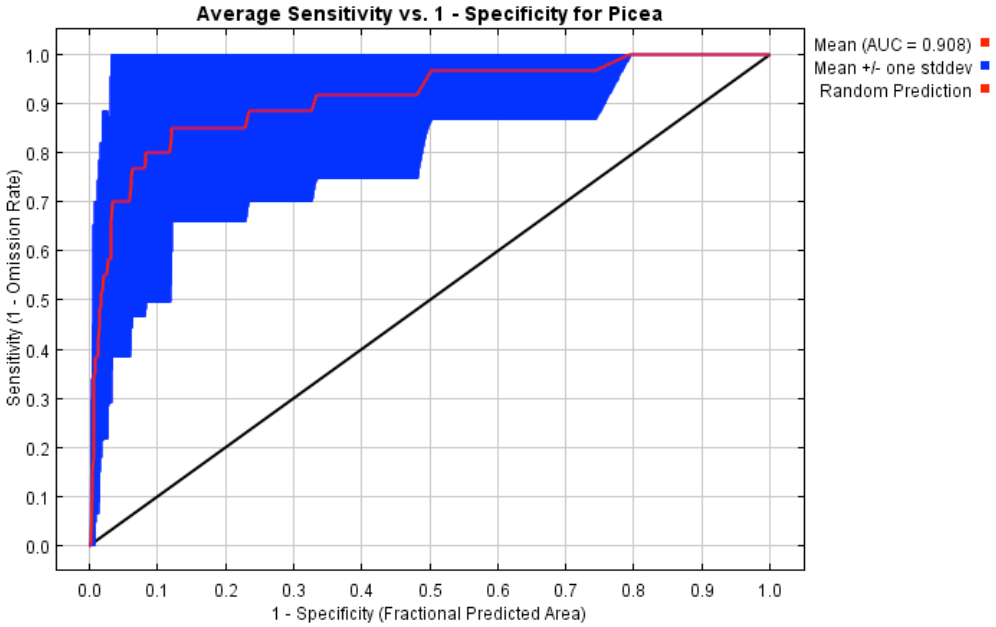

Figure 2.13: Sensitivity vs Specificity – 1 (ROC curve) for *Picea chihuahuana*

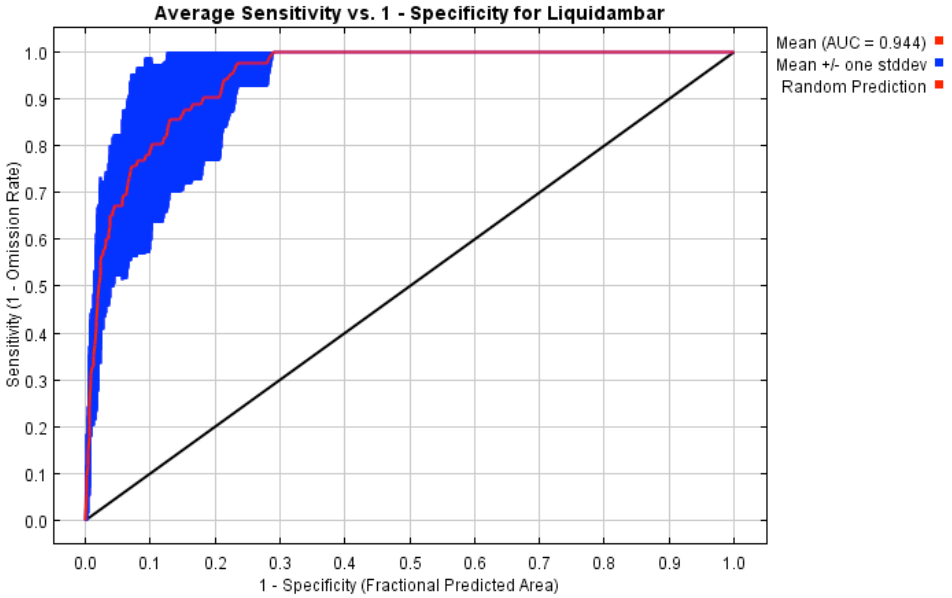

Figure 2.14: Sensitivity vs Specificity – 1 (ROC curve) for *Liquidambar styraciflua*

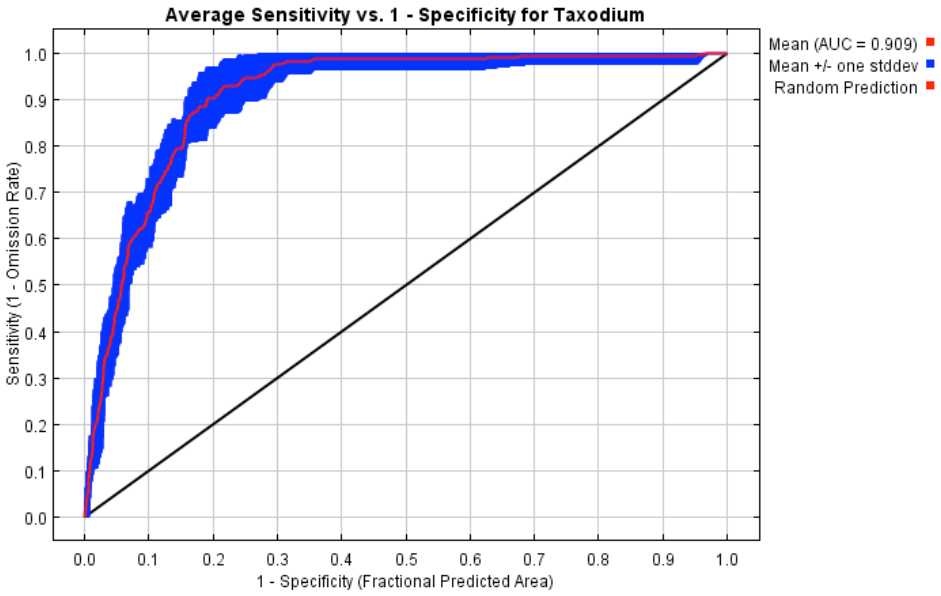

Figure 2.15: Sensitivity vs Specificity – 1 (ROC curve) for *Taxodium mucronatum*

Table 2.3: Threshold Levels

Taxon	Threshold based on ROC 0-1 shortest distance method
Abies religiosa	0.80
Picea chihuahuana	0.80
Artemisia ludoviciana	0.75
Liquidambar styraciflua	0.75
Taxodium mucronatum	0.70

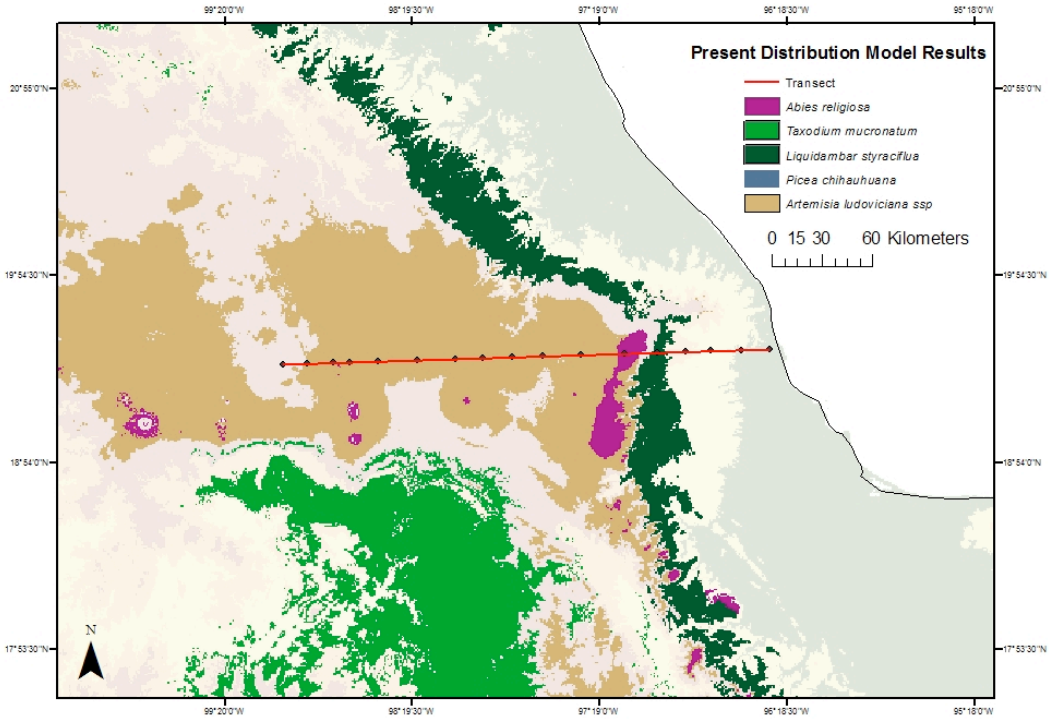

Figure 2.16: MaxEnt results for all species, including a transect from the central plain to the central plateau.

REFERENCES

Aguirre-Planter E, Furnier G.R., & L.E. Eguiarte (2000) Low levels of genetic variation within and high levels of genetic differentiation among populations of species of *Abies* from southern Mexico and Guatemala. *American Journal of Botany*, **87**, 362–371.

Aguirre-Planter E., Jaramillo-Correa, J., Gómez-Acevedo, S., Khasa, D.P., Bousquet, J., Eguiarte, L.E., Phylogeny, diversification rates and species boundaries of Mesoamerican firs (*Abies,* Pinaceae) in a genus-wide context. *Molecular Phylogenetics and Evolution*. **62**, 263-274.

Bernal-Salazar, S. & Terrazas-Salgado, T. (2000) Influencia climática sobre la variación radial de caracteres anatómicos de madera en *Abies religiosa*. *Madera y Bosques,* **6**, 73-86.

Bobbink, R., Heil, G.W. & Verduyn, B. (2003). Ecology and Man in Mexico's Central Volcanoes Area, G.W. Heil, R. Bobbink & N.T. Boix (Ed.), Dordrecht, The Netherlands: Kluwer Academic Publishers.

Byrne, R. (1982) Preliminary pollen analysis of Deep Sea Drilling Project Leg 64, Hole 480, cores 1-11. In: R. Curray and D.G. Moore, Editors, *Initial Reports of the Deep Sea Drilling Project*. **64**, U.S. Govt. Printing Office, Washington. 1225–1237 Pt. 2.

Calvert, W. H. & Brower, L. P. (1986) The location of the monarch butterfly (*Danaus plexippus L.*) overwintering colonies in Mexico in relation to topography and climate. *Journal of the Lepidoptera Society*, **40**, 164-187.

Cavazos, T. & Hastenrath, S. (1989). Convection and rainfall over Mexico and their modulation by the Southern Oscillation, *International Journal of Climate*, **10,** 377-386.

Chiang, J.C.H. (2010). Extraction of PMIP2 mid-Holocene and LGM anomalies for use in WORLDCLIM. Unpublished raw data (see Appendix 5 for methods).

Clisby, K.H. & P.B. Sears, (1955) Palynology in southern North America, 3: Microfossil profiles under Mexico City correlated with the sedimentary profiles, *Bulletin of the Geological Society of America*, **66**, 511–520.

D. Alvarado, de Bauer, L.I., J. Galindo, A. (1983) Decline of sacred fir (*Abies religiosa)* in a forest park south of Mexico City. *Environmental Pollution.* **80**, 115-121.

Douglas, MW, Maddox, RA, Howard, K., & Reyes, S. (1993) The Mexican Monsoon. *The Journal of Climate*, **6**, 1665-1677.

Elith, J., Graham, C. H., Anderson, R. P., Dudík, M., Ferrier, S., Guisan, A., Leathwick, J. *et al.* (2006) Novel methods improve prediction of species' distributions from

occurrence data. *Ecography* **29**, 129-151.

Elith, J., Phillips, S.J., Hastie, T., Dudík, M., Yung, E.C. & Yates, C.J. (2011) A statistical explanation of MaxEnt for ecologists. *Diversity and Distributions* **17**, 43–57.

http://www.gbif.org (See full citation in Appendix 3)

García, S., Durant McArthur, E., Pellicer, J., Sanderson, S.C., Valles, J., & Garnatje, T. (2011). A molecular phylogenetic approach to western North America endemic *Artemisia* and allies (*Asteraceae):* untangling the sagebrushes. *American Journal of Botany,* **98**, 638-654.

González Quintero, L. (1986). Análisis polinico de los sedimentos. In ‘‘Tlapacoya, 35,000 años de historia del lago de Chalco’’ (J. L. Lorenzo and L. Mirambell, Eds.) Coleccion Cientifica No. 115, pp. 113–132.

Gordon A.G. (1968) Ecology of *Picea chihuahuana* Martínez. *Ecology*, **49**, 880–896.

Graham, A. (1993) Historical factors and biodiversity in Mexico. *In* T. P. Ramammoorthy, R. Bye, A. Lot, and J. Fa [eds.], Biological diversity of Mexico: origins and distribution, 109–127. Oxford University Press, New York, New York, USA.

Hijmans, R.J., S.E. Cameron, J.L. Parra, P.G. Jones and A. Jarvis (2005) Very high resolution interpolated climate surfaces for global land areas. *International Journal of Climatology*, **25**, 1965-1978.

Huntley, B. (1991) How plants respond to climate change: migration rates, individualism and the consequences for plant communities *Annals of Botany,* **67,** 15-22.

Jaramillo-Correa JP, Beaulieu J, Ledig FT & Bousquet, J. (2006) Decoupled mitochondrial and chloroplast DNA population structure reveals Holocene collapse and population isolation in a threatened Mexican-endemic conifer. *Molecular Ecology,* **15**, 2787-2800

Jaramillo-Correa J.P., Aguirre-Planter E, Khasa D.P., Eguiarte L, Piñero D, Furnier G.R., & Bousquet, J. (2008) Ancestry and divergence of subtropical montane forest isolates: molecular biogeography of the genus *Abies* (Pinaceae) in southern Mexico and Guatemala. *Molecular Ecology*, **17**, 2476-2490.

Lauer, W. (1978) Timberline studies in central Mexico. *Arctic and Alpine Research,* **10**, 383-396.

Ledig FT, Hodgskiss P.D., Krutovskii K.V., Neale D.B., & Eguiluz Piedra, T. (2004) Relationships among the spruces (*Picea, Pinaceae*) of southwestern North America. *Systematic Botany*, **29**, 275–292.

Leopold A.S. (1950) Vegetation zones of Mexico. *Ecology*, **31**, 507–518.

Little, E.L., Jr. (1971) Atlas of United States trees, volume 1, conifers and important hardwoods: U.S. Department of Agriculture Miscellaneous Publication 1146, 9 p., 200 maps.

Liu, C., Berry, P.M., Dawson, T.P., & Pearson, R.G. (2005) Selecting thresholds of occurrence in the prediction of species distributions. *Ecography,* **28**, 385–393.

Lozano-García, M.S., Ortega-Guerrero, B., Caballero-Miranda, M. & Urrutia-Fucugauchi, J. (1993) Late Pleistocene and Holocene paleoenvironments of Chalco Lake, central Mexico. *Quaternary Research*, **40**, 332–342.

Lozano García, S. & Xelhautzi, S. (1997) Some problems in the late Quaternary pollen records of central Mexico: Basin of Mexico and Zacapu. *Quaternary International*, **43/44**, 117–123.

Lozano-García, S., Sosa-Nájera, S., Sugiura, Y. & Caballero, M. (2005) 23,000 yr of vegetation history of the Upper Lerma, a tropical high-altitude basin in Central Mexico. *Quaternary Research*, **64**, 70–82.

Luna-Vega, I., Alcántara Ayala, O., Espinosa Organista, D., & Morrone, J.J. (1999) Historical relationships of the Mexican cloud forests: a preliminary vicariance model applying parsimony analysis of endemicity to vascular plant taxa. *Journal of Biogeography*, **26**, 1299–1305.

Martin, P.S. & Harrell, B.E. (1957) The Pleistocene history of temperate biotas in Mexico and eastern United States. *Ecology*, **38**, 468-480.

McMillan, C. (1974) Differentiation in habitat response in *Taxodium distichum, Taxodium mucronatum, Platanus occidentalis*, and *Liquidambar styraciflua* from the United States and Mexico. *Plant Ecology,* **29**, 1-10.

Metcalfe, S.E., Bimpson, A., Courtice, A.J., O'Hara, S.L. & Taylor, D.M. (1997) Climate change at the monsoon/westerly boundary in northern Mexico. *Journal of Paleolimnology*, **17**, 155–171.

Metcalfe, S. E., S. L. O'Hara, M. Caballero, & Davies, S.J. (2000) Records of late Pleistocene–Holocene climatic change in Mexico—A review. *Quaternary Science Review*, **19,** 699–721.

Meyer, E.R. (1973). Late-Quarternary Paleoecology of the Cuatro Cienegas Basin, Coahuila, Mexico. *Ecology*, **54**, 982-995.

Mosiño, P. A. & García, E., (1974) The Climate of Mexico. World Survey of Climatology. Climates of North America. R. A. Bryson and F. K. Hare (editors). London: Elsevier **11**, 345–404.

E1-Moslimany, A.P. (1990) Ecological significance of common nonarboreal pollen: examples from drylands of the Middle East, *Review of Paleobotany and Palynology,* **64**, 343-350.

Muñoz-Jiménez, J., Rangel-Rios, K. & García-Romero, A. (2005) Plant colonization of recent lahar deposits on Popocatepetl Volcano, Mexico. *Physical Geography.* **26**, 192-215

Newton, A. C., L. Cayuela, C. Echeverría, J. J. Armesto, R. F. Del Castillo, D. Golicher, D. Geneletti, M. Gonzalez-Espinosa, A. Huth, F. López-Barrera, L. Malizia, R. Manson, A. Premoli, N. Ramírez-Marcial, J. Rey Benayas, N. Rüger, C. Smith-Ramírez, and G. Williams-Linera. 2009. Toward integrated analysis of human impacts on forest biodiversity: lessons from Latin America. *Ecology and Society* **14**, [online] URL: http://www.ecologyandsociety.org/vol14/iss2/art2/

Pearman, P.B., Guisan, A., Broennimann, O. & Randin, C.F. (2008) Niche dynamics in space and time. *Trends Ecology and Evolution*, **23**, 149–158.

Phillips, S. J., Anderson, R. P. & Schapire, R.E. (2006) Maximum entropy modeling of species geographic distributions. *Ecological Modelling*. **190**, 231-259.

Prentice, I.C., Guiot, J. & Harrison, S.P. (1992) Mediterranean vegetation, lake-levels and palaeoclimate at the Last Glacial Maximum. *Nature*, **360**, 658–660.

Rzedowski, J. 1978. Vegetación de México. Mexico DF (Mexico): Editorial Limusa.

Schultz, D.M., Bracken, W.E. & Bosart, L.F. (1998) Planetary- and synoptic-scale signatures associated with Central American cold surges. *Monthly Weather Review*, **126**, 5–27.

Straka, H. & Ohngemach, D. (1989) Late Quaternary vegetation history of the Mexican highland. *Plant Systematics and Evolution,* **162,** 115-32.

Subally, D & Quézel, P. (2002) Glacial or interglacial: *Artemisia*, a plant indicator with dual responses, *Review of Palaeobotany and Palynology* **120**, 123–130.

Thompson R.S., Anderson K.H. & Bartlein, P.J. (2008) Quantitative estimation of bioclimatic parameters from presence/absence vegetation data in North America by the modern analog technique. *Quaternary Science Review,* **27**,1234–1254

Villers-Ruiz, L., Rojas-Garcia, F., & Tenorio-Lezama, P. (2006) Guía de Botánica del Parque Nacional Malinche, Tlaxcala-Puebla. UNAM.

Watts,W.A. & Bradbury, J.P. (1982) Paleoecological studies at Lake Patzcuaro on the west-central Mexican Plateau and at Chalco in the basin of Mexico, *Quaternary Research*, **17**, 56-70.

Williams J.W., Jackson S.T. & Kutzbach J.E. (2007) Projected distributions of novel and disappearing climates by 2100 AD. *Proceedings of the National Academy of Sciences.* **104**, 5738-5472.

Xiang, Q.P, Xiang, Q.Y., Guo, Y.Y., Zhang, X.C. (2009) Phylogeny of *Abies* (Pinaceae) inferred from nrITS sequence data, Taxon, **58,** 141-152.

Woodward, F.I. (1987) Climate and plant distribution, Cambridge, Cambridge University Press.

Woodward, F.I. & Beerling, D.J. (1997) The dynamics of vegetation change: health warnings for equilibrium 'dodo' models. *Global Ecology Biogeography Letters*, **6**, 413–418.

3. CHAPTER THREE

Mid-Holocene distribution of five climatically sensitive plant species in central and northwestern Mexico

INTRODUCTION

The five species discussed in Chapter Two are often present in Mexican pollen diagrams covering the mid-Holocene and/or the Last Glacial Maximum (LGM). In this chapter, I present the Maxent model results for the five species under mid-Holocene climatic conditions defined by the GCM's discussed in Chapter Two.

Mid-Holocene climate change is reasonably well understood as having been driven by orbital (precessional) forcing. In addition, several Mexican pollen diagrams include the mid-Holocene and therefore provide a basis for testing climate simulations. Although the mid-Holocene was once thought to be a time period of higher global temperatures (compared to the present), it is now accepted that only northern hemisphere summer temperatures were higher than they are today (Kerwin *et al.,* 1999).

METHODS

As already discussed in Chapter Two, MaxEnt was used to model present-day distribution of each of the five species. MaxEnt also has a feature (not discussed in Chapter Two) through which a model trained on one set of environmental layers can be "projected" by applying it to another set of environmental layers. This process, in MaxEnt terminology, is called 'projection'. The process is useful to any study that is attempting to either predict or hindcast scenarios in different environmental settings. Although projection is a useful way to visualize ecological change under different environmental conditions, it does have limitations. These are detailed in Appendix 1.

Unlike Chapter Two, which focused on present-day climate, the mid-Holocene climate models used in this chapter are WorldClim variables which were adjusted based on the results of a multivariate Empirical Orthogonal Function (EOF) method applied across nine oceanic-atmospheric paleoclimate models (Chiang, unpublished, see Appendix 2 and Table 3). It is necessary to describe the importance of this step.

Ecological models are typically generated using only one collection of climate data, usually extracted from oceanic-atmospheric models. While this is a good way to approximate the climate to arrive at a species distribution, it does not tell the whole story. Because multiple climate models exist, it may be worthwhile to consider all the models. The additional step I am incorporating here essentially compares and combines multiple climate models to arrive at an "average" climate model. In order to find this "average", it is necessary to compare all the models and find a common response among them.

The purpose of the EOF analysis is to extract this common response across all the

available climate models. The projection of each model onto the leading EOF is has comparable magnitude and the same sign, verifying a common climatic response among the models (Chiang unpublished). However, the projection of the leading EOF onto each climate model is not quite the same, which implies subtle differences among the climate models. In this chapter, I have considered only the average response of all the models' anomalies. It is important to bear in mind that the resulting "climate model" I am using is merely one realization of the climate during the mid-Holocene. Given the models in the EOF analysis, there are potentially nine separate realizations that can be incorporated into the model, each of them ultimately yielding a slightly different ecological model. The extremes of these realizations provide an opportunity to observe the range of sensitivity of the ecological model, which I discuss later in this chapter.

Finally, in terms of the mid-Holocene climate, the leading component for each model is most likely the effect of changes in Earth's orbital parameters during the mid-Holocene.

RESULTS AND DISCUSSION

The modeled mid-Holocene climates summarized in Figures 3.1 to 3.4. In general, the models suggest mid-Holocene winters (Figure 3.3) that were slightly cooler (on the order of 0.3º to 1º C) throughout Mexico, and wetter, with exceptions in the southern areas. Differences in summer precipitation are more obvious (Figure 3.2), however, and should be noted when interpreting the pollen evidence. Finally, the modeled summer temperatures show generally higher mean temperatures compared to the present, although in southern Mexico, the modeled summer temperatures are slightly cooler (a maximum difference of 1.1º C, see Figure 3.4).

The MaxEnt species distribution maps are shown in Figures 3.5 to 3.10. Bivariate graphs comparing relevant temperature and precipitation variables for the climate envelopes during the mid-Holocene are also included in Figures 3.11 to 3.15. Two maps illustrating a range of sensitivity have been generated for *Liquidambar styraciflua* to demonstrate the importance of the climate data source (Figures 3.16a and 3.16b). Figures 3.19 to 3.23 illustrate the overall changes in modeled distribution between 6K and 0K BP. Figure 3.22 is a map of the five predicted species distributions over a hypothetical transect from the Gulf coast to the Valley of Mexico during the mid-Holocene.

Abies religiosa

The projected mid-Holocene distribution for *Abies religiosa* during the mid-Holocene is shown in Figure 3.5. The variables used to construct the map, and their approximate contributions to the present-day models, according to MaxEnt, are in Table 2.1b. The projection to the mid-Holocene is supported by the accuracy of the present-day model.

There are populations around the eastern peaks of Pico de Orizaba and Cofre de Perote, and around high elevations in the central regions, specifically throughout Mexico and Tlaxcala. It is notable that the predicted areas of distribution in the high elevations appear more expansive than present-day distribution (Figure 2.15).

González-Quintero's pollen diagram from Tlapacoya, in the Valley of Mexico

(González-Quintero, 1986), shows an increase in deciduous taxa in the mid-Holocene which suggests more humid conditions. Lozano-Garcia *et al.'s* study from Chalco (1993) illustrates a potential conflict between the diatom and pollen records in the Valley of Mexico. Their pollen record indicates that *Abies* was present in the mid-Holocene and that *Quercus* increased while *Pinus* decreased (Lozano-Garcia *et al.*, 1993). However diatom evidence suggests ongoing drying beginning before the mid-Holocene (Bradbury, 1989).

Lozano-Garcia & Ortega-Guerrero's in a later paper reporting on the research at Chalco and Texcoco (1998) also suggests that *Abies* was present in the Valley of Mexico during the mid-Holocene, albeit in small amounts (<1-2%). They also concluded that increases in *Alnus, Abies* and *Quercus* were the result of drier conditions due to warmer annual temperatures during the mid-Holocene. However, rises in *Abies* and *Alnus* may also indicate a wetter but warm environment, rather than a dry one. Furthermore, the latter interpretation is supported by the high-resolution mid-Holocene climate model, which suggests enhanced summer precipitation compared to today (Figure 3.1).

Straka & Ohngemach (1989), in their Tlaloqua record from Volcan Malinche shows a gradual decrease and disappearance of *Picea* slightly after 8500 BP. This is followed by a slow increase in *Abies* with a concurrent rise in other mesophytic taxa such as *Liquidambar, Fagus,* and *Carpinus*. The presence of the mesophytic taxa is additional evidence supporting a wet and slightly warmer mid-Holocene in the TMVB. As the percentage of *Abies* increases, its persistence may be due to a tolerance to warming conditions. *Picea* may not have been able to compete with *Abies* in these warmer conditions.

At the Guanajuato sites of San Nicolas and Rincon de Parangueo, Park *et al.,* (2005) found pollen evidence suggestive of a wetter climate throughout the early to mid-Holocene. Conserva (2003) also suggests that increases in *Quercus, Alnus* and *Abies* in the early Holocene (Hoya de Alberca, Guanajuato) may be indicative of a wetter climate. Watts & Bradbury (1982) also imply that drying may have occurred only after the mid-Holocene mark, i.e. around 5000 BP. Although mid-Holocene summers were more likely wetter than summers today, it is more likely to have been the case based on both orbital parameters and the fossil data, the model here shows a modest expansion in *Abies* compared to the modern distribution, and this reconstruction is supported by the fossil pollen records.

Picea chihuahuana

MaxEnt suggests a mid-Holocene *Picea* distribution (Figure 3.8) similar to the present-day (Figure 2.4) throughout the Sierra Madre Occidental. The model also shows *Picea* reaching to lower elevations on the western slopes of the Sierra Madre Occidental. Despite *Picea* reaching to lower elevations, the MaxEnt prediction is not exactly in agreement with, Ortega-Rosas *et al's* (2008) pollen diagram from the Sierra Madre Occidental (Figure 3.18). It shows *Picea* pollen in the mid-Holocene in small amounts (2% or less) at elevations around 1900 m. MaxEnt predicts *Picea* within 35 km of Ortega-Rosas *et al's* pollen site. The lack of exactness in MaxEnt may be due to inaccurate environmental variable selection or the inability of MaxEnt to account for the microclimatic influence on *Picea's* distribution. In the Sierra Madre Occidental, *P.*

chihuahuana grows in cool canyons (barrancas) that are difficult to define using only the climate model data, even with the downscaled data used in the model here. A finer scale study may help to isolate the barrancas.

There are several small populations of *Picea chihuahuana* in the Sierra Madre Occidental. Very little pollen evidence supports the idea that *Picea* covered larger areas during the mid-Holocene in the Sierra or the TMVB, although Lozano-Garcia & Ortega-Guerrero (1993) report *Picea* pollen in the Valley of Mexico during the early Holocene. Similarly, Ortega-Rosas *et al.* (2008) have shown that *Picea* did occur in the Sierra Madre Occidental at lower elevations during the mid-Holocene, perhaps aided by a wetter climate. The wetter conditions during the mid-Holocene may account for the presence of *Picea* in the TMVB, although there is no pollen evidence of *Picea*'s presence there after 8500 BP. Ledig *et al.* (2010) investigated future climate change scenarios for *Picea* using a different modeling method, and found that some regions in the eastern TMVB will have climatic conditions suitable for *Picea.* While mid-Holocene climate is different than a future climate change scenario, both models suggest that *Picea* can potentially grow in the eastern TMVB under slightly warmer and presumably wetter conditions. Most inferences have suggested that post-glacial warming alone is to blame for *Picea's* demise, however a cool and wet early Holocene should have, at least in theory, helped *Picea* persist longer than it did in the eastern TMVB. Furthermore, the abrupt disappearance of *Picea* in the eastern TMVB around 8500 BP (Straka & Ohngemach, 1989) coincides with the 8200 BP cold event in the north Atlantic. The sudden influx of very cold water into the Gulf is an event whose impacts on Mexico are not clearly understood (Alley *et al.,* 1997).

Finally, Lozano-Garcia & Ortega-Guerrero (1998) report *Picea* in the mid-Holocene sections of cores from Chalco and Texcoco, evidence that supports the model results presented here. This is the only pollen evidence indicating that *Picea* was present during the mid-Holocene.

Artemisia ludoviciana

The MaxEnt predicted distribution for *Artemisia ludoviciana* for the mid-Holocene shows a slight contraction of range in the north central highlands compared to the present, with very little change in central Mexico (Figure 3.6). *Artemisia* pollen is often considered an indication of dry summers and cool winters. One problem with the MaxEnt predictions for both the mid-Holocene and the present is that they do not show *Artemisia* in northwestern Mexico. *Artemisia* pollen is reported in diagrams from northwest sites, both in the present and the mid-Holocene, albeit in low percentages, between 1-4% (Ortega-Rosas *et al.,* 2008; Byrne 1982). The unsatisfactory MaxEnt results may be due to clustering in the herbarium data, and further subsampling and stratifying of data could address clustering issues in MaxEnt. Also, additional field sampling in the northern regions would strengthen the present-day distribution, which in turn affects the projected distributions. Another possibility is that the *Artemisia* pollen in the northwest represents species other than *Artemisia ludoviciana.*

Artemisia is present in the mid-Holocene sections of several central Mexican pollen diagrams, including the long Patzcuaro record (Watts & Bradbury, 1982), the Upper Lerma (Lozano-Garcia *et al.,* 2005), and the Tlaloqua site in the state of Puebla (Straka &

Ohngemach, 1989). Straka & Ohngemach (1989) interpret *Artemisia* in the Pleistocene section of the Tlaloqua diagram as evidence of a "species-rich herb/grassland" characteristic of dry alpine conditions, and that toward the end of the Pleistocene, *Artemisia* declined as summer precipitation and temperature increased. The late Pleistocene decline is also apparent at Patzcuaro (Watts & Bradbury, 1982) the Gulf of California (Byrne, 1982), both of which clearly show the decline of *Artemisia* approximately 10000 BP.

There is little difference between the present-day and mid-Holocene predicted distribution of *A. ludoviciana*: the present distribution is slightly expanded relative to the mid-Holocene. According to the mid-Holocene climate projection used in MaxEnt shows average summer temperatures in highlands were warmer during the mid-Holocene, particularly in the east. The shift to lower summer temperatures in the northeast highlands during the late Holocene may have contributed to the change in distribution that we see today.

Liquidambar styraciflua

The last three pollen types discussed (*Picea, Abies* and *Artemisia*) are primarily indicators of cool climates with differences in moisture sensitivity. *Picea, Abies* and *Artemisia* are typically important during glacial periods of the late Pleistocene and then decrease significantly or disappear during the Holocene. As an interglacial begins, pollen types indicative of warmer climates begin to appear. Depending on how much moisture is available, mesophytic taxa may also appear. *Liquidambar styraciflua* is one such mesic species, and is particularly prominent in the present-day Mexican cloud forest.

L. styraciflua's modeled mid-Holocene distribution is shown in Figure 3.7. The difference between the mid-Holocene projection and the present distribution suggests a contraction in the *L. styraciflua* range since the mid-Holocene. The differences are more prominent in the southern regions of Mexico and parts of Guatemala, due to more prominent warming and drying in the south than in the east since the mid-Holocene. The mid-Holocene models of the eastern distribution of *L. styraciflua* are close to the present-day distribution.

Several pollen diagrams from central Mexico show low percentages of *L. styraciflua* during the mid-Holocene. González-Quintero (1986) identified *Liquidambar* to be present in the mid-Holocene. This is interesting because there is no cloud forest in the Valley of Mexico. However, it is possible that *Liquidambar* pollen at Tlapacoya is due to long-distance dispersal. & Ohngemach (1989) also report a low percentage of *L. styraciflua* during the mid-Holocene in their Tlaloc I core. Lozano-Garcia's diagram from the Chalco core (Lozano-Garcia & Ortega-Guerrero, 1998) contained *L. styraciflua* during the mid-Holocene. Lozano-Garcia, *et al.* (2005) also document an appearance of a mesophytic assemblage including *Liquidambar* at the Upper Lerma site in Central Mexico during the late Pleistocene, but the assemblage is not present during the mid-Holocene.

In brief, MaxEnt suggests a more extrusive distribution for areas clarified as cloud forest (Rzedowski, 1975) *L. styraciflua* during the mid-Holocene, but there is no pollen evidence to confirm or refute this prediction. The Taloquoa diagram suggests that *L. styraciflua* may have been growing in the area, but long-distance dispersal is also a

possibility.

Taxodium mucronatum

Taxodium mucronatum has a wide distribution in Mexico and is common in riparian areas within the TMVB, and the south near Oaxaca. It also appears in riparian ravines in northwestern Mexico (Rzedowski, 1975).

The MaxEnt mid-Holocene distribution is shown in Figure 3.9. It shows a reduced range in the distribution compared to the present-day, but most notably, an absence throughout the Valley of Mexico. Not surprisingly, most of the Valley of Mexico is above 2300 m.

As discussed in Chapter Two, the present-day MaxEnt results are not in close agreement with either the herbarium data or previously mapped estimates of *T. mucronatum.* Given the poor result for the present, the projection of the MaxEnt present-day envelope into past conditions is less reliable as well. Although there are no detailed discussions about the distribution of *T. mucronatum* during the mid-Holocene in central Mexico, it is unlikely that *T. mucronatum* disappeared entirely. Watts and Hansen's diagram from Lake Tulane in Florida shows *T. distichum* dwindling almost to almost zero in the early Holocene and appearing increasing during the late Holocene (Watts & Hansen, 1994).

Taxodium pollen is easily confused with *Cupressus* and *Juniperus* pollen, and as a result this pollen type is often reported as TCT (*Taxoodiaceae, Cupressaceae, Taxaceae*). Because the types are similar, conclusive evidence regarding *Taxodium's* presence based on fossil pollen records is uncertain. On the other hand, the absence of this pollen type strongly suggests that the *Taxodium* is not present.

MaxEnt's difficulty in modeling *T. mucronatum's* present and past distributions is attributable to several factors covered in Chapter 2. One is that *T. mucronatum* is a riparian species and is therefore not directly dependent on rainfall for its water supply. This is not taken into account in MaxEnt, which only includes macroclimatic variables. The net result is the model will predict the species to be present in areas with low rainfall and no appropriate riparian habitat.

On the other hand, temperature controls of the *T. mucronatum* distribution are clearly evident. Figure 3.15 illustrates the parameters within which MaxEnt modeled *T. mucronatum.* The results show a mean winter temperature range between 15° and 22° C, and a clearly defined range of values for precipitation seasonality.

Despite the apparent failure of the MaxEnt model to accurately model *T. mucronatum's* distribution, a few locations within the resulting maps (Figure 3.10) do show a close adherence to river valleys. Given these small successes, future attempts to incorporate hydrological data into the MaxEnt model alongside climate variables may yield much better results.

A second potential reason that the MaxEnt model has not effectively predicted *T. mucronatum's* distribution may lie in the choice of environmental variables for the climate envelope. However, the climate envelope is unlikely the main reason for the poor prediction. The incorporation of hydrological data remains more important and its incorporation may vastly improve the model output.

Range of Sensitivity: *Liquidambar*

The final point in this discussion focuses on the potential differences in MaxEnt models based on different climate realizations (discussed earlier). Using climate data based on a maximum and minimum PC loading (Appendix 2), two such realizations were used to generate two distinct MaxEnt models for *Liquidambar* (Figures 3.16a and 3.16b). Although the WorldClim climate variables used for the both models are identical, the resulting maps are slightly different, with the map from a minimum PC loading *Liquidambar's* presence slightly further south than the map generated using the maximum PC loading. While the differences are subtle in this case, they do illustrate how the different climate models can affect model predictions. This is an important finding that is rarely addressed in species distribution model discussions.

CONCLUSIONS

In this chapter, I present mid-Holocene distribution maps for five climatically sensitive species in Mexico. Based on the results, I draw the following conclusions:

1. The inaccuracies in the MaxEnt models for the present-day distribution of *T. mucronatum* and *A. ludoviciana* in Chapter 2 are clearly relevant to the mid-Holocene projections. The model results for *A. ludoviciana* are not in full agreement with the pollen record, while *T. mucronatum's* model is difficult to confirm, because of limited pollen data and the difficulty of distinguishing *Taxodium* pollen from that of other members of the *Taxaceae, Cupressesaceae* and *Taxodiaceae* families. In the model presented here, *T. mucronatum* appears to disappear completely from central Mexico during the mid-Holocene, although this is difficult to fathom, since it has a wide distribution in Mexico today.

2. The mid-Holocene distribution for *L. styraciflua* matches the general distribution of present-day cloud forest as defined by Rzedowski (1975). The Tlaloqua diagram suggests that this species was growing on volcan Malinche (Straka & Ohngemach, 1989), and pollen diagrams from sites outside the cloud forest (González-Quintero, 1986; Bradbury, 1989; Lozano-Garcia, 1993) also show *Liquidambar* in the mid-Holocene. Reports of *Liquidambar* pollen in small amounts from areas outside its present distributions may be attributable to long distance dispersal.

3. According to MaxEnt, *P. chihuahuana* was widely distributed during the mid-Holocene in central Mexico. However, its disappearance in the Tlaloqua diagram (Straka & Ohngemach, 1989) refutes this possibility. Lozano-Garcia & Ortega-Guerrero (1998) report *Picea* during the mid-Holocene (Chalco and Texcoco). Ledig *et al.*'s (2010) recent conservation projections for future warming scenarios also suggest a future presence of *Picea* in the Valley of Mexico, raising the question of whether or not *Picea* can thrive in the region under slightly warmer conditions. The question is interesting because *Picea* is

rare in Mexico, and an important candidate for conservation efforts (Ledig *et al.,* 2010).

4. The mid-Holocene result for *Abies religiosa* illustrates a modest expansion in distribution. This result is supported by the pollen data, particularly Conserva's report of *Abies* pollen at Alberca, Guanajuato (2003). The Tlaloqua diagram (Straka & Ohngemach, 1989) also shows a slow increase in mesophytic taxa appearing concurrently with *Abies* during the early and mid-Holocene.

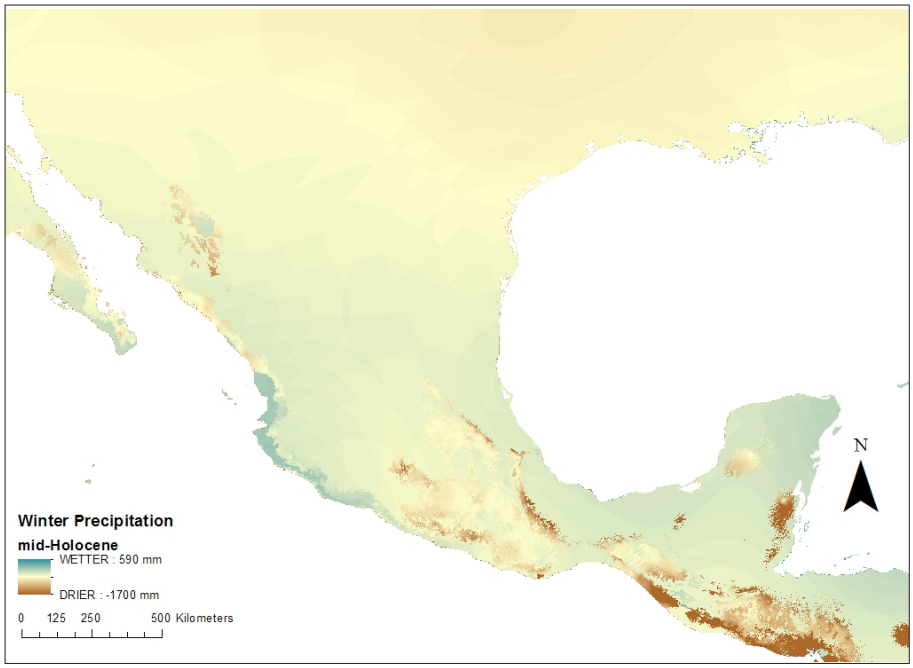

Figure 3.1: Differences in winter precipitation during the mid-Holocene, based on climate models.

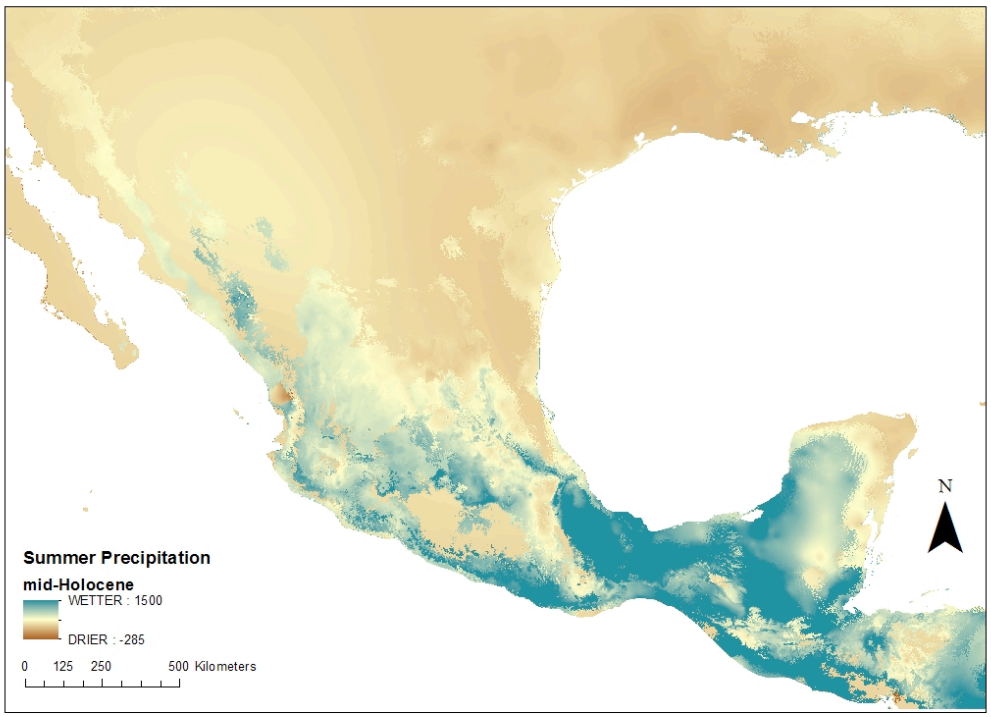

Figure 3.2: Differences in summer precipitation during the mid-Holocene, based on climate models

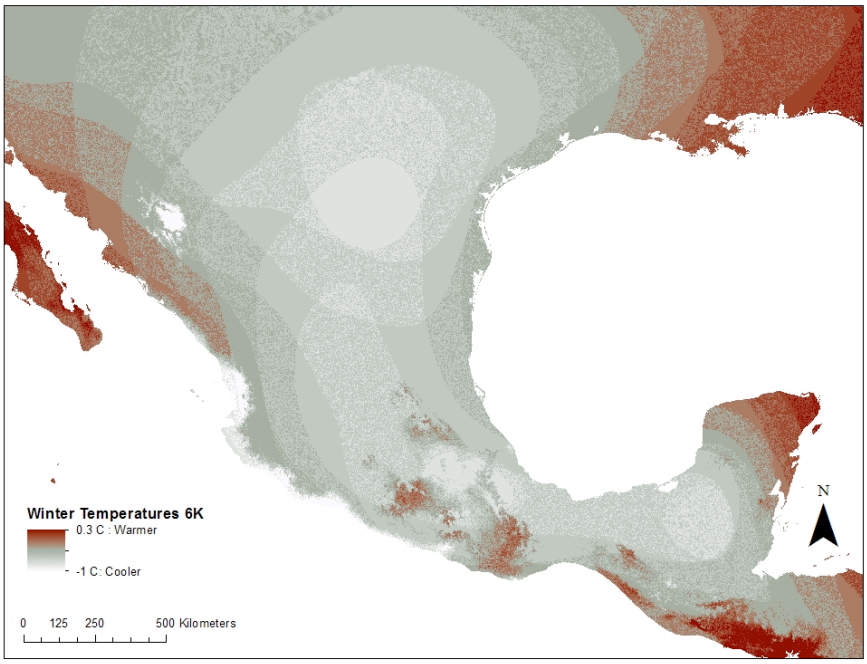

Figure 3.3: Differences in winter temperatures during the mid-Holocene (compared to the present), based on climate models.

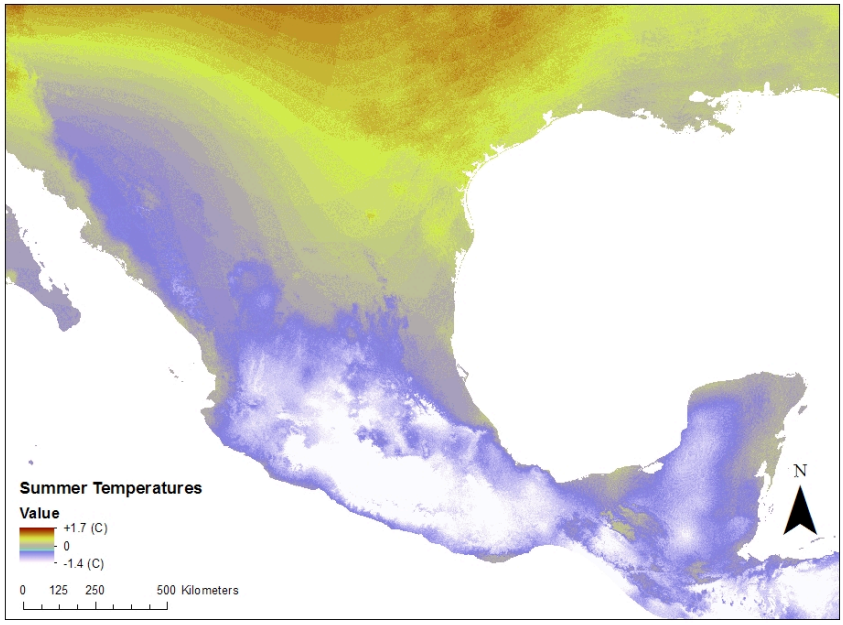

Figure 3.4: Differences in summer temperatures during the mid-Holocene (compared to the present), based on climate models

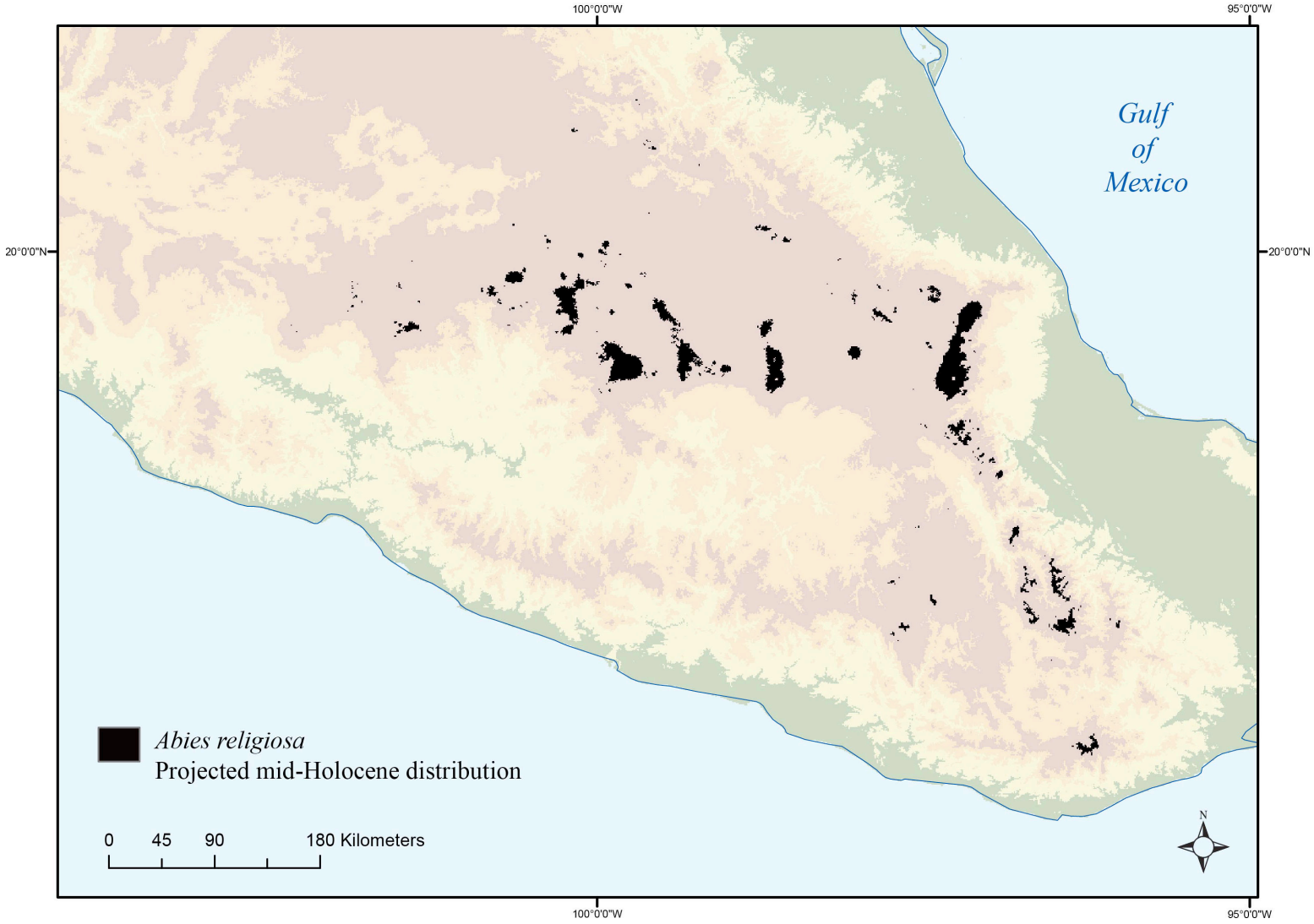

Figure 3.5: Projected mid-Holocene distribution for *Abies religiosa*

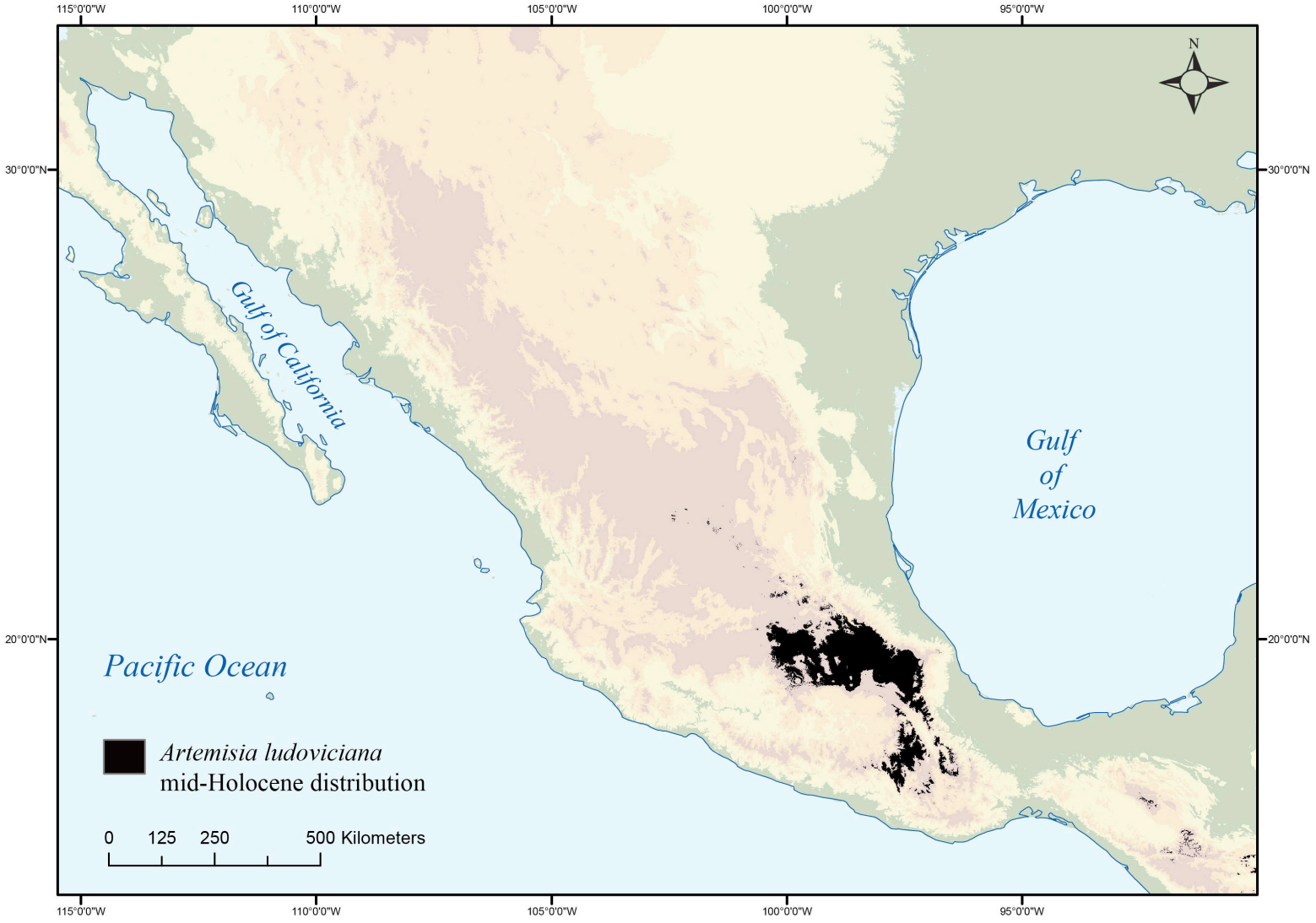

Figure 3.6: Projected mid-Holocene distribution for *Artemisia ludoviciana*

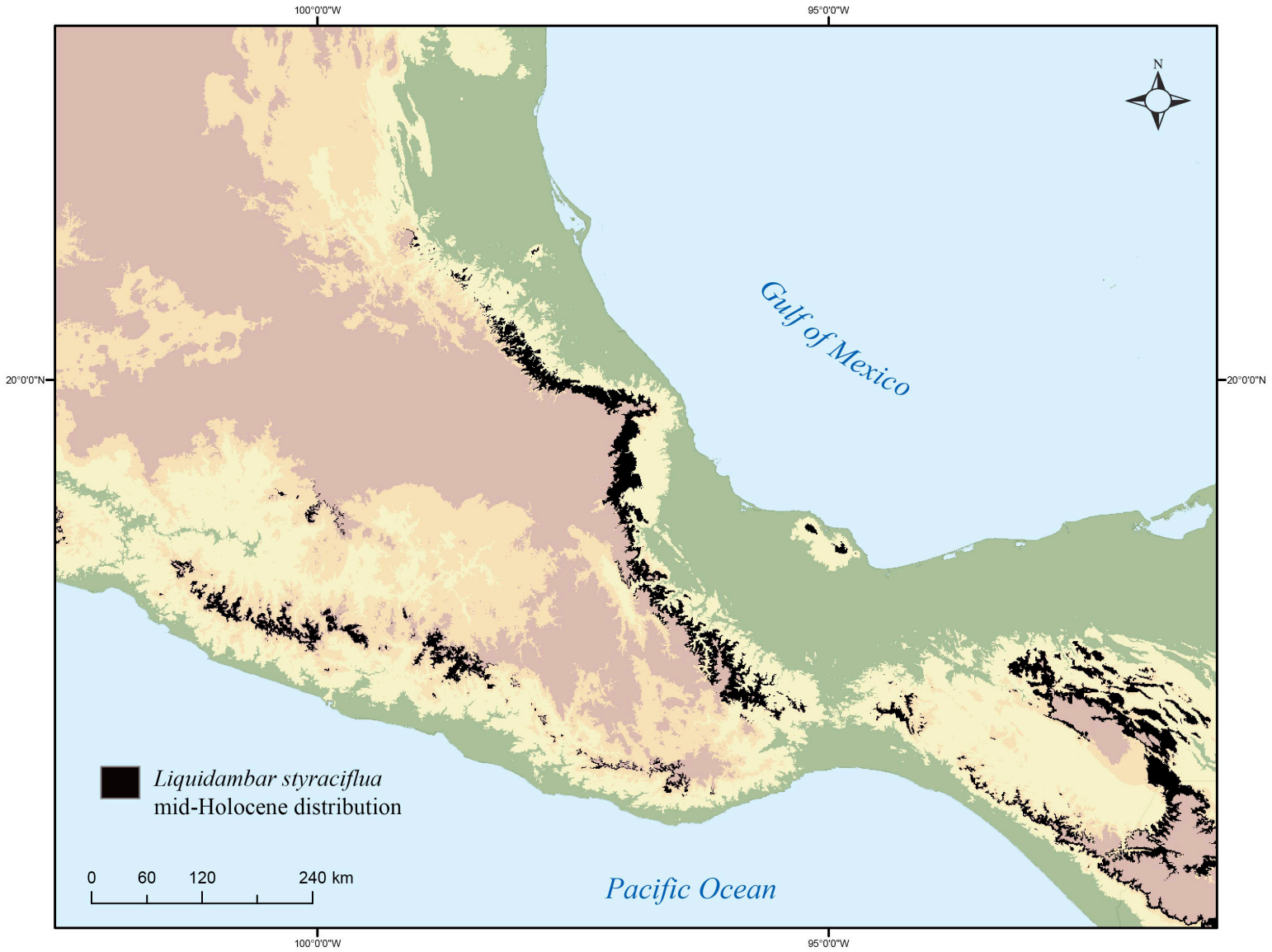

Figure 3.7: Projected mid-Holocene distribution –*Liquidambar styraciflua*

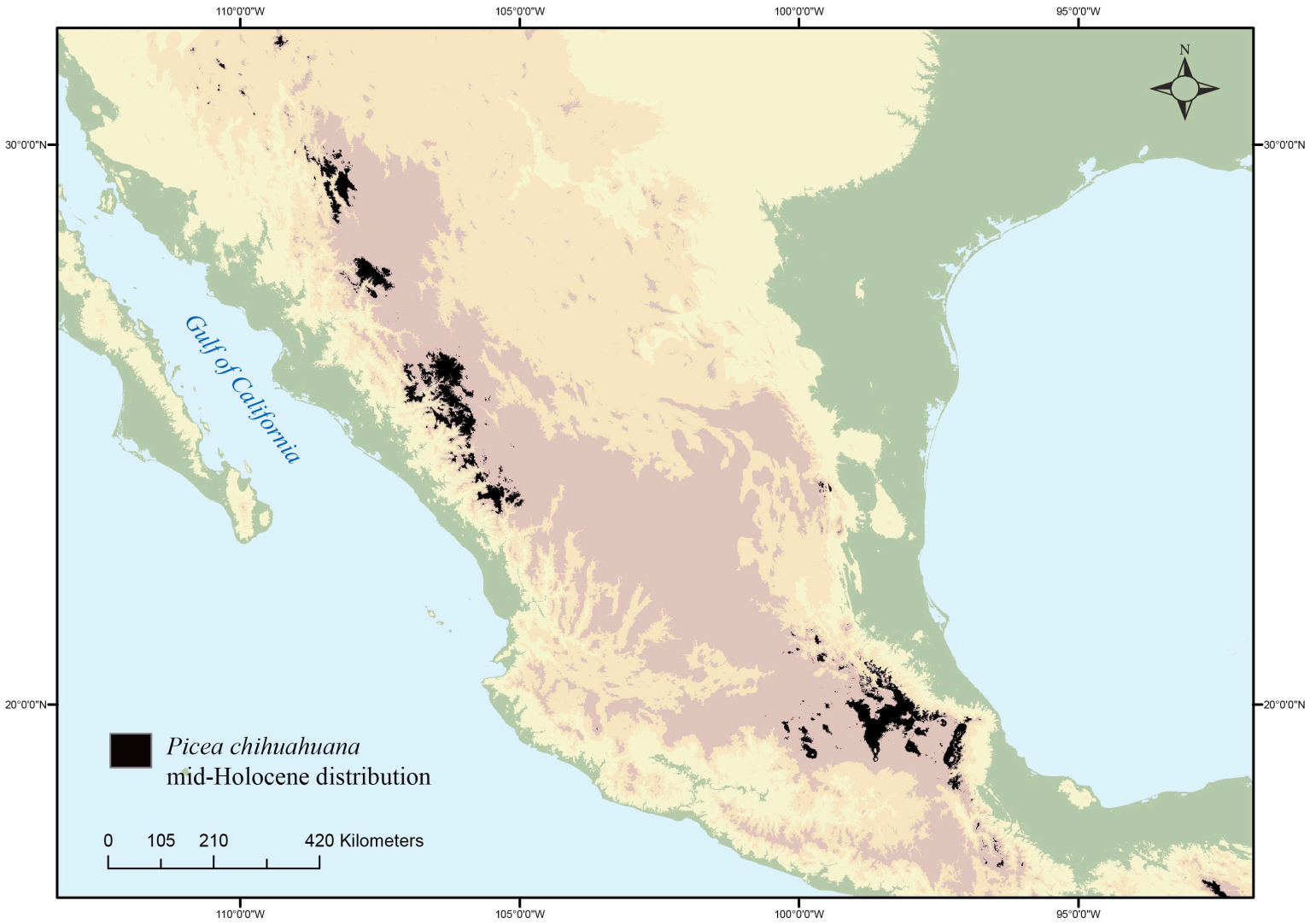

Figure 3.8: Projected mid-Holocene distribution –*Picea chihuahuana*

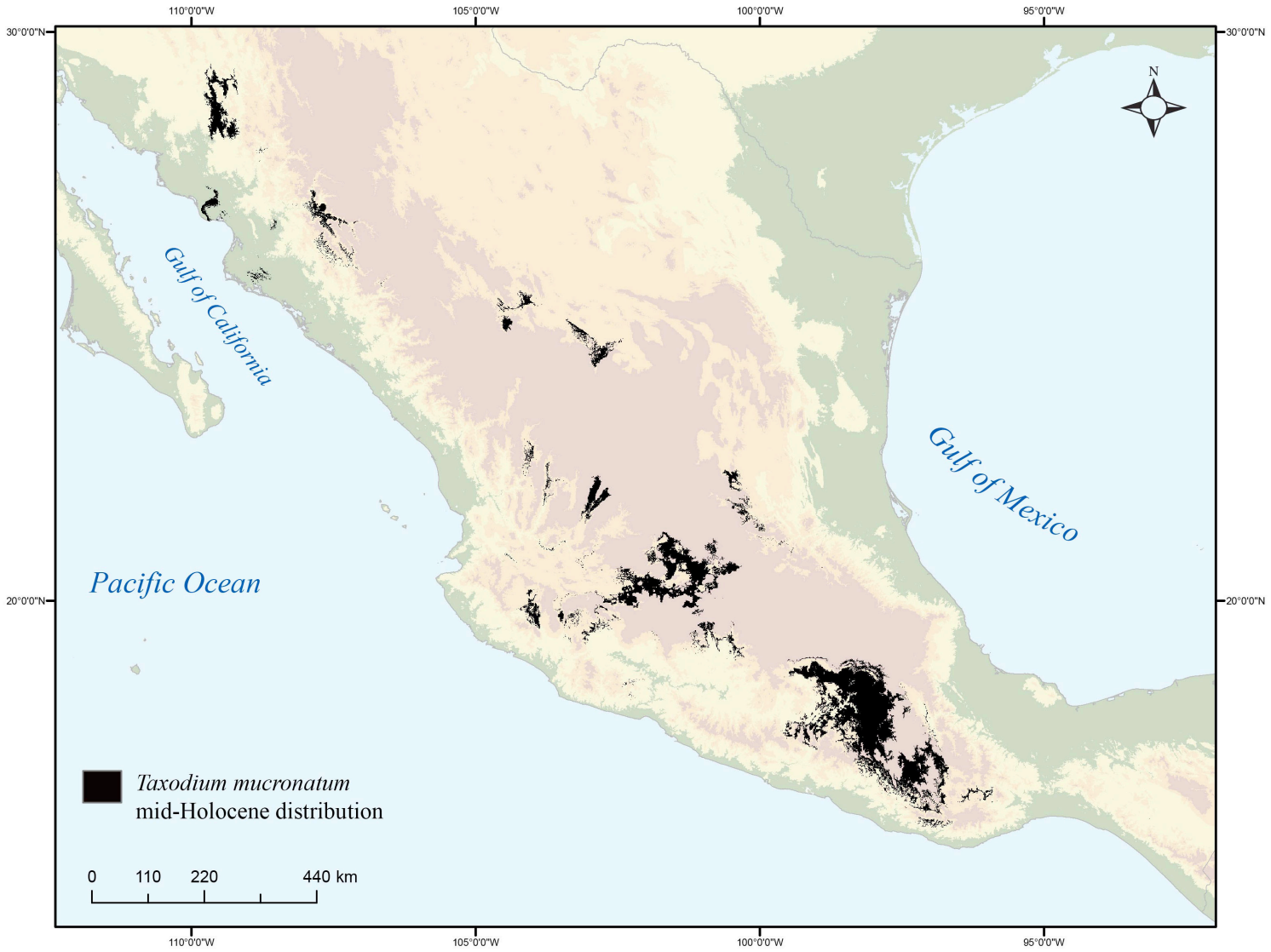

Figure 3.9: Projected mid-Holocene distribution for *Taxodium mucronatum*

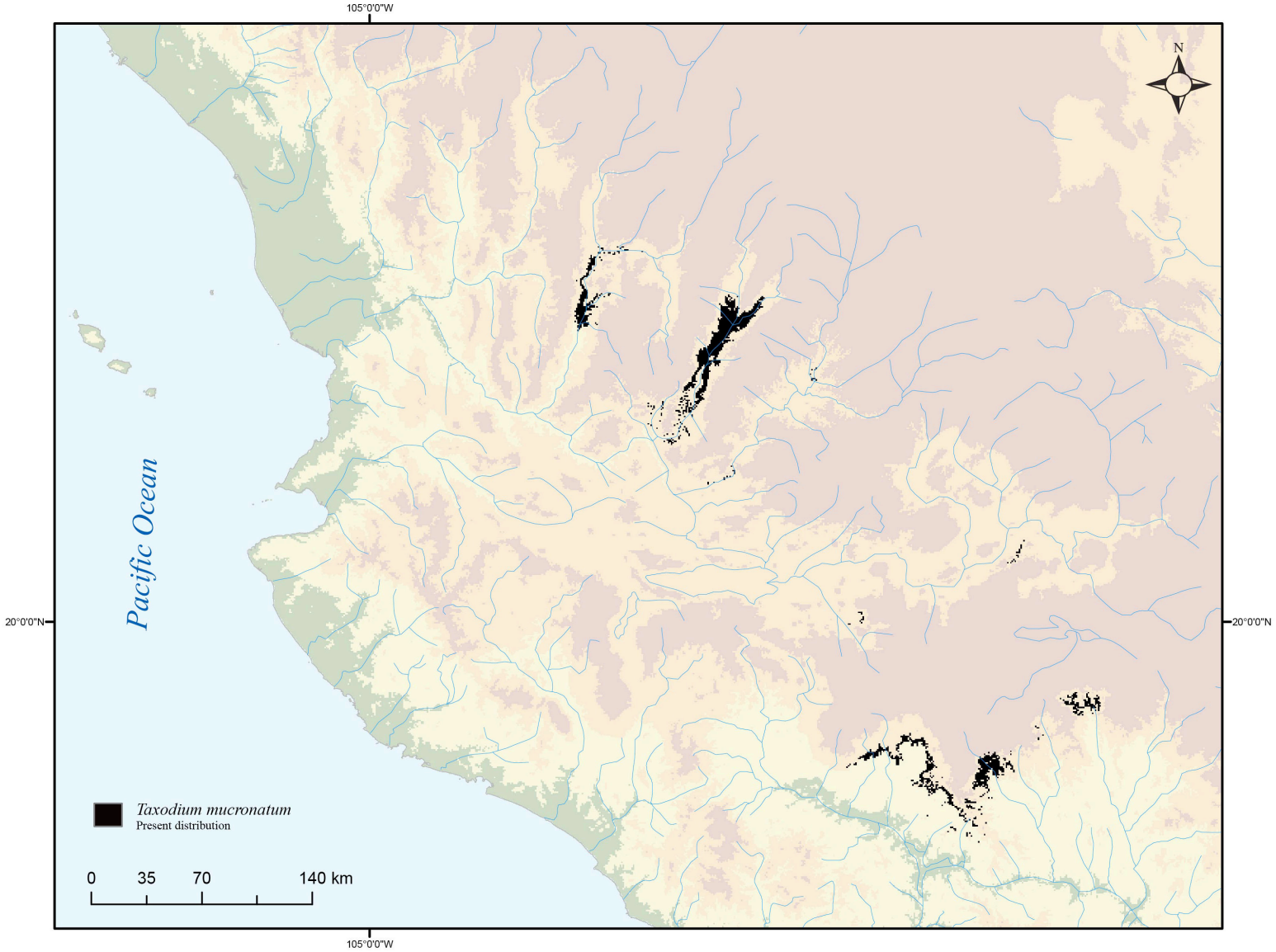

Figure 3.10: *Taxodium mucronatum* riparian growth pattern (MaxEnt)

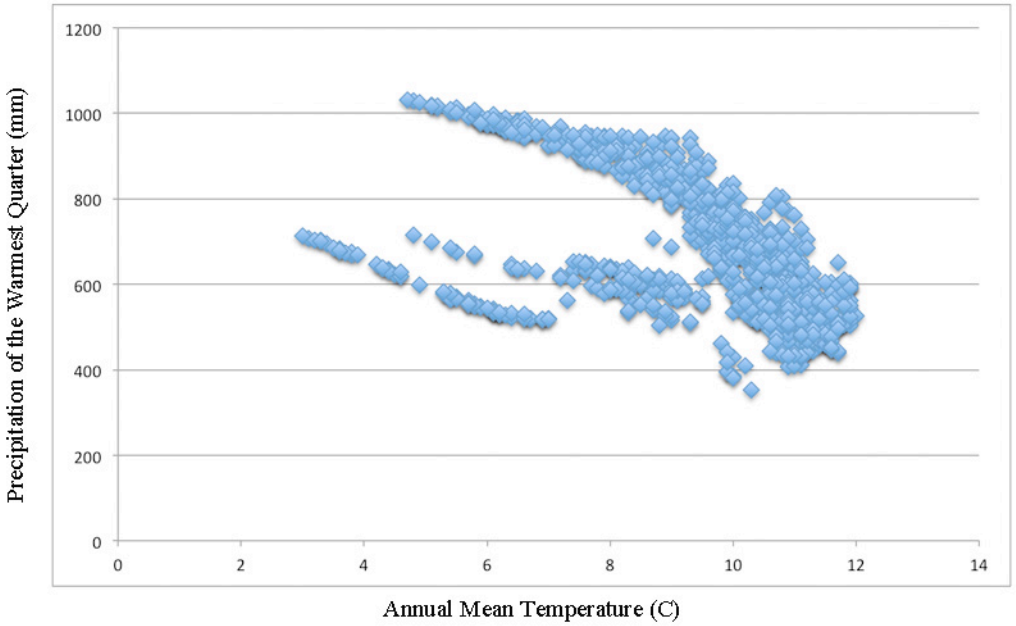

Figure 3.11: Precipitation vs. Temperature relationship for *Abies religiosa* MaxEnt model

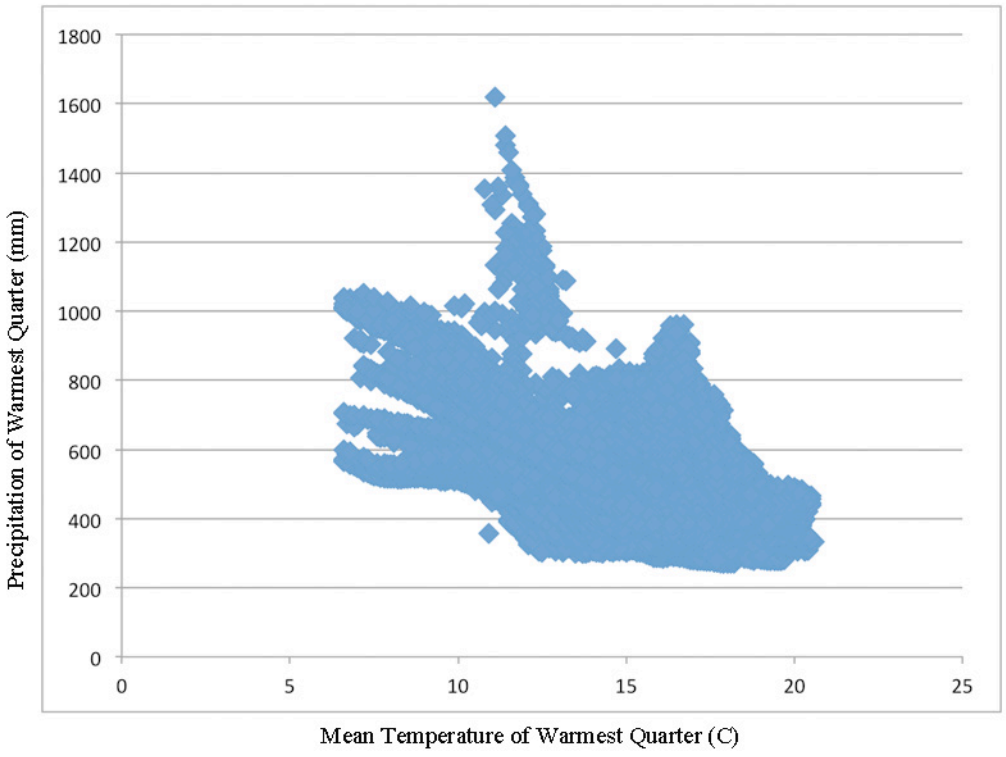

Figure 3.12: Precipitation vs. Temperature relationship for *Picea chihuahuana* MaxEnt model

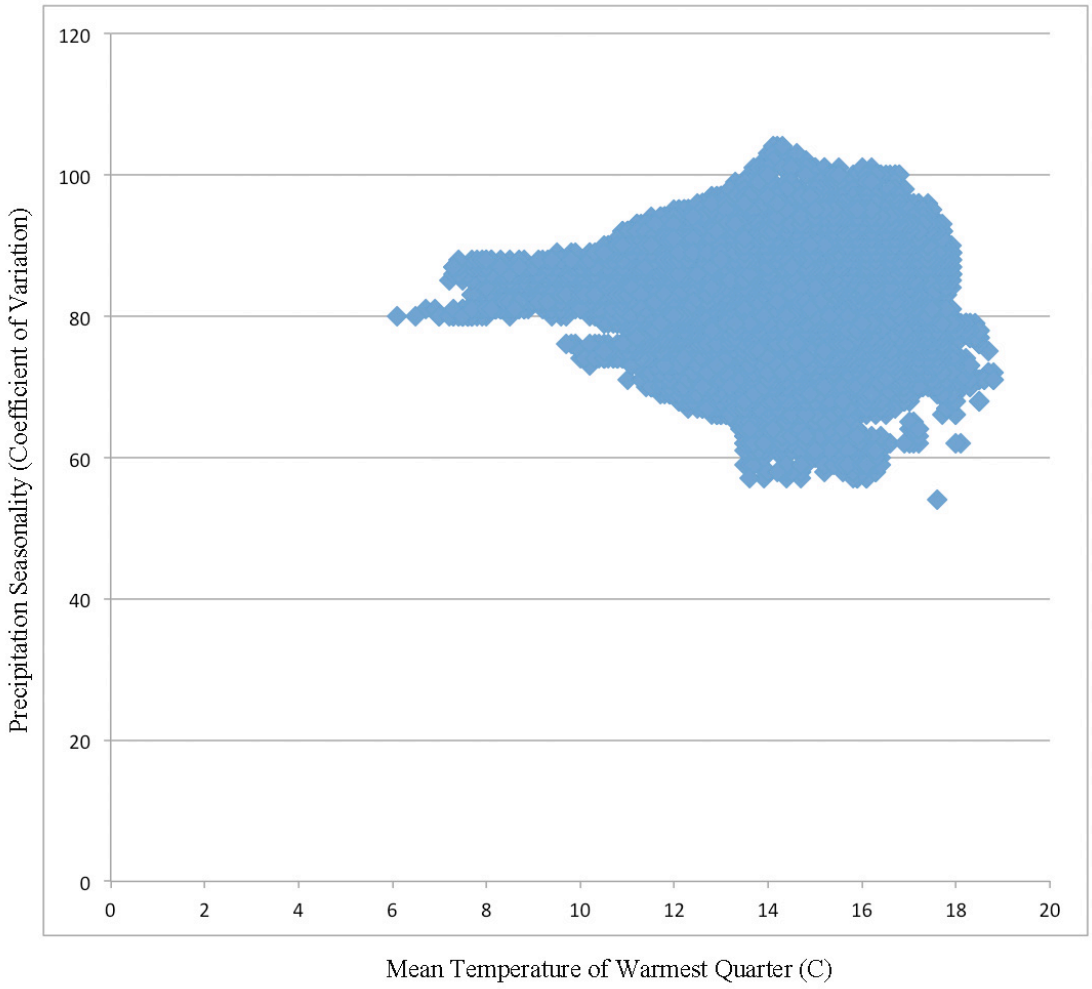

Figure 3.13: Precipitation vs. Temperature relationship for *Artemisia ludoviciana* MaxEnt model

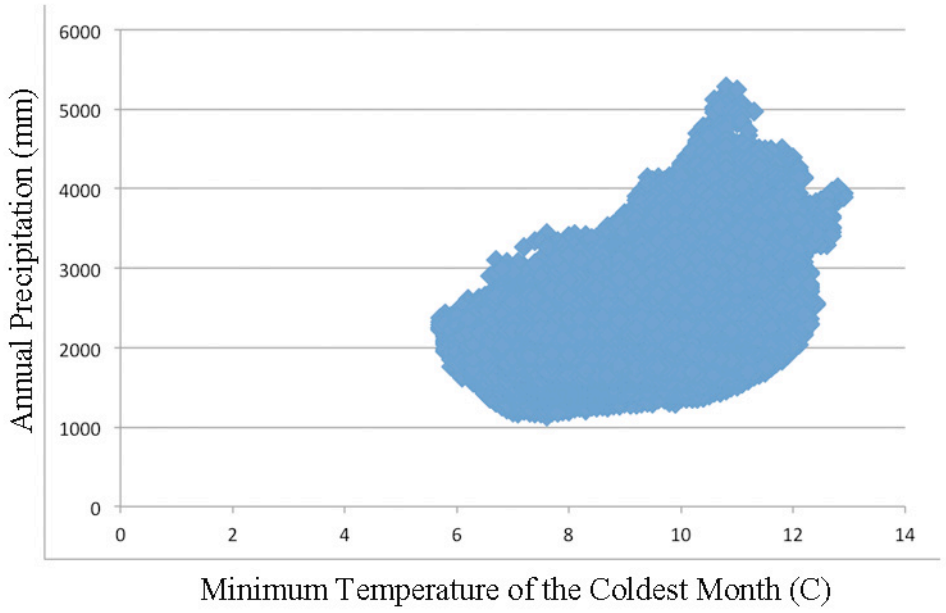

Figure 3.14: Precipitation vs. Temperature relationship for *Liquidambar styraciflua* MaxEnt model

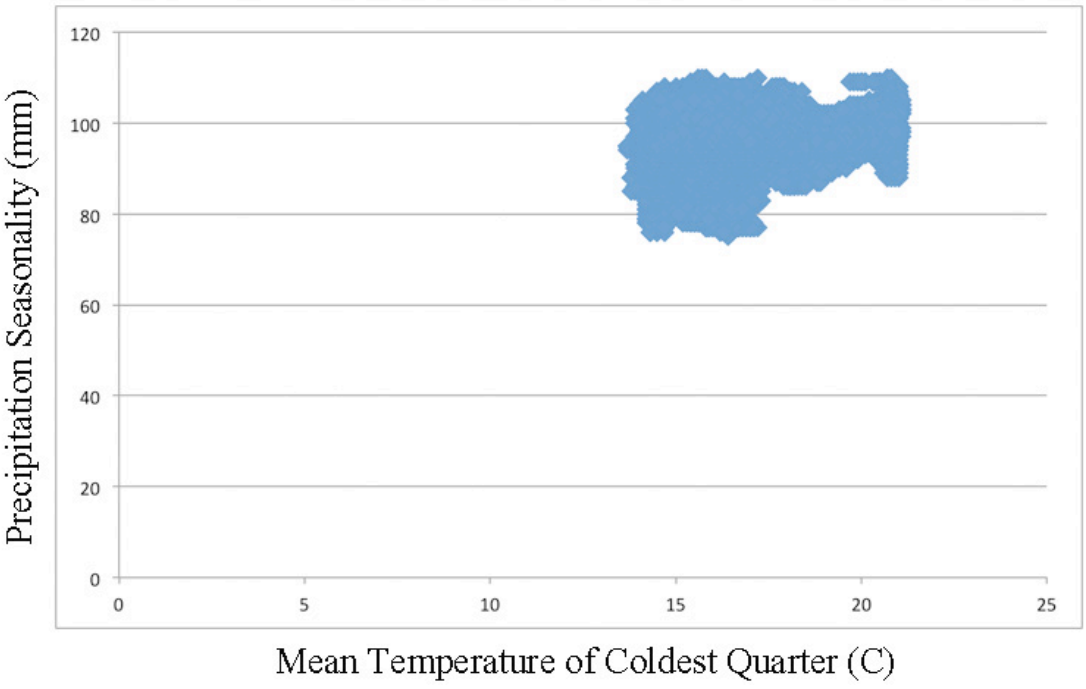

Figure 3.15: Precipitation vs. Temperature relationship for *Taxodium mucronatum* MaxEnt model.

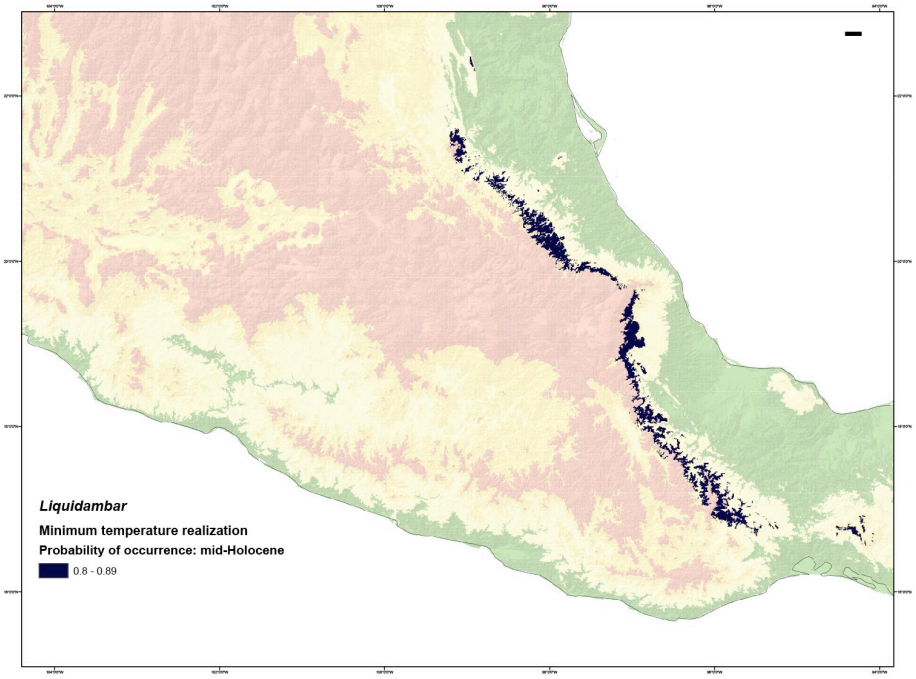

Figure 3.16a: Minimum PC loading for mid-Holocene, *Liquidambar styraciflua*

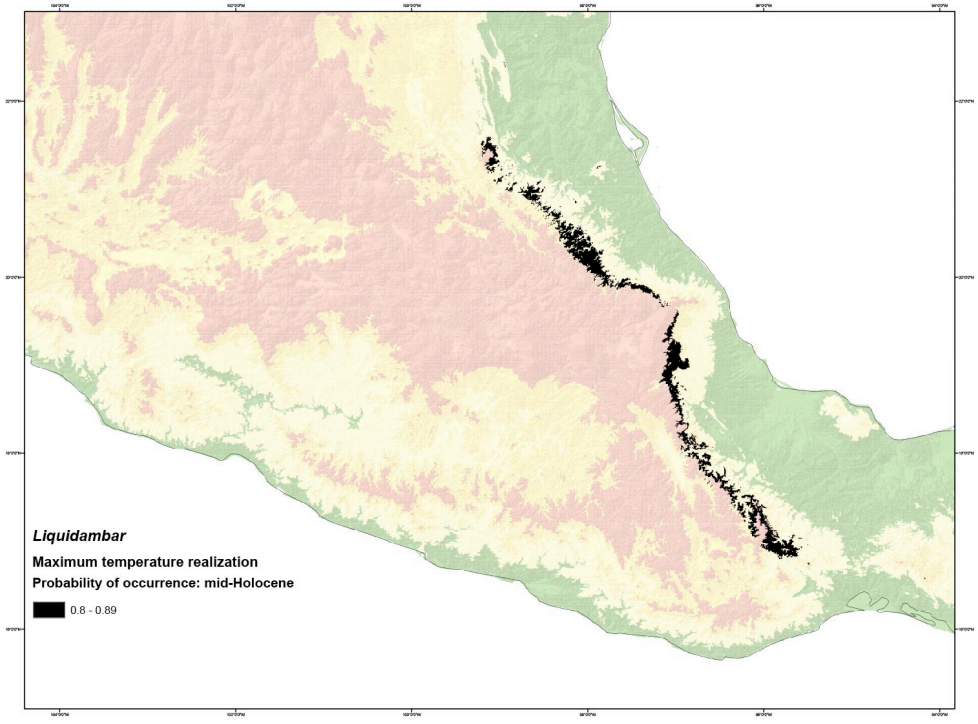

Figure 3.16b: Maximum PC loading for the mid-Holocene, *Liquidambar styraciflua*

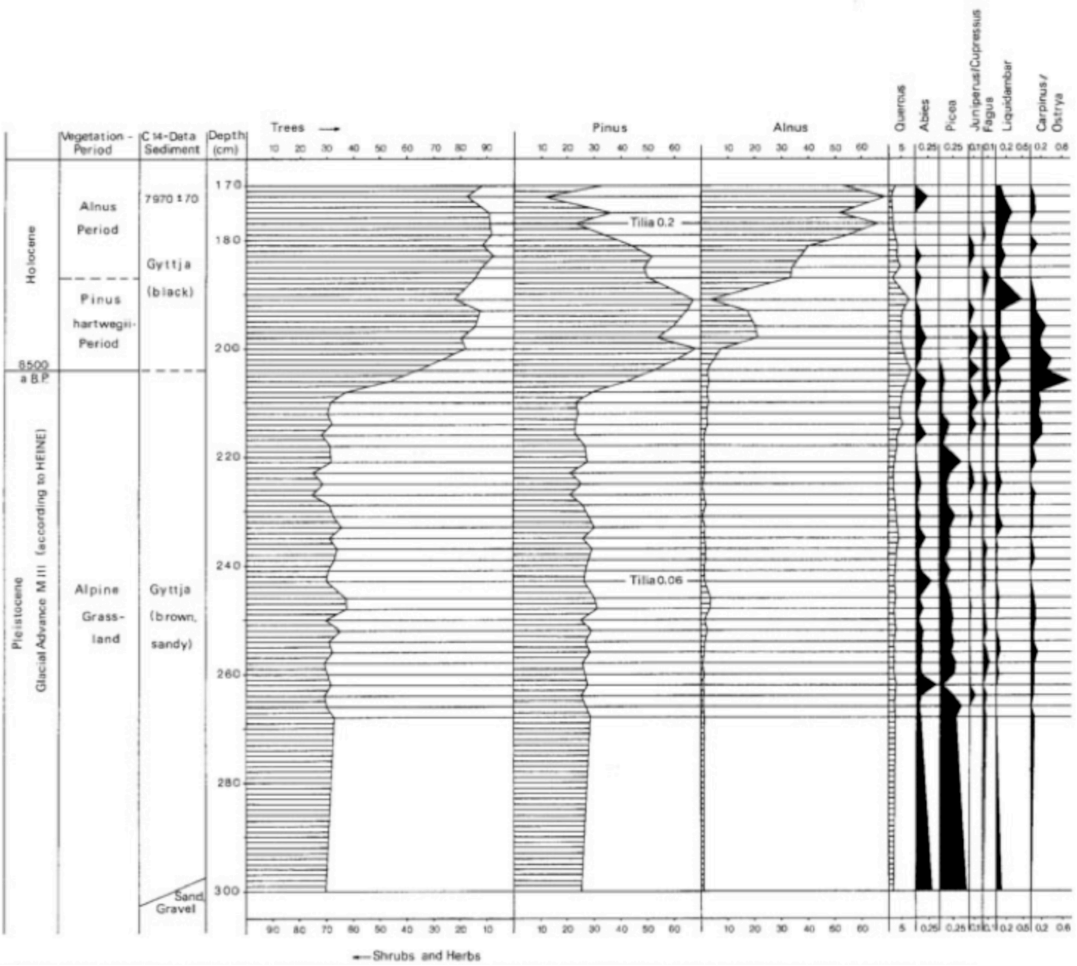

Figure 3.17: *Picea's* early Holocene disappearance in the TMVB gives rise to *Abies* and *Quercus* increases (Straka & Ohngemach, 1989).

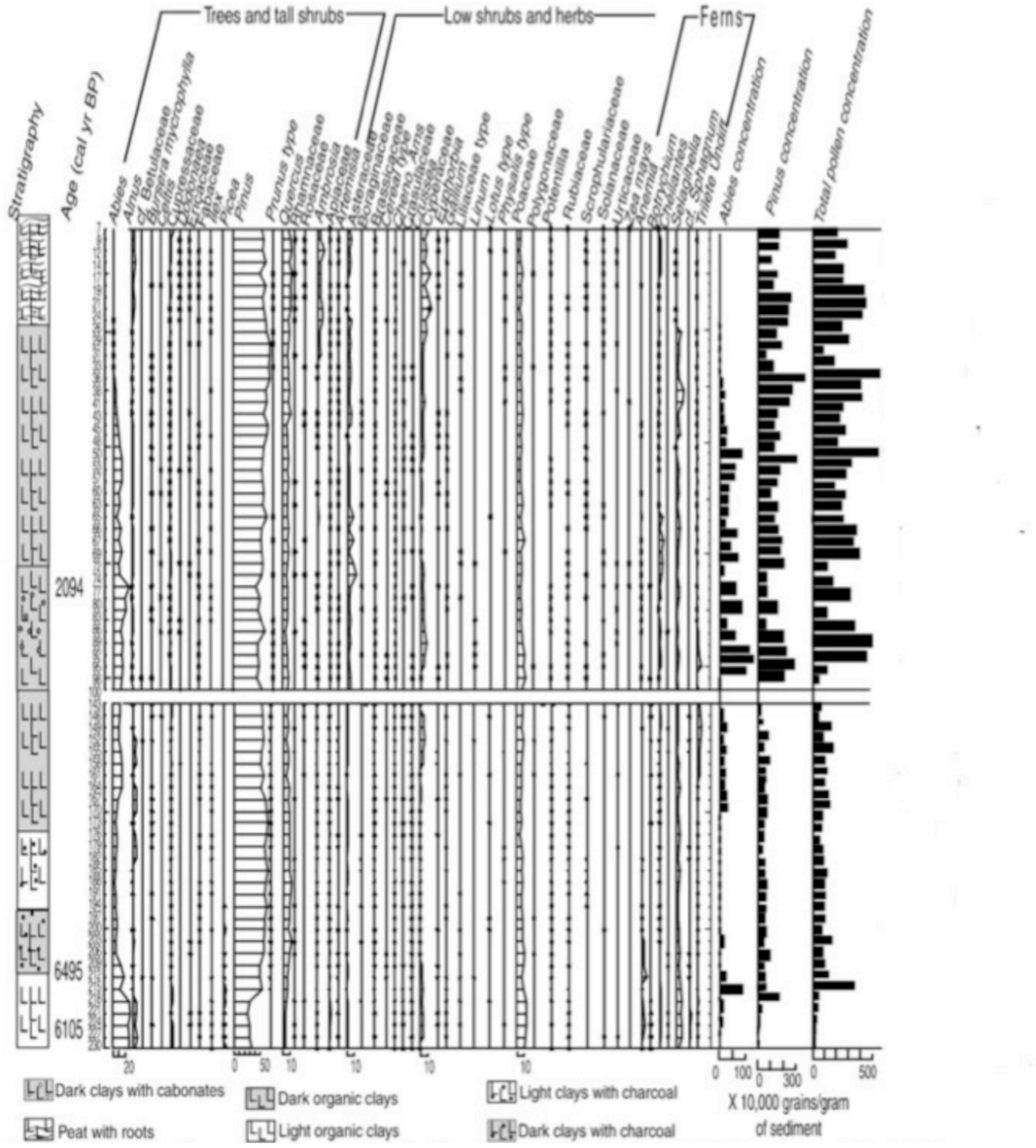

Figure 3.18: Pollen diagram and core stratigraphy Cienega Pino Redondeado (Ortega-Rosas *et al*, 2008). Chihuahua, MX 28°22'39" N, 108°23'05" W, 1810 m a.s.l.

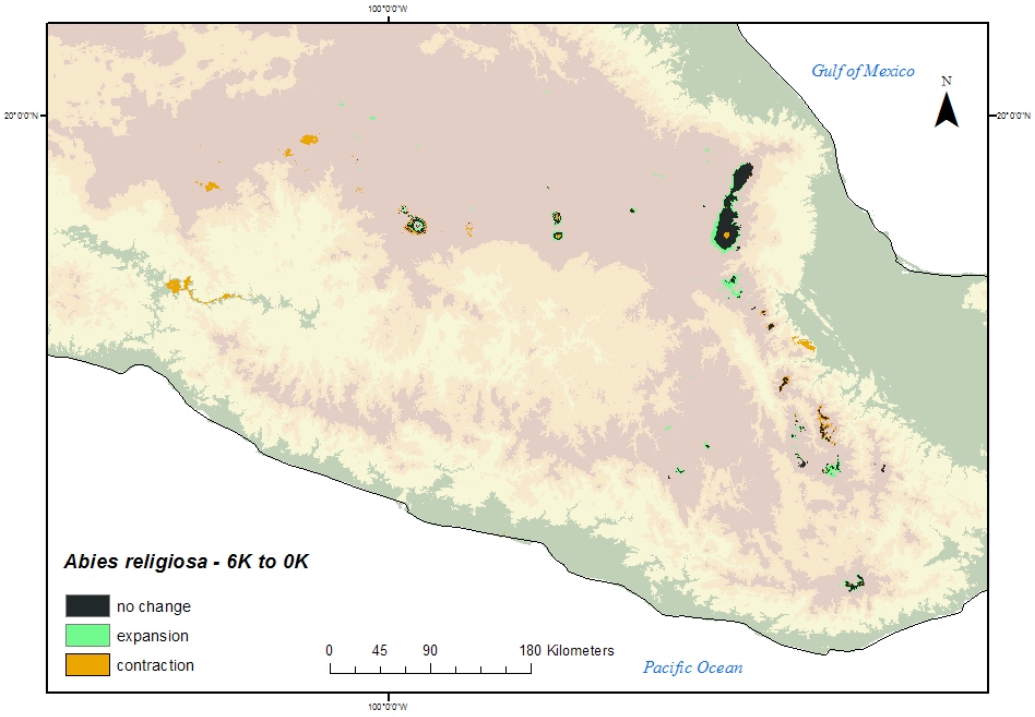

Figure 3.19: *Abies religiosa* change map between 6K and 0K.

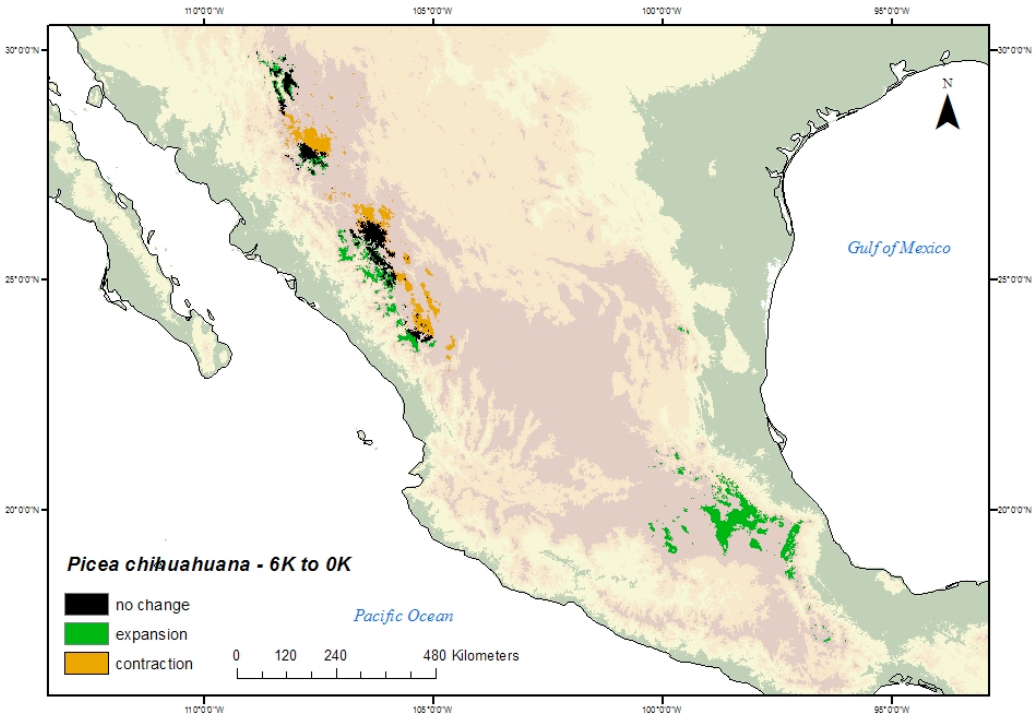

Figure 3.20: *Picea chihuahuana* change map between 6K and 0K.

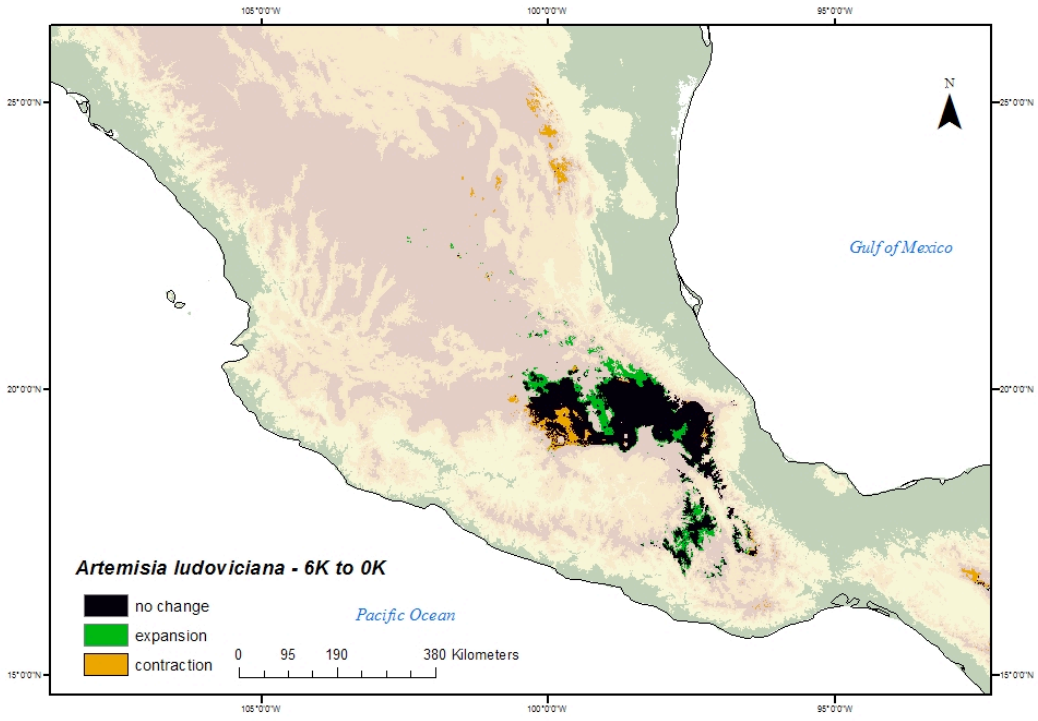

Figure 3.21: *Artemisia ludoviciana* change map between 6K and 0K.

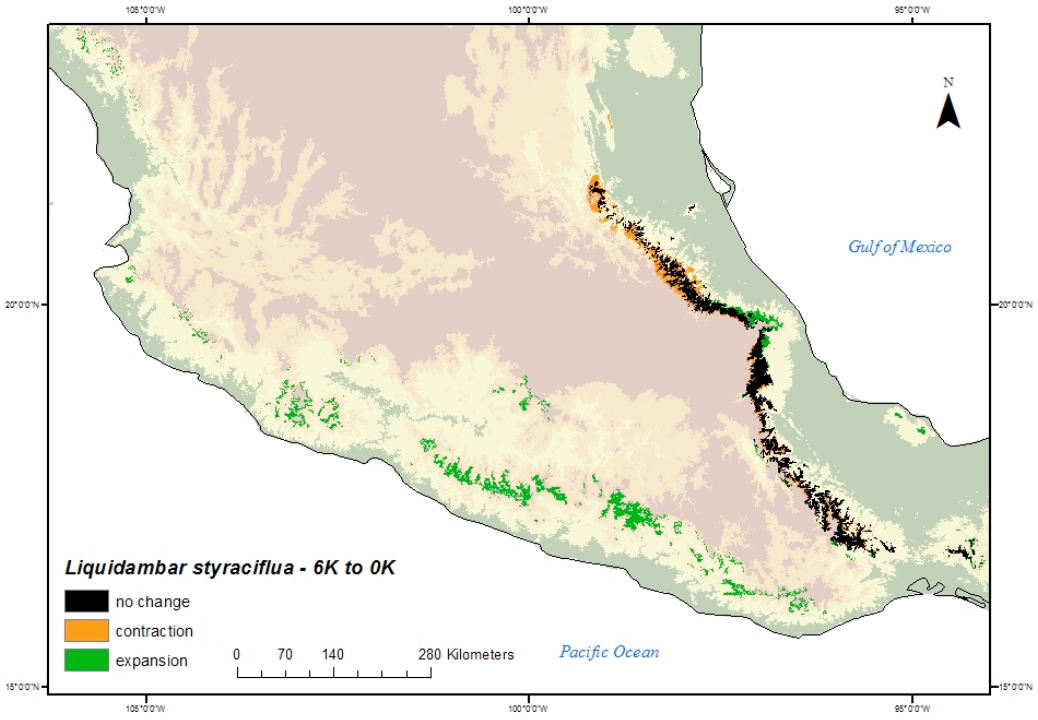

Figure 3.22: *Liquidambar styraciflua* change map between 6K and 0K.

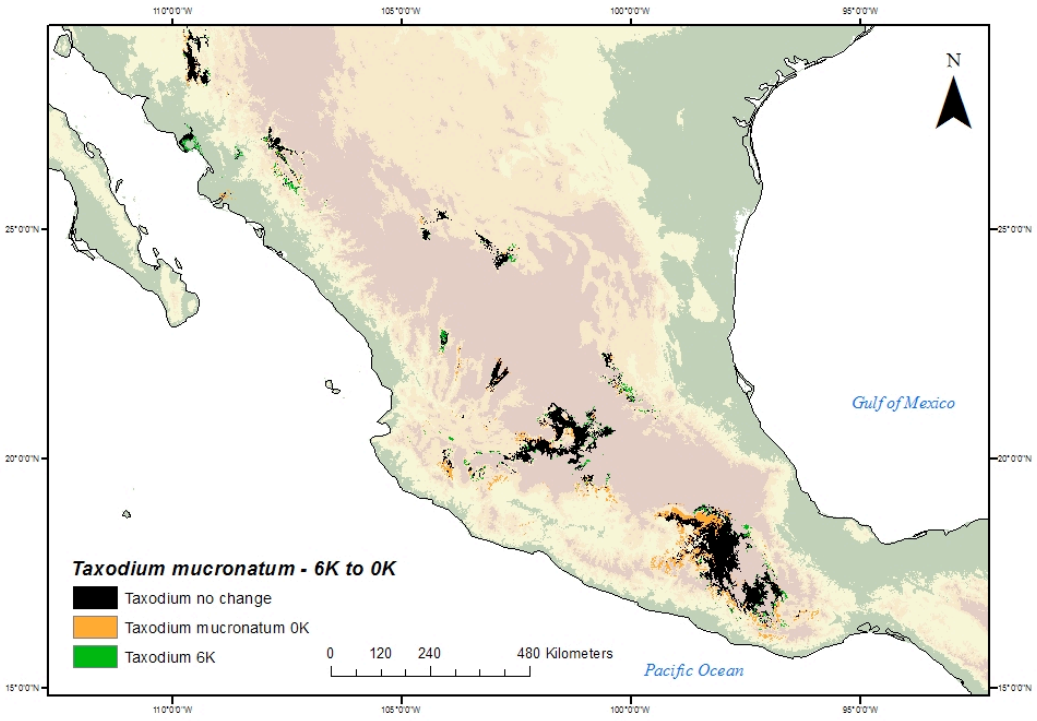

Figure 3.23: *Taxodium mucronatum* change map between 6K and 0K.

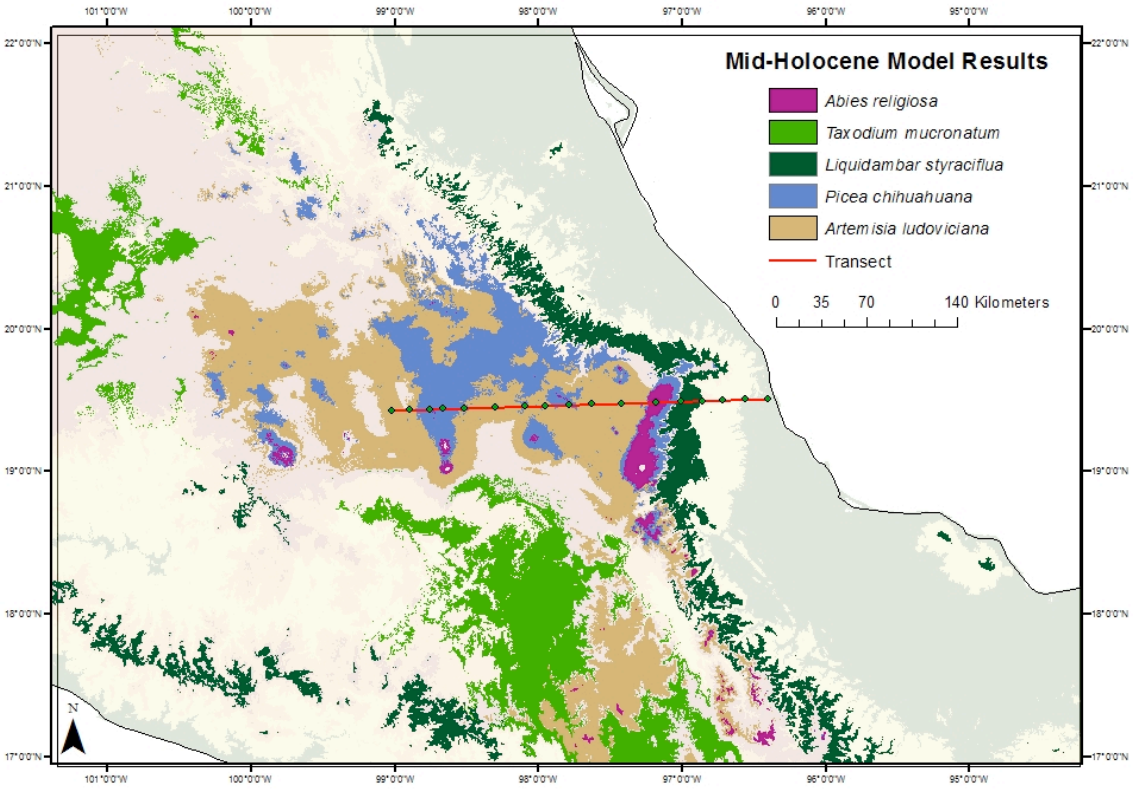

Figure 3.24: MaxEnt results for all species, including hypothetical transect from the Valley of Mexico to the coastal plain. The large area of *Abies religiosa* is mixed with *Picea chihuahuana*.

REFERENCES

Alley, R. B., Mayewski, P. A., Sowers, T., Stuiver, M., Taylor, K. C., & Clark, P. U. (1997). Holocene climatic instability: A prominent, widespread event 8200 yr ago. *Geology*, **25,** 483-486.

Bartlein, P. J., K. H. Anderson, P. M. Anderson, M. E. Edwards, C. J. Mock, R. S. Thompson, R. S. Webb, T. Webb III, C. Whitlock. (1998) Paleoclimate simulations for North America over the past 21,000 years: features of the simulated climate and comparisons with paleoenvironmental data. *Quaternary Science Reviews* **17**, 549-585.

Bradbury, J.P. (1989) Late Quaternary lacrustine paleoenvironments in the Cuenca de Mexico. *Quaternary Science Reviews* **8,** 75-100.

Byrne, R. (1982) Preliminary pollen analysis of Deep Sea Drilling Project Leg 64, Hole 480, cores 1-11. In: R. Curray and D.G. Moore, Editors, *Initial Reports of the Deep Sea Drilling Project*. 64, U.S. Govt. Printing Office, Washington. 1225–1237 Pt. 2.

Chiang, J.C.H. (2010). Extraction of PMIP2 mid-Holocene and LGM anomalies for use in WORLDCLIM. Unpublished raw data.

Conserva, M. (2003) Climate and Vegetation Change in Central Mexico: Implications for Mesoamerican Prehistory. Unpublished Ph.D. Thesis, University of California, Berkeley.

Elith, J., Graham, C. H., Anderson, R. P., Dudík, M., Ferrier, S., Guisan, A., ... & Zimmermann, N. E. (2006) Novel methods improve prediction of species' distributions from occurrence data. *Ecography* **29** (2): 129-151.

Elith, J., Phillips, S.J., Hastie, T., Dudík, M., Yung, E.C. & Yates, C.J. (2011) A statistical explanation of MaxEnt for ecologists. *Diversity and Distributions* **17** 43–57.

Farjon, A. (Conifer Specialist Group) 2003. *Taxodium mucronatum*. In: IUCN 2012. IUCN Red List of Threatened Species. Version 2012.2. http://www.iucnredlist.org Downloaded on 29 November 2012.

http://www.gbif.org (See full citation in Appendix 3)

González -Quintero, L. (1986). Análisis polinico de los sedimentos. In ‘‘Tlapacoya, 35,000 años de historia del lago de Chalco’’ (J. L. Lorenzo and L. Mirambell, Eds.) Coleccion Cientifica No. 115, pp. 113–132.

Hijmans, R.J., S.E. Cameron, J.L. Parra, P.G. Jones & Jarvis, A. (2005) Very high resolution interpolated climate surfaces for global land areas. International Journal of Climatology, **25**, 1965-1978.

Holmgren, C., Betancourt, J., Rylander, K. (2011) Vegetation history along the eastern, desert escarpment of the Sierra San Pedro Mártir, Baja California, Mexico, *Quaternary Research*, **75**, 647-657.

Lozano-García, M.S., Ortega-Guerrero, B., Caballero-Miranda, M. & Urrutia-Fucugauchi, J. (1993) Late Pleistocene and Holocene paleoenvironments of Chalco Lake, central Mexico. *Quaternary Research*, **40**, 332–342.

Lozano-Garcia, M.S., Ortega-Guerrero, B. (1998) Late Quaternary environmental changes of the central part of the Basin of Mexico: correlation between Texcoco and Chalco basins. *Review of Palaeobotany and Palynology,* **99**, 77-93.

Lozano-García, M.S., Sosa-Nájera, S., Sugiura, Y. & Caballero, M. (2005) 23,000 yr of vegetation history of the Upper Lerma, a tropical high-altitude basin in Central Mexico. *Quaternary Research*, **64**, 70–82.

Martin, P. (1963) "The last 10,000 years: a fossil pollen record of the American Southwest". University of Arizona Press, Tucson.

Metcalfe, S.E. A. Say, S. Black, R. McCulloch & O' Hara, S.L. (2002) Wet conditions during the last glaciation in the Chihuahuan desert, Alta Babicora Basin, Mexico. *Quaternary Research*, **57**, pp. 91–101.

Ortega-Rosas C. I., Peñalba M. C., Guiot J. (2008) Holocene altitudinal shifts in vegetation belts and environmental changes in the Sierra Madre Occidental, Northwestern Mexico, based on modern and fossil pollen data. *Review of Palaeobotany and Palynology,* **151**, 1-20.

Park, J. (2005). Holocene Climate Impacts and Human Environmental Impacts in Guanajuato Mexico. (Doctoral Dissertation) University of California, Berkeley.

Park, J., Byrne, R., Bohnel, H., & Conserva, M. (2010) Holocene climate change and human impact, central Mexico: a record based on maar lake pollen and sediment chemistry, *Quaternary Science Reviews*, **29**, 618-632.

Phillips, S. J. & Dudík, M. (2008) Modeling of species distributions with MaxEnt: New extensions and a comprehensive evaluation. *Ecography*, **31**, 161-175.

Ruter, A., Arzt, J., Vavrus, S., Bryson, R. A. & Kutzbach, J. E. (2004) Climate and environment of the subtropical and tropical Americas (NH) in the mid-Holocene: comparison of observations with climate model simulations. *Quaternary Science Reviews,* **23,** 663-679.

Straka, H. and D. Ohngemach, (1989) Late Quaternary vegetation history of the Mexican highland. *Plant Systematics and Evolution* **162,** 115-32.

Watts,W.A., Bradbury, J.P. (1982) Paleoecological studies at Lake Patzcuaro on the west-central Mexican Plateau and at Chalco in the basin of Mexico, *Quaternary Research*, **17,** 56-70.

4. CHAPTER FOUR

Distributions of five climatically sensitive plant species in central and northwestern Mexico during the Last Glacial Maximum

INTRODUCTION

In this chapter, I project the current distributions achieved by the MaxEnt onto a climate space representing the Last Glacial Maximum (LGM). The motivations are as follows: 1) the climate and vegetation of central and northwestern Mexico during the LGM are poorly understood, 2) current high-resolution climate data are often used to predict LGM ecological conditions, but the results are rarely compared to proxy climate records, and 3) environmental history reconstructions based on fossil pollen evidence during the LGM in Mexico remain sparse, and the climatic envelope models may offer some clarification.

At least nine Mexican pollen records span the Last Glacial Maximum (see Table 4.1), and not all are reliable in terms of chronology. Despite the limited evidence, researchers do have some limited insight into climate and environmental conditions in central and northwestern Mexico during the LGM. These records will be discussed later in the chapter.

METHODS

Like the previous chapter, my goal is to project the current distribution model for each species into a past climate setting (the LGM in this case). The methods used in this section are identical to those used in Chapter Three, with the exception of the LGM climate modeling data which consists of five total EOF outputs, rather than eight (Appendix 2). The leading component in the LGM climate models is most likely the influence of the North American ice sheet.

RESULTS AND DISCUSSION

Several WorldClim variables from the climate model outputs are summarized in Figures 4.1 to 4.4. I simplified the legends in order to ease map interpretation (e.g. warmer, cooler), and discuss the numerical results in the next paragraph.

In general, the climate models show LGM winters that were on the order of 2º C cooler in central Mexico, and up to 3º C cooler in northern Mexico (Figure 4.4). The maps also show more extreme differences in the southern United States and southwest. The models show summer temperatures during the LGM (Figure 4.3) to also be 2-3º C cooler than the present, which the most significant cooling in the central highlands (3º C).

The climate model for the LGM summer precipitation (Figure 4.1) shows variation throughout Mexico with some areas modeled wetter today and others more wet during the LGM. The map's greener areas imply up to 100 mm more precipitation, while the

dark brown areas experienced up to 160 mm less precipitation during the LGM. Finally, winter precipitation during the LGM was generally less prevalent than today (Figure 4.2). The dark brown areas on the map range from 50-100 mm less precipitation than today, while the green areas of the model results are 50-100 mm more precipitation.

A decrease of only 2-3º C during the LGM in Mexico conflicts with Caballero *et al.* (2010), who suggest that a much larger decrease, between 6-8º C was likely. They base their estimate on glacial and fossil pollen records. While the question of which is correct is out of the scope of this dissertation, it will be covered in later work.

The MaxEnt results for each taxon are shown in Figures 4.5 to 4.0. Bivariate graphs of leading variables for precipitation and temperature are in Figures 4.11 to 4.15.The MaxEnt model comparison based on two different climate model realizations are shown in Figures 4.18a and 4.18b. The MaxEnt model ROC plots, which are used to help determine threshold levels, are in Appendix 3, and the predictor variables used for each taxon are in Table 2.1a to 2.1e (same as the present-day distribution model). Figures 4.19 to 4.23 illustrate the overall change in modeled distribution between the present (0K) and 21K BP. Figure 4.24 is a map of the five predicted species distributions over a hypothetical transect from the Gulf coast to the Valley of Mexico during the LGM.

Mexican Climate: the Last Glacial Maximum (LGM)

During the LGM (21K BP), the ice sheets covering the northern and southern hemispheres were at their maximum extent. In North America, the Laurentide ice sheet reached from approximately 56º W to 112º through modern-day Canada, and as far south as 40º N near present-day Indiana and Illinois in the United States. The Cordillieran ice sheet extended from 112º W to 120º W, with a southern edge at approximately 48º N (Dyke & Prest, 1987). Recent high-resolution climate simulations for the LGM suggest that westerly jet flow split into two branches over the Laurentide ice sheet. Of these two branches, the southern branch in thought to have influenced Mexico, particularly during the northern hemisphere winter (Kim, *et al.,* 2008). The same high-resolution model also indicates overall decreased precipitation in the Gulf of Mexico (both summer and winter), but increases in precipitation in western Mexico.

In northwestern Mexico and the Sierra Madre Occidental, the consensus among various climate models and proxy evidence is that the Mexican Monsoon had not yet developed, only emerging during the early Holocene with maximum influence during the mid-Holocene (Poore, *et al.,* 2005; Harrison, *et al.,* 2003).

The influence of the Gulf of Mexico on Mexican climate during the LGM was considerably different than it is today. With a near 130 m drop in sea level, more of the continent was exposed. This change in topography influenced flow patterns throughout the Gulf. Brunner's (1982) study of planktonic foraminifera concluded that during LGM winters, a warm core region was surrounded by cooler waters to the west, while the warm Caribbean-fed Loop current kept eastern waters as warm as the core region. The coastal waters, however, were generally much cooler, according to the analysis. In terms of salinity, Brunner found considerably fresher surface waters in the Valley of Mexico during the winter months, suggesting reduced evaporation and a more humid climate, while summer waters around the Gulf coast were more saline than today, suggesting increased summer evaporation and more arid conditions.

Brunner's description of the Gulf of Mexico is supported by the climate model data I used in this study (Brunner, 1982). The data used in this study does illustrate the absence of the Mexican Monsoon during the LGM, but also suggests increased winter precipitation compared to today, contradicting Kim *et al.'s* (2008) results. The lack of a monsoonal climate is illustrated by only a small change in precipitation during the warmest quarter of the year compared to the cool quarter (Figures 4.1 and 4.2), while the increase in winter precipitation may suggest increased Pacific storms in the west, and higher frequencies of Nortes reaching into the Gulf and southeastern Mexico, which do not necessarily bring increased precipitation, but do contribute to cooler overall temperatures and decreased evaporation in the Gulf.

Abies religiosa

I chose to model the species *Abies religiosa,* which is primarily restricted to the TMVB. Several species of *Abies* exist in Mexico, but they do not all have the same environmental tolerance (Farjon 1990). Furthermore, phylogenetic studies assert the fact that the southern species of *Abies* have diverged strictly due to glacial expansions and interglacial contractions, although at the time of this writing, phylogenetic studies have not yet determined the exact sequence of divergence amongst the three southern *Abies* species. (*Abies religiosa, A. guatemalensis* and *A. hickelii)*. What is known is that the limitation on gene flow amongst the populations is due largely to barriers in dispersal - topography and climate (Jaramillo-Correa *et al,* 2008). In light of this fact, it is reasonable to assume that if *A. religiosa* exists today in a location near palynological sites containing *Abies*, the likelihood of the ancient pollen grain being that of *A. religiosa* is high.

Much of the literature points to a "large expansion" of *Abies* sometime during the late Pleistocene, but the actual extent of that expansion remains unknown. MaxEnt (Figure 4.15) shows that the LGM expansion was modest in more southern regions, and that contraction appears to be associated with the LGM climate in the central and eastern TMVB.

Although it is to some degree drought resistant, *A. religiosa* thrives in the TMVB under cool and moist conditions. Huante & Rincon (1991) report a typical setting for a fir forest as having a temperate climate with a mean precipitation of roughly 1300 mm (mostly summer precipitation) and a mean minimum and maximum temperatures as 0.13º C and 21.9º C, respectively. In a study of monarch butterfly colonies, Calvert and Brower (1986) mention that *A. religiosa* expands to lower elevations if conditions become wetter.

In the 21K projection for *A. religiosa* (Figure 4.5)*,* MaxEnt shows a larger range for the species than exists today in the southern state of Oaxaca. In this case, the climate model predictions show lower summer temperatures, and modest increases in both summer and winter precipitation in this area (Figures 4.1 and 4.2). A cooler and slightly wetter environment supports such an expansion.

The more northern expansions illustrated in Figure 4.15 corresponds to the climate models, which show a slight cooling in the TMVB both during summer and winter (Figure) as well as modest increases in winter precipitation (Figure).

The fossil evidence is limited, yet useful as a check on the predictions. One point of agreement between the two lies in Watts and Bradbury's (1982) record from Patzcuaro. The pollen record shows traces of *Abies* during the LGM and MaxEnt does predict in the

vicinity of Patzcuaro during the LGM. Deevey (1944) found no *Abies* pollen in surface samples from the region, while Watts' pollen diagram shows pollen in the LGM (Watts & Bradbury, 1982).

To the east, González-Quintero's (1986) record in Chalco contains only "scarce" amounts of *Abies* during the LGM. González -Quintero attributes the Chalco presence to northern populations approximately 100-150 km away, a hypothesis that also fits with the MaxEnt model output. Other potential sources of the pollen in the Chalco record may have been due to populations on nearby volcanic peaks such as Popocatépetl, where the model results show very little change in *Abies* extent between the LGM and present time.

Finally, the full glacial section of the Chingahuapan Upper Lerma record (Lozano-Garcia *et al*., 2005) contains small amounts of *Abies* as well, in accordance with MaxEnt, which predicts small populations in the same area.

One question that remains is if indeed MaxEnt reflects what actually happened during the LGM, is how did *A. religiosa* recolonize high altitude regions from places where it appears to have "disappeared" during the LGM. Since the MaxEnt model threshold was set to 0.80 probability, the possibility remains that *Abies* continued to exist in high altitude pockets to the west of its distribution (Figure 4.5) and then later expanded as the climate grew more favorable during the early to mid-Holocene.

Artemisia ludoviciana

MaxEnt shows that *Artemisia* (Figure 4.6) projects a more expansive range than the present in central Mexico. This is in agreement with cooler and drier conditions, but little confirmation can be made for the northern parts of the central highlands since the fossil pollen records are limited to the TMVB. Nearly all the pollen diagrams in the TMVB show *Artemisia's* as present at the LGM.

The model predicts almost no *Artemisia* for the northwestern part of Mexico although *Artemisia* averages between 5-10%, of the pollen record from DSDP Site 480 (Byrne 1982). As noted previously, the *Artemisia* subspecies in the northwest and the subspecies in the TMVB are different. The subspecies in central Mexico (*A. ludoviciana* ssp *Mexicana)* may be more in agreement with the climate envelope I defined (see Results section), whereas the northern subspecies, *A. ludoviciana* ssp *sulcata* and possibly *A. tridentata*, may require a climate envelope that accounts for the conditions northwestern Mexico. That is, the present-day envelope (Chapter 2) should have accounted for possibly warmer conditions. The subspecies *sulcata* is common throughout New Mexico and southern Arizona, both regions with climate and terrain similar to Sonora in northwestern Mexico. It is possible that the *Artemisia* found in Byrne's study is more akin to the subspecies found throughout New Mexico and Arizona, and if indeed it is the same, then it did occur in unique assemblages that are suggestive of a non-analog climate.

In summary, the pollen record shows the presence of *Artemisia* in both the central and northwestern regions of Mexico. In central Mexico, *Artemisia's* presence is attributed to cool, arid conditions (Watts & Bradbury, 1982; Ohngemach & Straka 1989; Lozano-García *et al.,* 2005), while in the northwest, Byrne states that a non-analog climate may have existed. Only Watts & Bradbury point out a similar possibility for the Patzcuaro site in central Mexico, where they found a "unique" assemblage containing *Artemisia*.

Liquidambar styraciflua

As it was introduced in Chapter Two, *Liquidambar styraciflua* is characteristic of the Mexican cloud forest, most prominently in eastern Mexico. The timing of the arrival of the temperate cloud forest in Mexico has remained a debated topic in the literature, although genetic techniques have helped clarify some of the issues, particularly in the case of *L. styracaflua.* Specifically, studies by both Hoey & Parks (1994) and Morris *et al.* (2008) confirm that *L. styracaflua's* presence in Mexico likely goes back to the early Miocene, with an entrance from the north. Furthermore, both studies agree that during glacial episodes such as the Pleistocene, the northern populations of *L. styracaflua* expanded and contracted while the Mexican refugia has remained relatively intact.

Pollen evidence suggests that *Liquidambar* was rare in central Mexico during the LGM. The Ohngemach & Straka record from Tlaloc I (1989) contains trace amounts, as does Lozano-Garcia *et al's* Texcoco record (1998). However, these two records are the only two with evidence for *Liquidambar* during the LGM.

The model result (Figure 4.7, 4.22) shows a slightly expanded distribution of *L. styraciflua* for the LGM. The distribution appears to expand downslope toward the Gulf side. The direction of expansion may be due to wet LGM winters and cooler temperatures that inhibited evapotranspiration, and helped maintain moisture in the forest. Arid LGM summers (Brunner, 1982) were cooler than today, and were likely able to maintain significant moisture throughout the cloud forest due to the higher elevation. Although speculative, it is possible that summer fog (warm days and cool evenings) contributed to available moisture in the cloud forest (see *Picea* discussion).

Finally, the LGM predictions for *Liquidambar* are difficult to in the areas of predicted distribution, simply because so few records exist from the LGM period in Mexico from cloud forest regions. Both the aforementioned records suggest a very sparse presence of *Liquidambar* during the LGM, including that of Ohngemach & Straka Jalapasquillo (1989), whose sites are the closest to the cloud forest where most of the *Liquidambar* is predicted to occur. However, that diagram does not include any other cloud forest taxa, which may point to long distance transport and deposition of *Liquidambar* pollen. The MaxEnt model results cannot explain the presence of cloud forest taxa in the Valley of Mexico, as was found in Lozano-Garcia's Texcoco core (1998).

Picea chihuahuana

The LGM distribution generated using MaxEnt (Figure 4.8) predicts *Picea* in the TMVB, primarily along volcanic slopes La Malinche's slopes have extensive *P. chihuahuana* coverage, along with Popocatépetl and Itzaccíhuatl. Palynological evidence suggests that small populations of spruce certainly grew in the Cuenca Oriental and the Valley of Mexico (Straka & Ohngemach 1989; González-Quintero 1986). Both these records contain *Picea* at low levels (<5%) during the LGM. Interestingly, MaxEnt did not predict *Picea* for the eastern volcanoes, including as Pico de Orizaba. *Picea's* absence points to potentially unique Valley of Mexico conditions that were likely more complex than simply "dry" or "cool", as is frequently described in palynological interpretations.

Generally, *Picea* grows in high altitude regions (2300 m to 3200 m) that have consistently cool, moist conditions (Gordon, 1968). *Picea* is less drought-tolerant than *Abies religiosa* and *Pinus hartwegii,* although both of these conifers quite possibly

occurred alongside *Picea* during the LGM. An inability to cope with drought may explain why only *Picea* no longer exists in the TMVB, which has become much drier since the mid-Holocene.

Gordon (1968) characterizes *Picea's* climatic requirements with warm summer days and cool evenings leading to fog, which provides much needed moisture. Effects such as long-term decreased evapotranspiration and summer fog formation are not included as variables in a climate model per se, but they are both consequences of cooler temperatures after warm summer days. The slopes surrounding the Valley of Mexico may have experienced the following conditions: cooler temperatures helped to retain whatever moisture was present in the basin longer, therefore providing appropriate conditions for *Picea*. Since present-day temperatures are higher than they were during the LGM, and precipitation has decreased *Picea* has disappeared while the drought-tolerant trees such as *Abies* continue to persist.

In the northwest, MaxEnt shows *Picea* occupying a significantly larger area of the Sierra Madre Occidental during the LGM than it does today. Included is a shift to lower elevations. The climate models show increased summer precipitation (Figure 4.1) in and lower winter temperatures throughout the Sierra Madre Occidental (Figure 4.4).

Palynologists agree that *Picea* likely had a wider distribution throughout the Sierra Madre Occidental and the TMVB during the LGM, but was eventually forced into refugial patterns in the early Holocene, both in northwestern Mexico and central Mexico (Byrne, 198; Metcalfe et al., 2000; Lozano-Garcia et al.; 1993, Straka & Ohngemach 1989). Pollen records show that *Picea* in central Mexico disappeared completely shortly after the mid-Holocene (Straka & Ohngemach 1989), presumably after the modern climate regime was established.

Phylogenetic evidence associated with *Picea* strongly suggests that *P. chihuahuana*, the species found only in the Sierra Madre Occidental, is likely the same species that occurred in the TMVB during the LGM (Jaramillo-Correa et al., 2008) in Mexico. Ledig, Hodgskiss, Krutovskii, Neale & Eguiluz-Piedra (2004) make clear that the other two species of *Picea* found in the eastern ranges of Mexico separated as species long before the LGM, and McDonald (1993) states that dispersion along the TMVB and toward the western ranges was the most likely path to take if *Picea's* population expanded. This points to *P. chihuahuana* being the most likely species found in the Valley of Mexico and TMVB during the LGM.

Byrne (1982) reports low percentages (1-2%) of *Picea* in the LGM section of a Gulf of California marine record (DSDP 480), and suggested a wider distribution of *Picea* together with *Artemisia* during the LGM. Metcalfe *et al.* (2002) report significant amounts of *Picea* (20%) during the LGM, which is in agreement with the MaxEnt model output. However, one cannot ignore the fact that an earlier pollen diagram at the same site does not include *Picea*, but instead shows *Abies* as the dominant conifer (Montúfar Lopez, 1987). If in fact the pollen type is *Abies*, then MaxEnt's prediction at the Alta Babicora site is not confirmed.

Taxodium mucronatum

On first glance, the MaxEnt LGM map for *Taxodium mucronatum* (Figure 4.9) suggests a contraction in the interior highland. However, this "contraction" is more a shift toward the southwest. The pushing of the taxon out from the highlands may be due to cooler LGM temperatures and aridity leading to a general drying of the streams and

rivers. However, the overall scenario is largely in disagreement with the fossil pollen records from the TMVB. There is evidence of *Taxodium* in the Valley of Mexico, most notably in the form of a dated fossil log at the Tlapacoya site (Quintero-González, 1986). The MaxEnt model shows no *Taxodium* in the Valley of Mexico under the LGM climate conditions used with the model. The model results point to *Taxodium* having a far more pronounced population to the south of the fossil sites, in southern Puebla, northern Guerrero and Oaxaca.

As stated in previous chapters, *Taxodium* is found predominantly in riparian habitats, but hydrology was not included as a variable in the model construction. Despite the lack of hydrological variables, the model captured some riparian features (Figure 4.10). I suggested in Chapter Two that using only the bioclimate envelope inadequately predicted *T. mucronatum's* present-day distribution and therefore the subsequent projections are flawed.

Range of Sensitivity: *Liquidambar*

As in Chapter Three, I tested the range of sensitivity of *Liquidambar* for the LGM under two climate realizations. Two distinct MaxEnt models for *Liquidambar* (Figures 4.14a and 4.14b) were generated from WorldClim data based on a maximum and minimum PC loading (Appendix 2). Although the WorldClim climate variables used for the both models are identical, the resulting maps are slightly different, with the map from a PC loading for the minimum LGM temperature showing *Liquidambar's* distribution to be much less widespread than an LGM climate model with maximum temperature. In the case of *Liquidambar,* the important variables in the climate envelope were the mean annual precipitation and the minimum temperature during the coldest month. In this case, the minimum temperature during the coldest month during the LGM probably contributes to the extremity between the two maps. As mentioned in Chapter Two, the lower temperature limit for *Liquidambar* is around -4°C, so if a climate realization that tends toward lower temperatures is used for the climate envelope then it is possible that the resulting species distribution will reflect the difference.

CONCLUSIONS

Only five records covering the LGM are available for central Mexico, and three for northwestern Mexico. Because so few records exist, the bioclimatic envelope method lends itself well to the problem of visualizing and reconstructing the paleo landscape. On applying the bioclimatic envelope method in this chapter, I was able to arrive at the following conclusions:

The MaxEnt reconstruction for *A. religiosa* (Figure 4.15) illustrates a wider distribution in the central highland (Michoacán-Mexico border) populations at high elevations, and also the southeastern and southern ranges in Puebla and Oaxaca. Model results for areas in the west-central region of the TMVB (Patzuaro) did predict a wider distribution *A. religiosa* during the LGM, which is in general agreement with Watts & Bradbury's pollen diagram (1982), but finer scale studies will better confirm the agreement.

MaxEnt results for *Artemisia's* during the LGM suggest expansion throughout north central Mexico. While this makes sense since the central highlands north of the

TMVB are thought to have been cooler, the climate model shows slightly wetter summers in some highland areas, but drier winters overall. It is difficult to confirm *Artemisia's* expansion in the northern highlands, due to limited proxy evidence. The MaxEnt model did not show increases in *Artemisia* distribution in northwestern Mexico, although this pollen type is frequently present in diagrams from this area. In this case, different species of *Artemisia* were probably involved.

Picea appears prominently along volcanic peaks in the TMVB, according to the MaxEnt model's LGM results. This result is in agreement with pollen evidence showing *Picea* in this area at that time. However, *Picea* is restricted to elevations above approximately 2000 m and did not extend into the Valley of Mexico. MaxEnt also projected *Picea* to expand in the northwestern area, which is in agreement with the pollen evidence.

MaxEnt shows a slightly wider distribution for *Liquidambar* during the LGM than today's distribution, particularly downslope toward the Gulf of Mexico. However, the MaxEnt results show no LGM populations in the Valley of Mexico, which is in conflict with the fossil pollen evidence. Although the bioclimatic envelope used here may be imperfect, *Liquidambar*, like *Picea*, has very specific climatic requirements and is a good candidate for this type of modeling.

As was the case for *Liquidambar, Taxodium* does not appear in the Valley of Mexico during the LGM. There is very little pollen evidence available for this taxon, but a *Taxodium* log dated to nearly 23K BP was found in Tlapacoya, Mexico City (Quintero-González, 1986). The LGM sections of several pollen diagrams from the Valley of Mexico include the *Cu-Ju* (*Cupressus-Juniperus)* pollen type, which is usually interpreted as an indicator of a drier climate. Unfortunatley *Taxodium*, *Juniperus,* and *Cupressus* pollen cannot be identified to the species level, so the evidence is not conclusive.

Finally, *Liquidambar* was used to test two different realizations of LGM climate models. The results show that there is a significant effect on the results. This is particularly true if the climate variables used are especially sensitive, as was the case with the coldest temperature of the coolest month during the LGM. Although annual precipitation was another important variable in *Liquidambar's* distribution, the cool temperature variable was more crucial to the prediction of presence or absence of *Liquidambar.*

Table 4.1: Summary of palynological records spanning the LGM and key taxa present.

Author	**Taxa of interest**	**Details**
Byrne (1982) DSDP480	*Picea, Artemisia*	Both appear in the record. *Picea* is sporadic (1-2%), but present through the early Holocene. *Artemisia* has a steady presence during the LGM, increasing later, around 15K BP.
Meyer (1973) Cuatro Cienegas	complacent	
Metcalfe *et al* (2002) Alta Babicora	*Picea*	*Picea* is present at high percentages (20%) through the LGM.
Watts and Bradbury (1982) Patzcuaro	*Abies, Artemisia, Isoetes*	*Artemisia* and *Abies* both present in trace amounts. *Isoetes* takes on importance (increase) during the LGM as a moisture indicator.
González-Quintero (1986) Lorenzo and Mirambell (1986) Chalco, Tlapacoya	*Taxodium, Picea, Abies*	*Taxodium* log dated immediately prior to LGM (23K BP). Traces of *Picea, Abies*.
Lozano-Garcia *et al* (2005) Santa Cruz Atitzlipan, Upper Lerma	*Poaceae*, *Artemisia, Abies*	Authors focus on *Poaceae,* but both *Artemisia* and *Abies* appear during the LGM in minor amounts.
Ohngemach and Straka (1989) Tlaxcala, Jalapasquillo	*Picea, Abies, Liquidambar*	All three taxa appear in the record. *Liquidambar* possibly result of long-distance dispersal.
Lozano-Garcia and Ortega-Guerrero (1998) Texcoco	*Picea, Isoetes, Abies, Liquidambar*	Low, but steady percentages.
Montúfar-Lopez (1987) Alta Babicora	*Abies*	Predominant conifer in the diagram. Contradicts Metcalfe *et al.* (2002)
Sears and Clisby (1955) Texcoco	*Abies*	Presence of *Abies* in Valley of Mexico

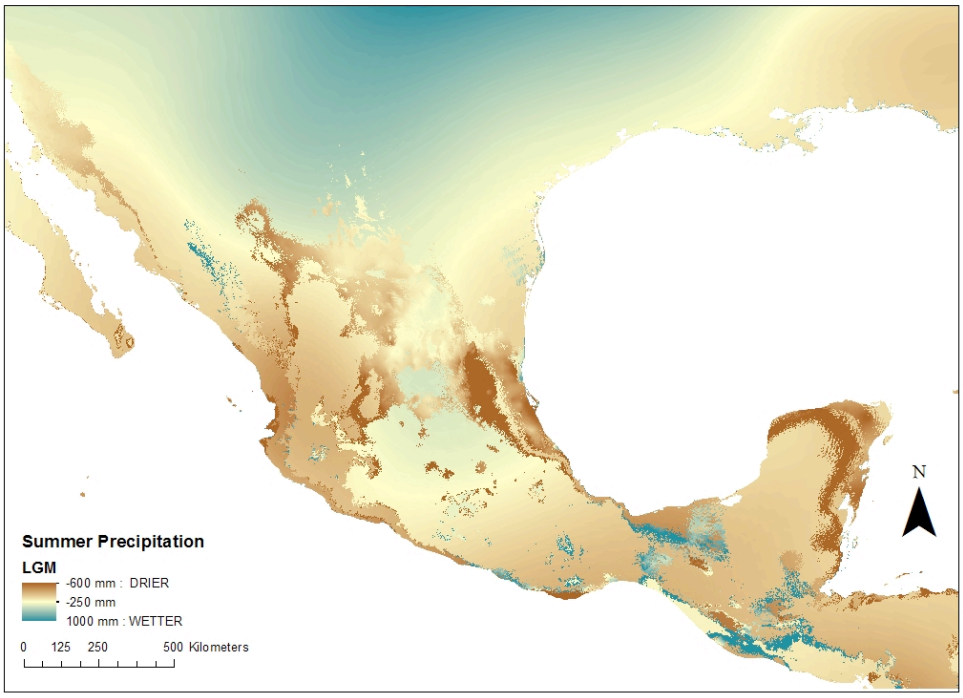

Figure 4.1: Differences in summer precipitation during the LGM, based on climate models.

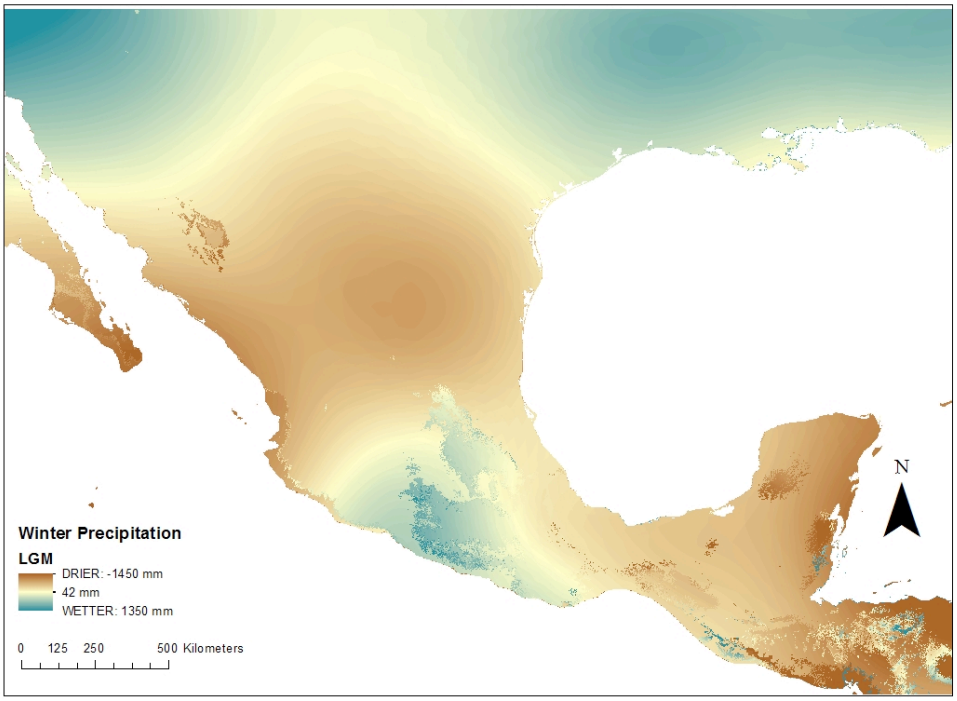

Figure 4.2: Differences in winter precipitation during the LGM, based on climate models.

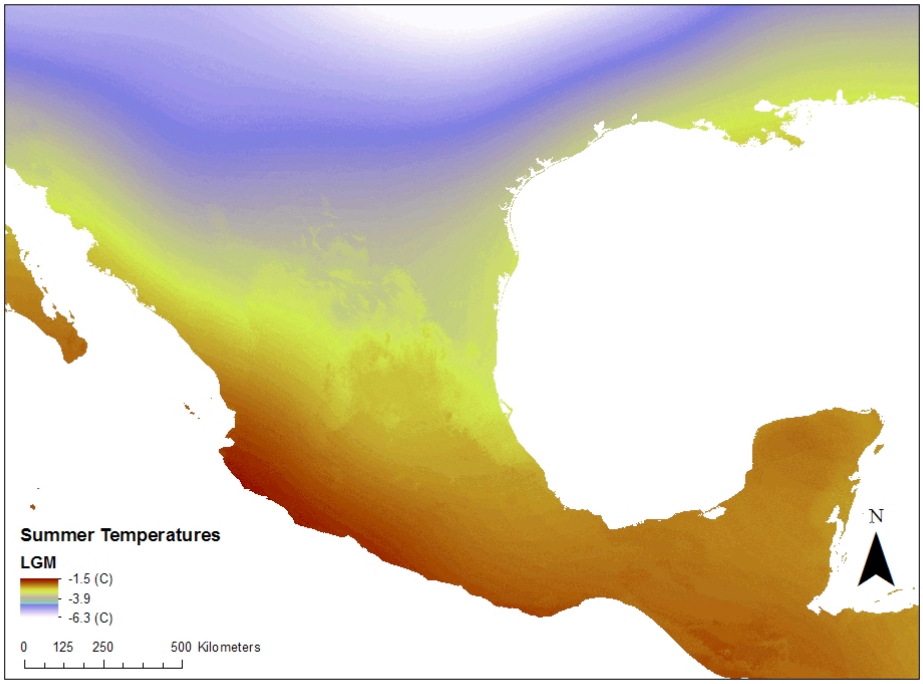

Figure 4.3: Differences in summer temperatures between the LGM and the present.

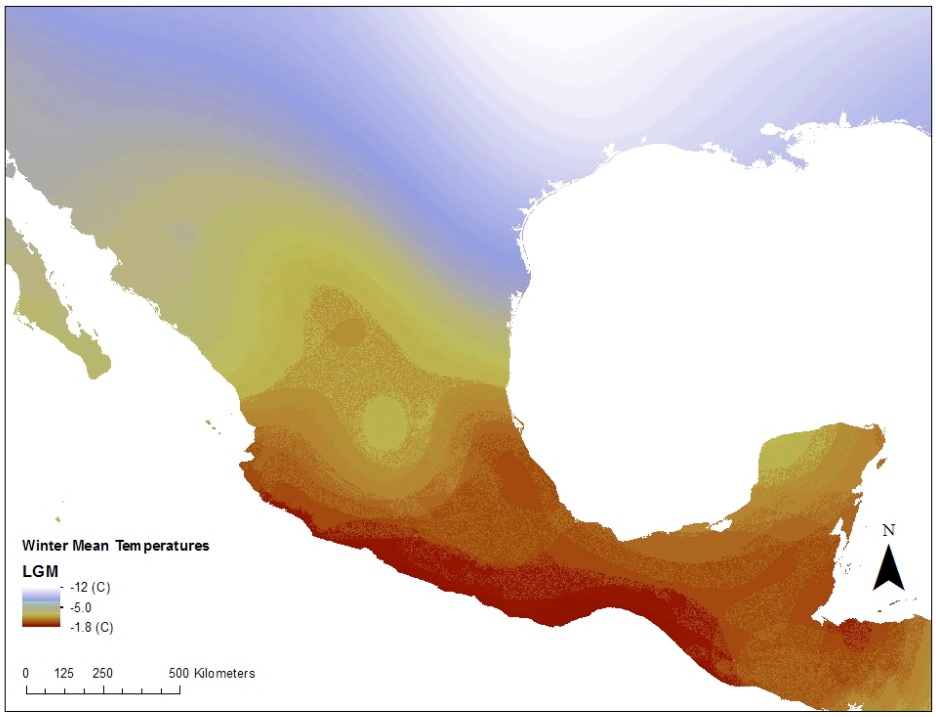

Figure 4.4: Differences in winter mean temperatures between the LGM and present.

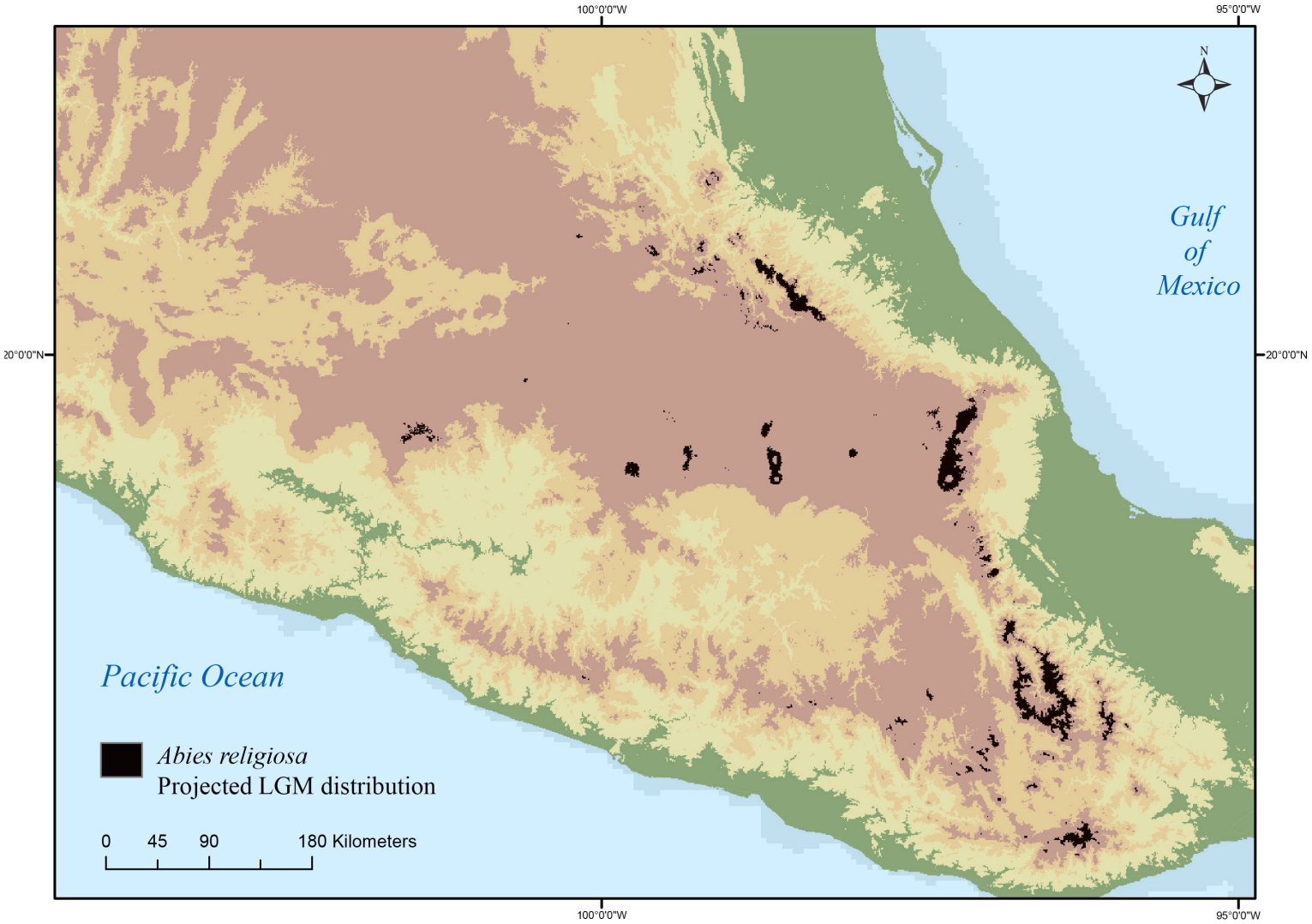

Figure 4.5: Projected LGM distribution for *Abies religiosa*

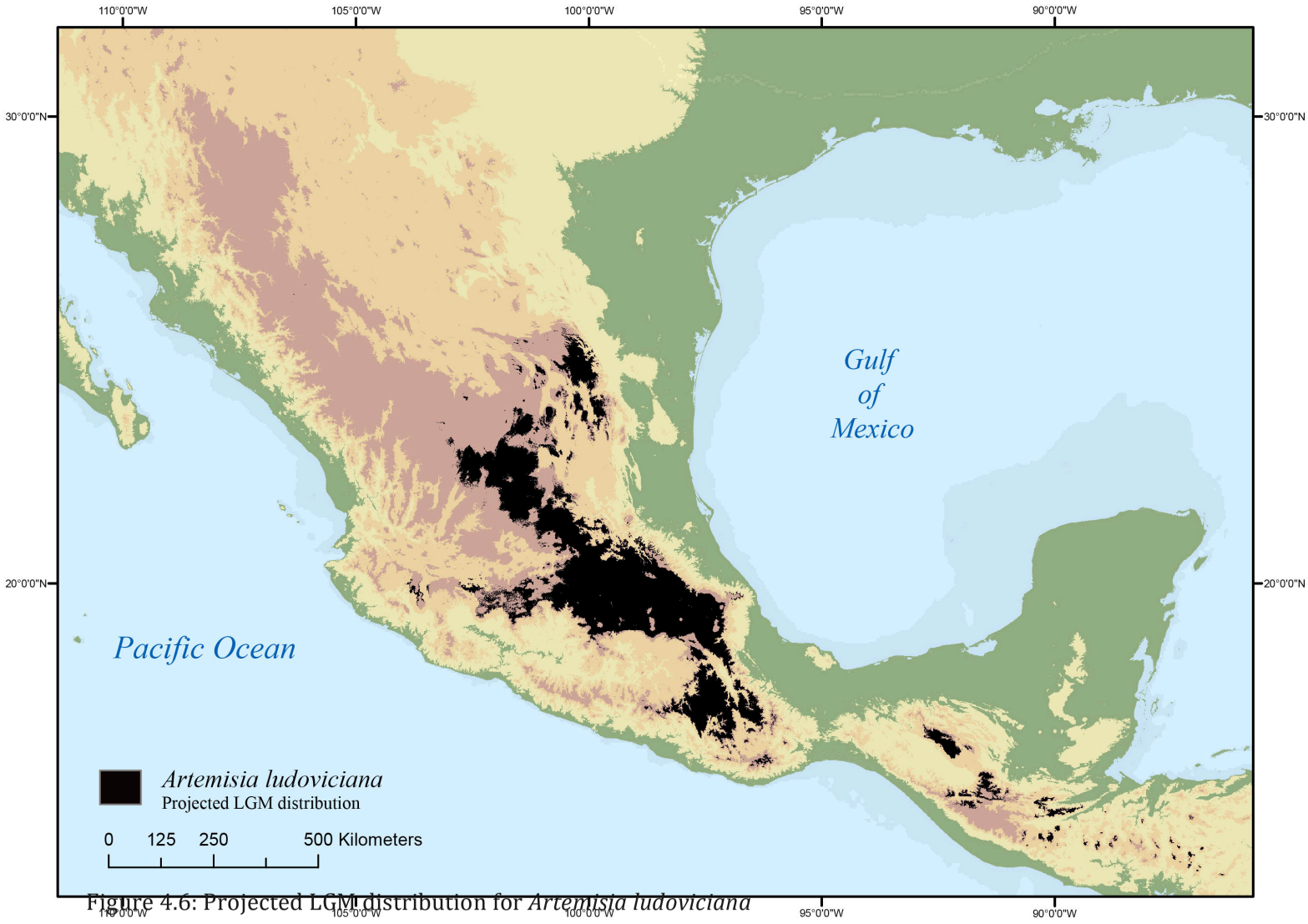

Figure 4.6: Projected LGM distribution for *Artemisia ludoviciana*

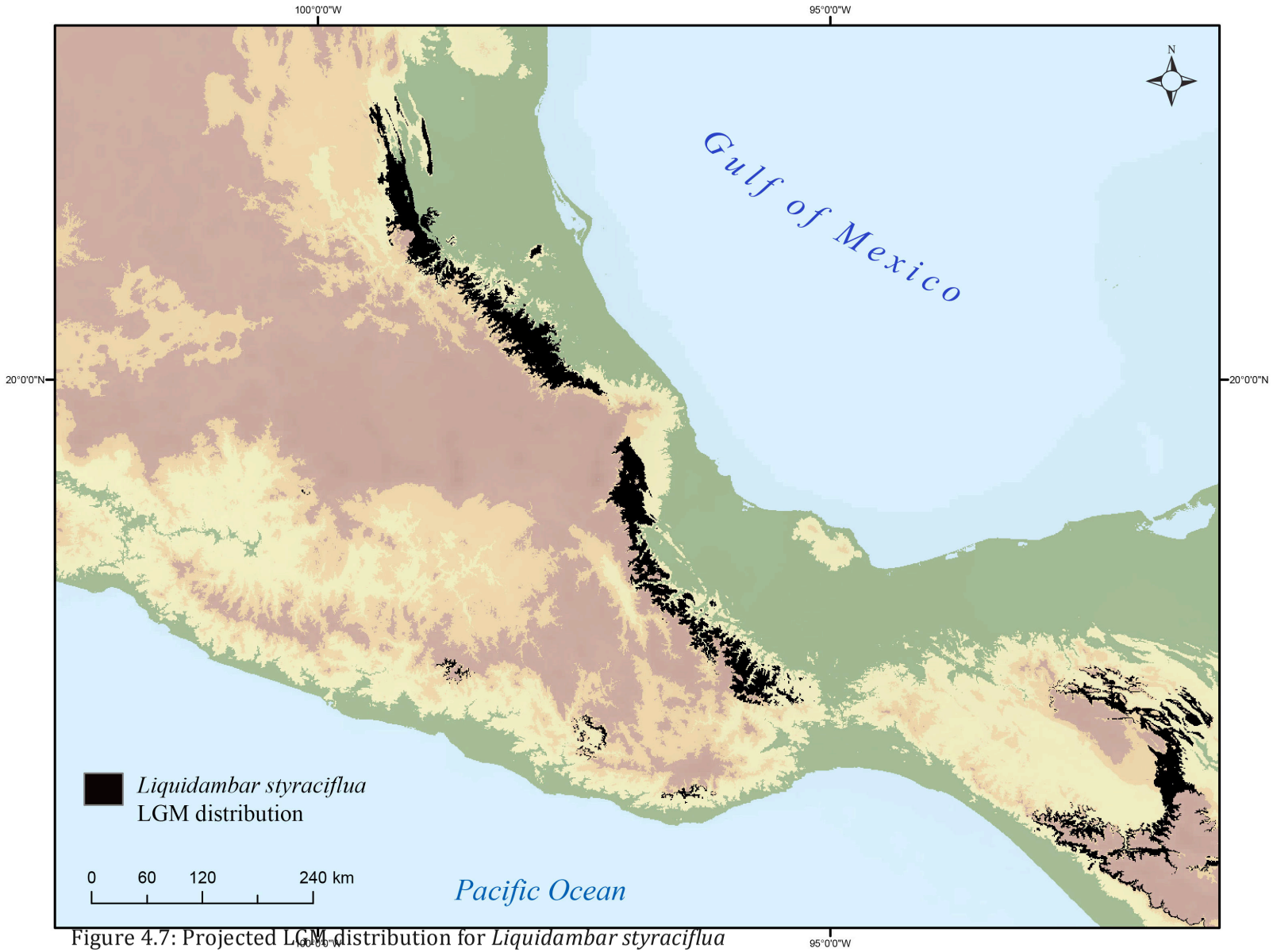

Figure 4.7: Projected LGM distribution for *Liquidambar styraciflua*

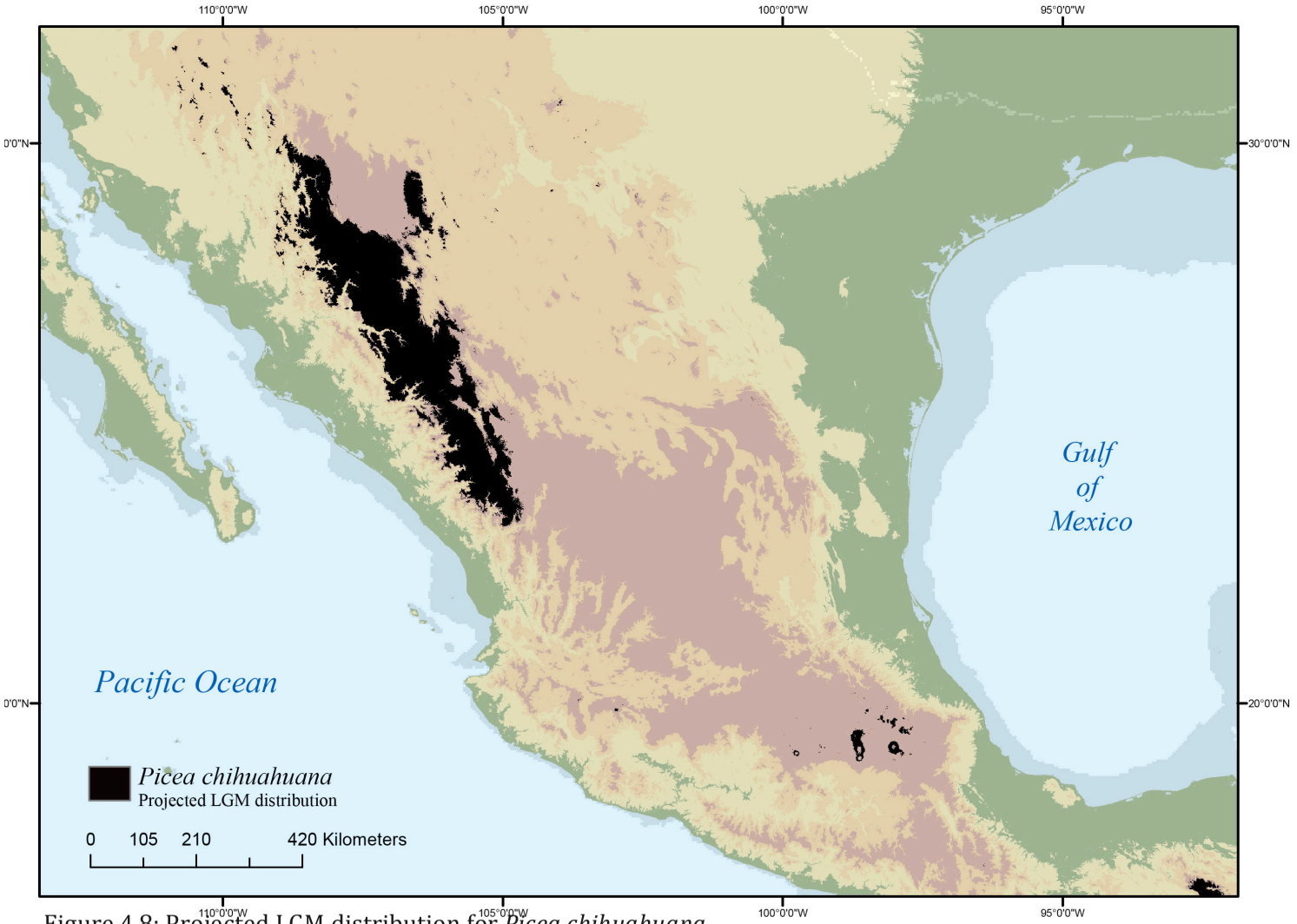

Figure 4.8: Projected LGM distribution for *Picea chihuahuana*

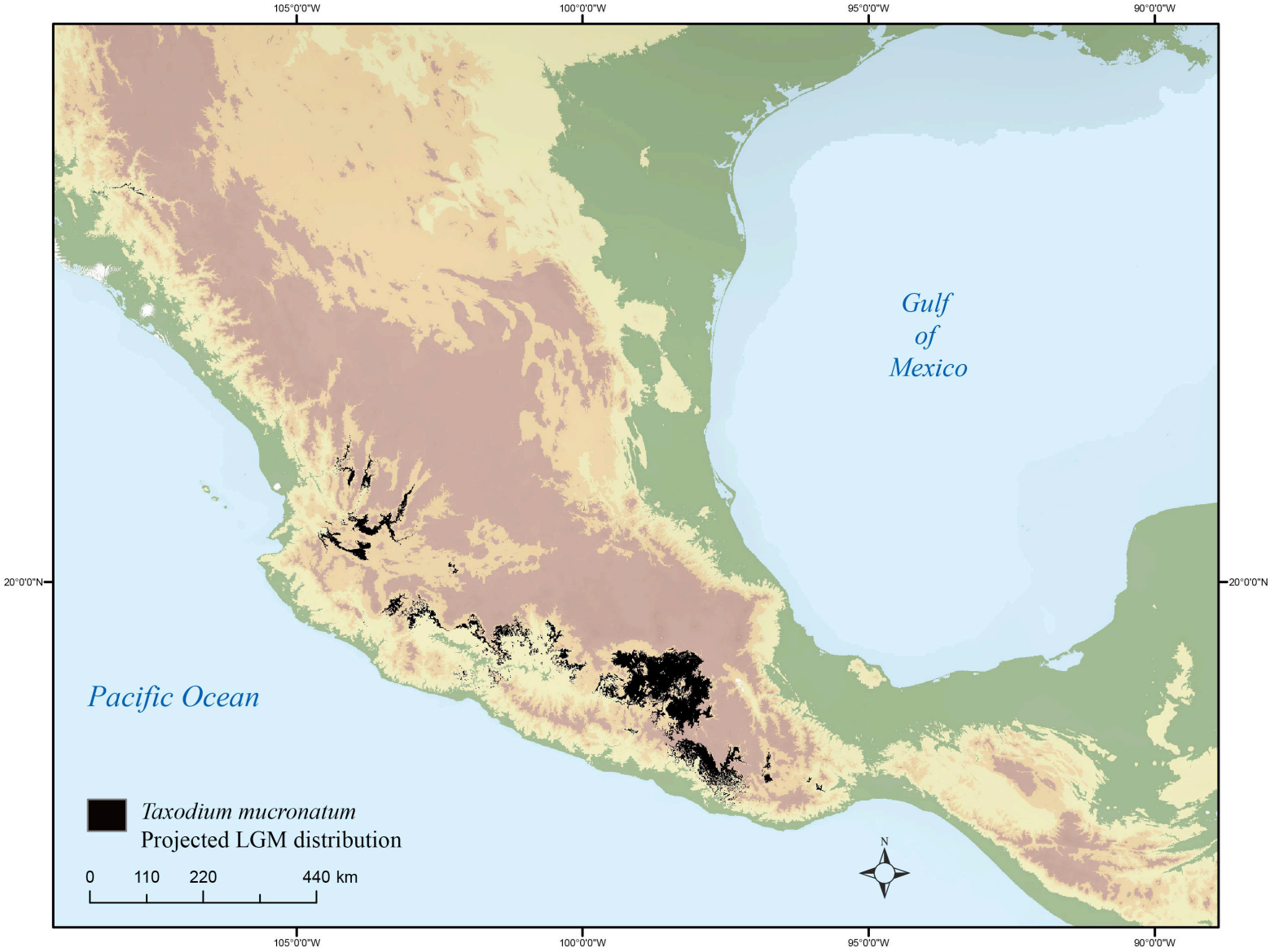

Figure 4.9: Projected LGM distribution for *Taxodium mucronatum*

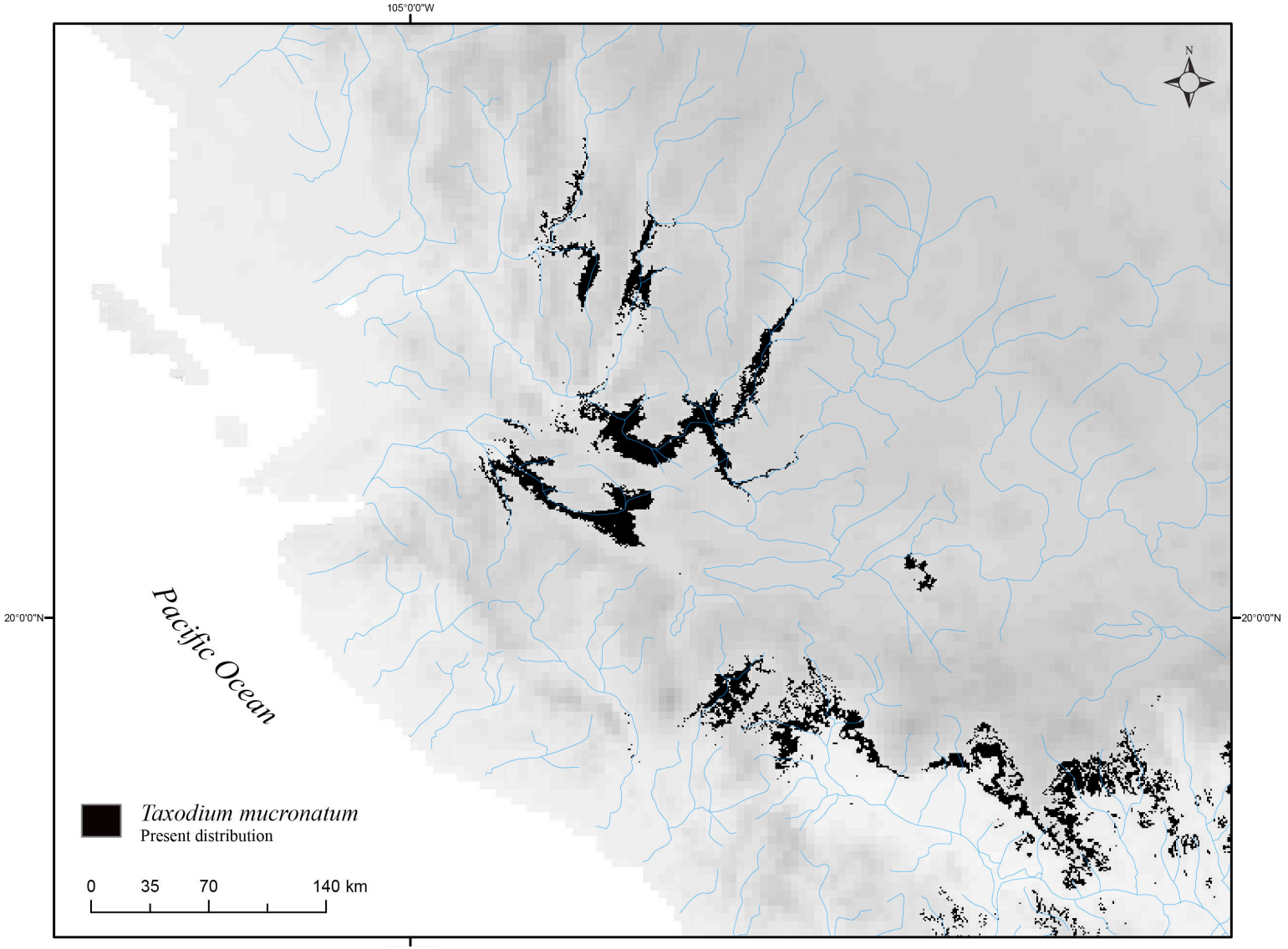

Figure 4.10: *Taxodium mucronatum's* riverine pattern (MaxEnt)

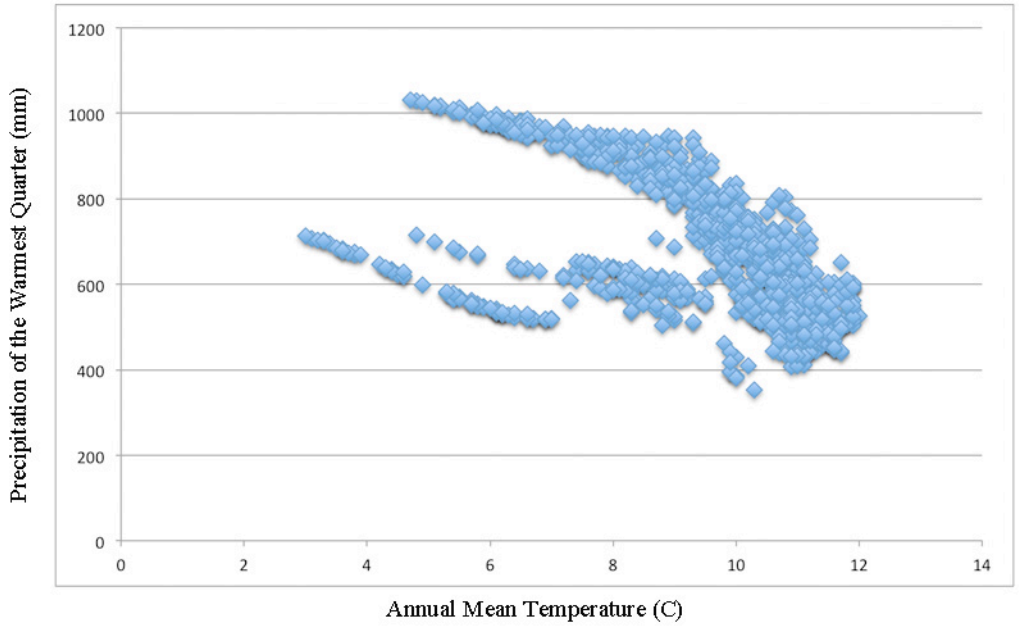

Figure 4.11: Precipitation vs. Temperature relationship for *Abies religiosa* MaxEnt model

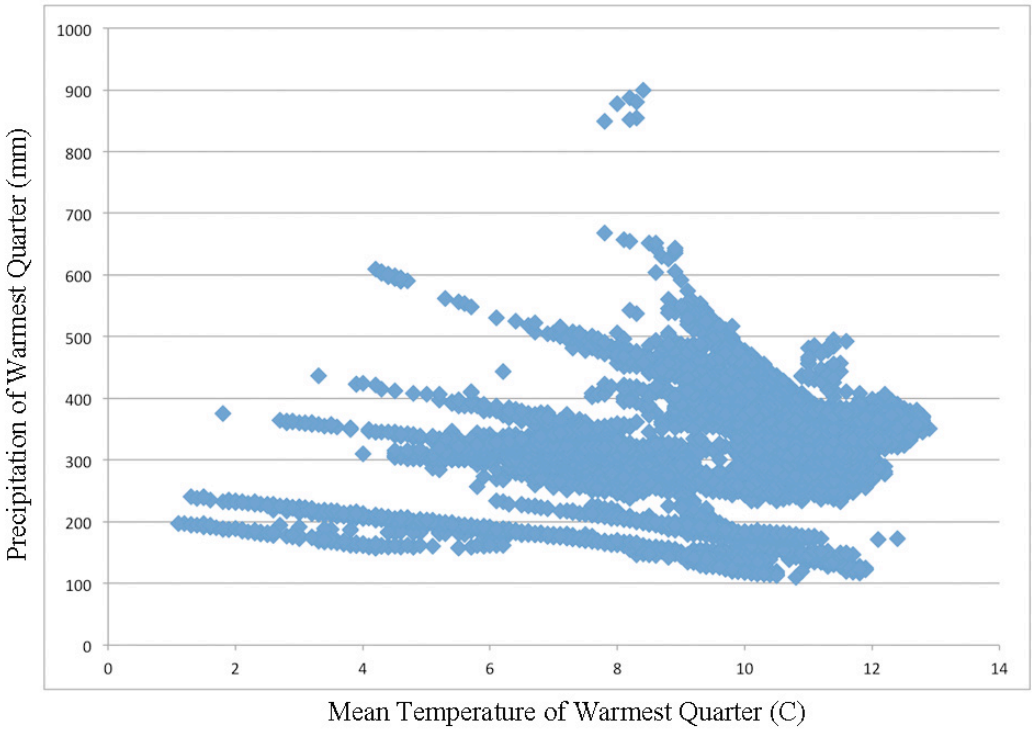

Figure 4.12: Precipitation vs. Temperature relationship for *P. chihuahuana* MaxEnt model

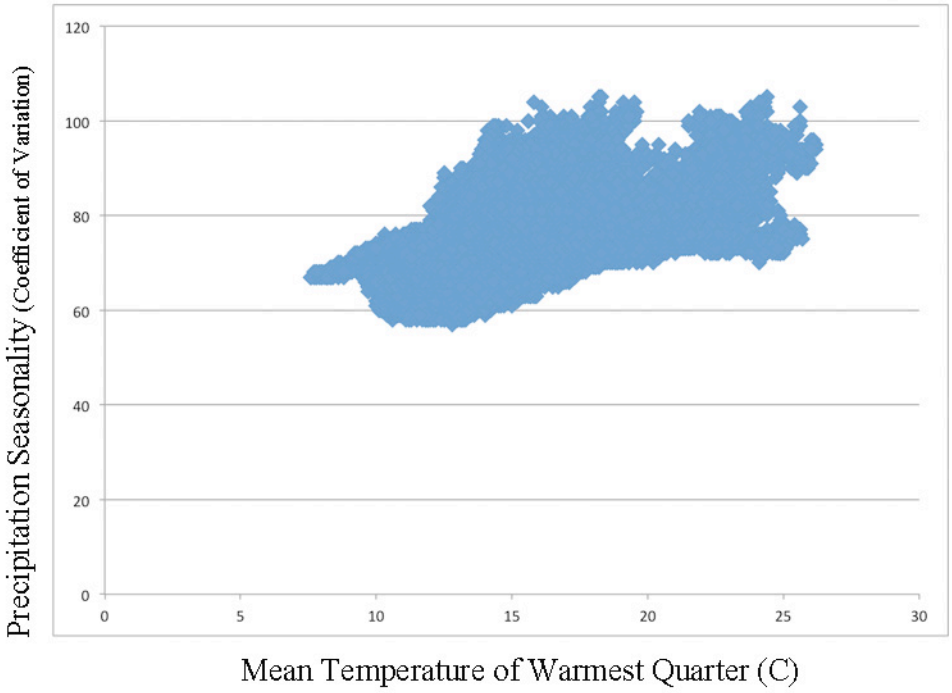

Figure 4.13: Precipitation vs. Temperature for *Artemisia ludoviciana* MaxEnt model

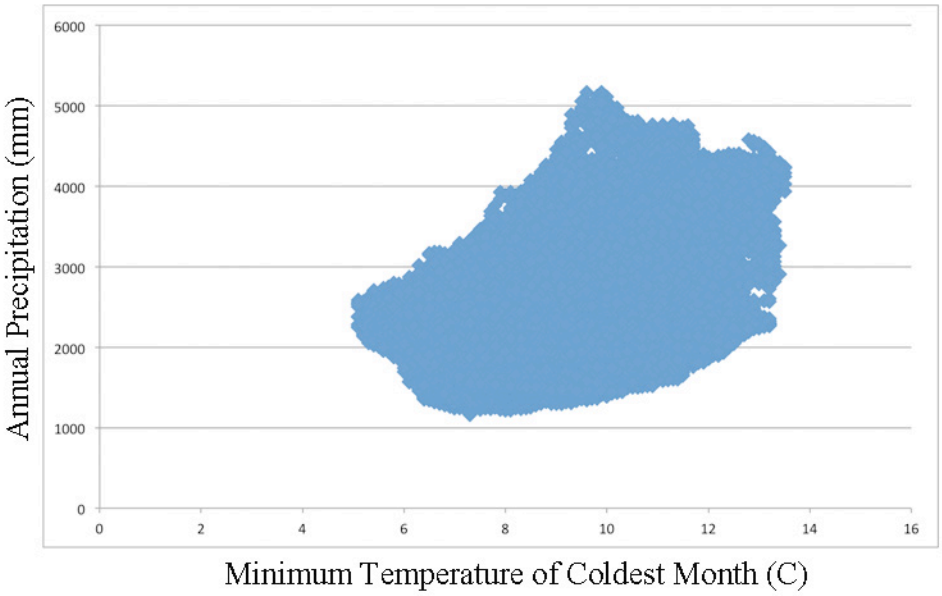

Figure 4.14: Precipitation vs. Temperature for *Liquidambar styraciflua* MaxEnt model

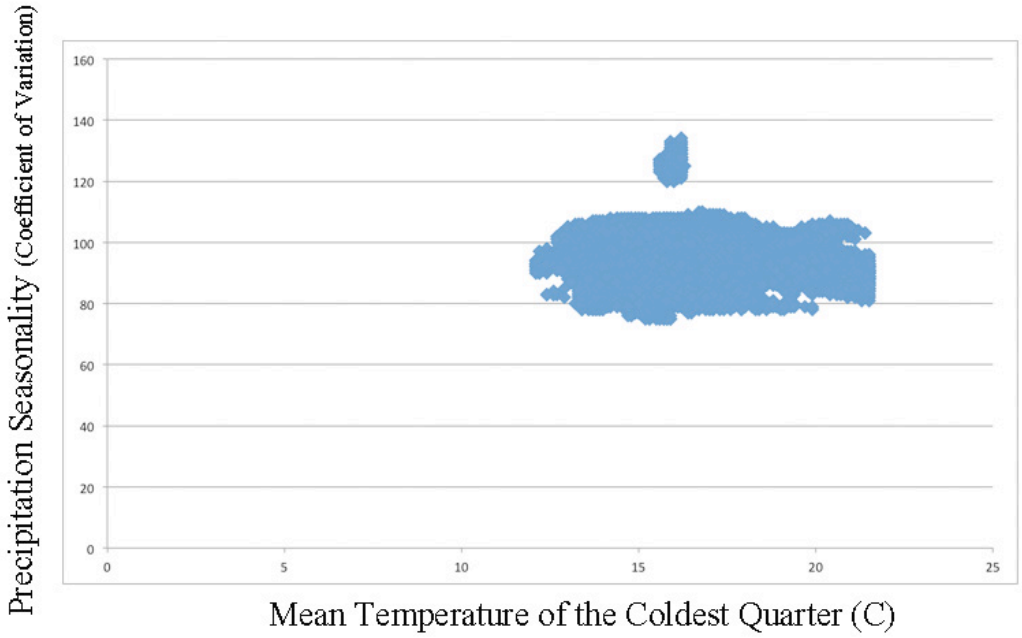

Figure 4.15: Precipitation vs. Temperature for *Taxodium mucronatum* MaxEnt model

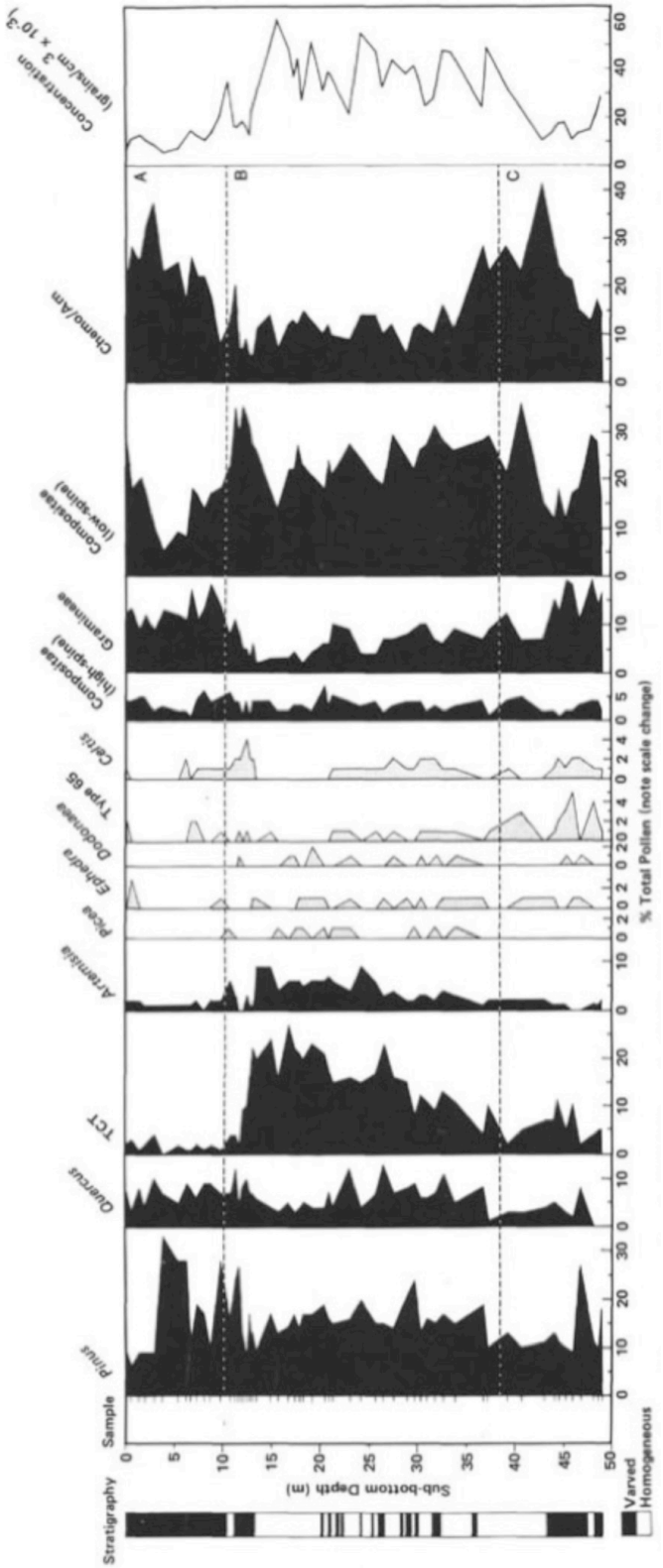

Figure 4.16: Byrne's (1982)record from the Gulf of Mexico, DSDP 480

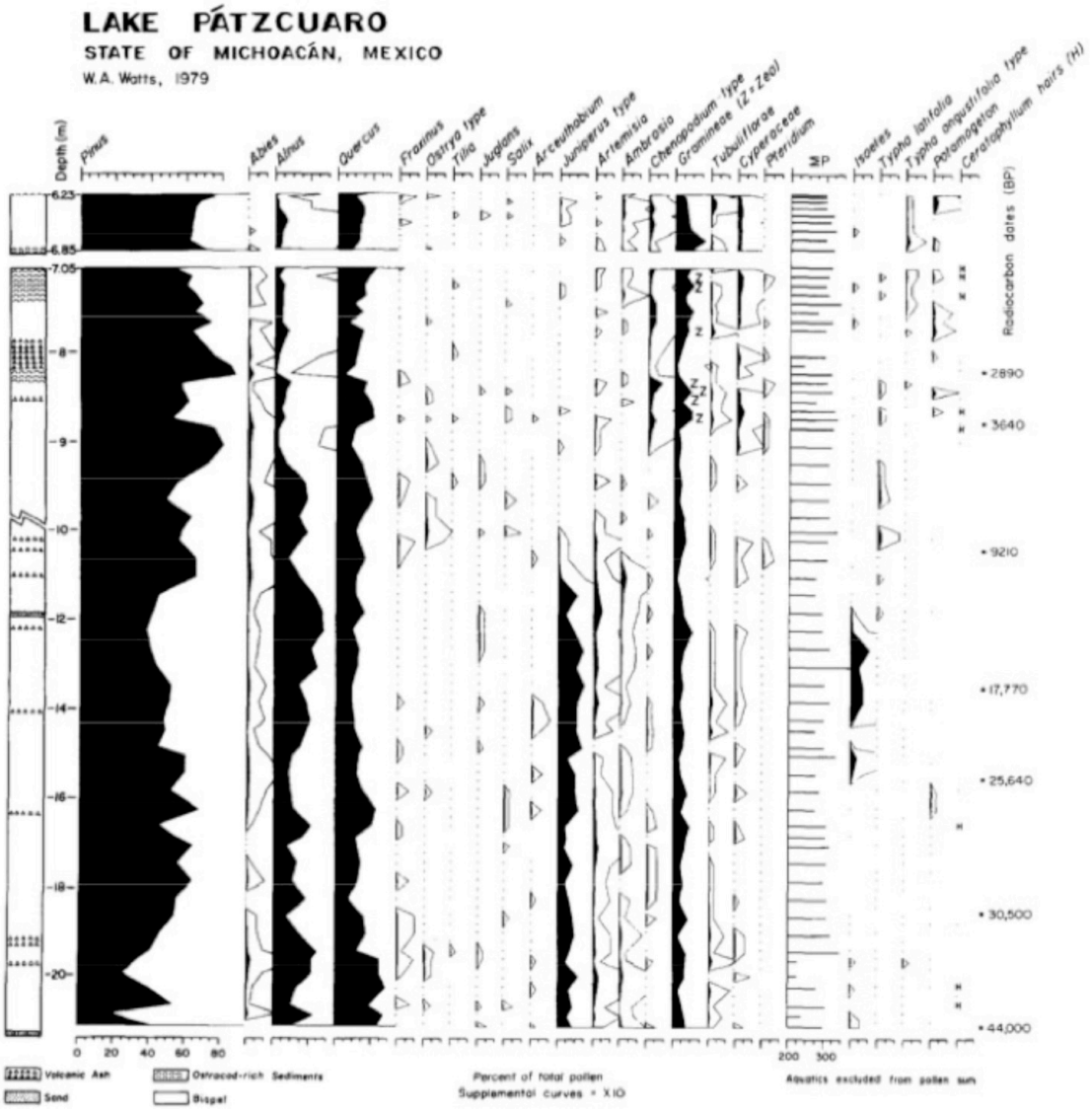

Figure 4.17: Watts & Bradbury's (1982) long record from Patzcuaro.

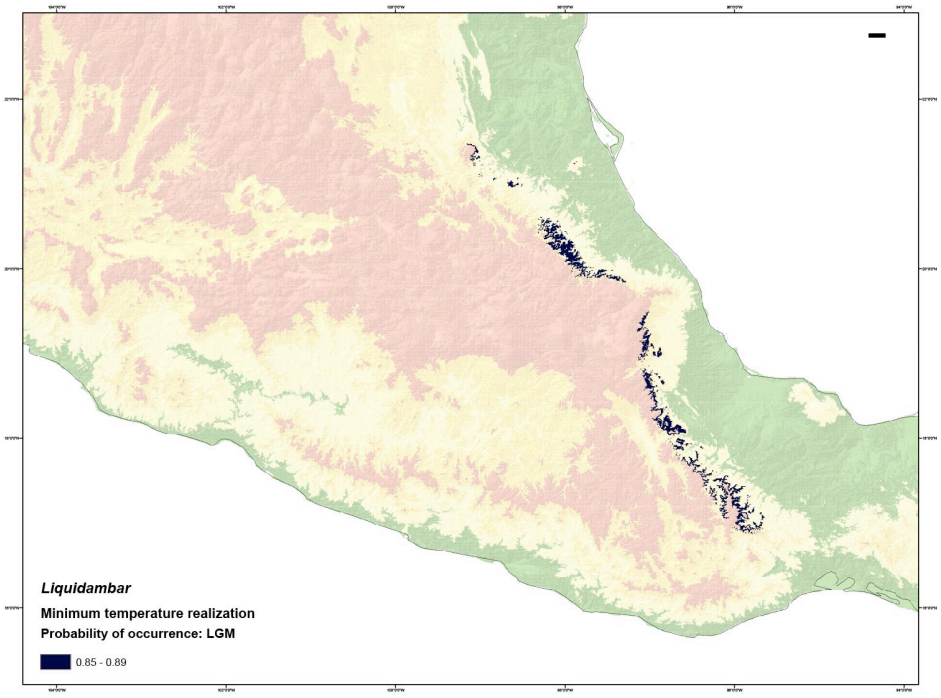

Figure 4.18a: Minimum PC loading for LGM, *Liquidambar styraciflua*

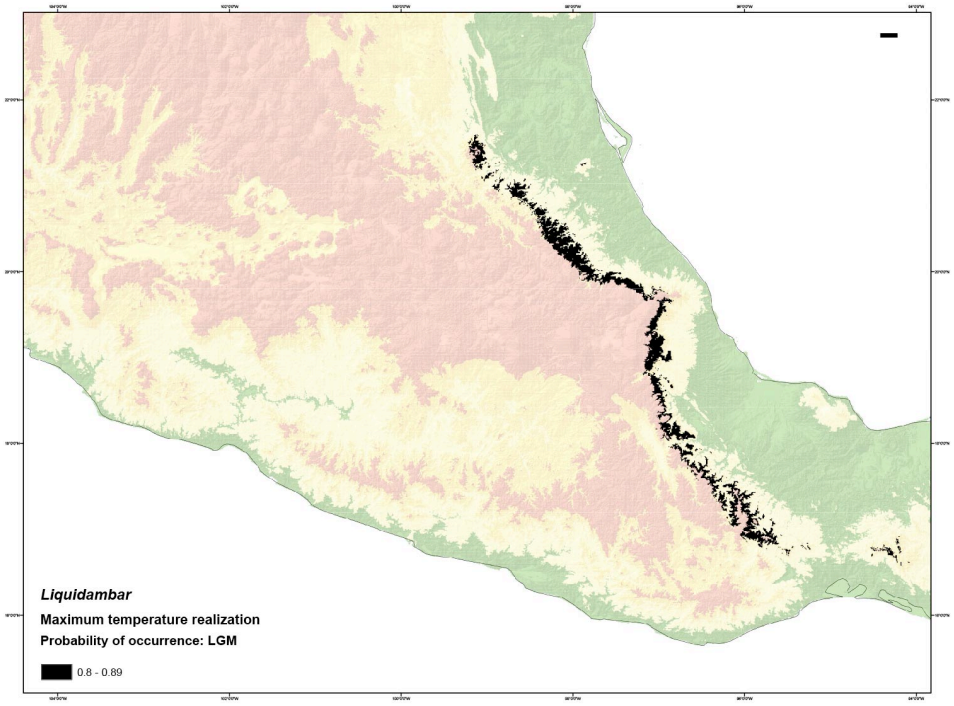

Figure 4.18b: Maximum PC loading for LGM, *Liquidambar styraciflua*

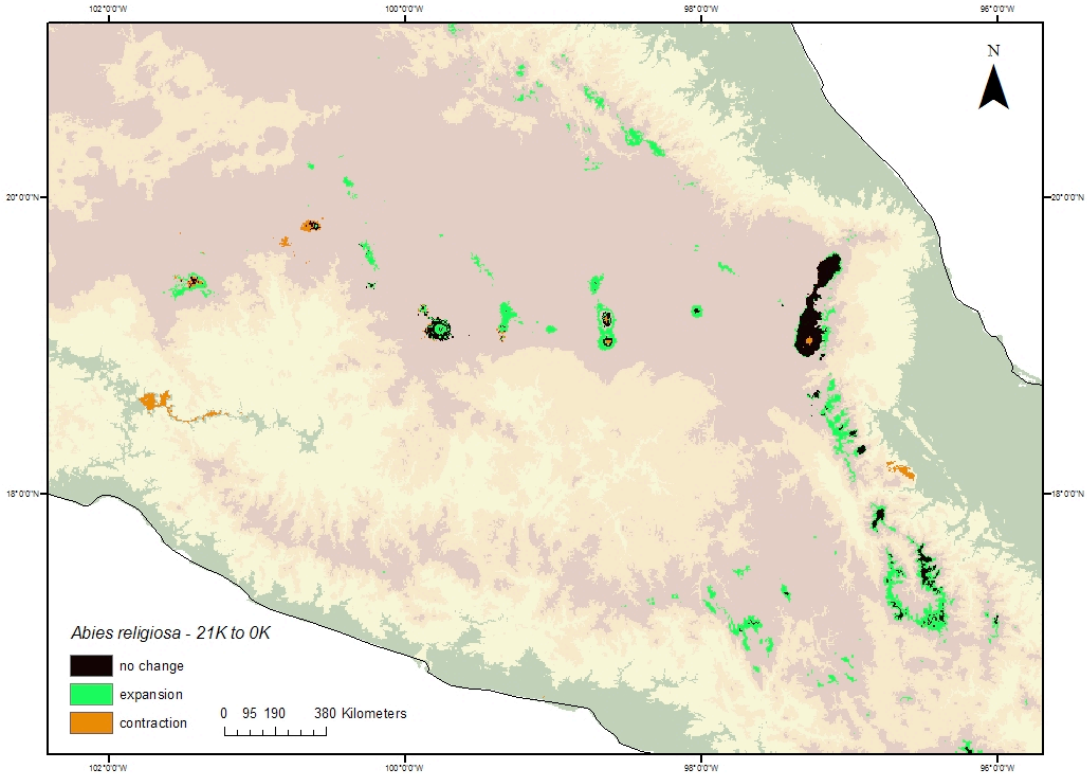

Figure 4.19: *Abies religiosa* change map between 21K and 0K.

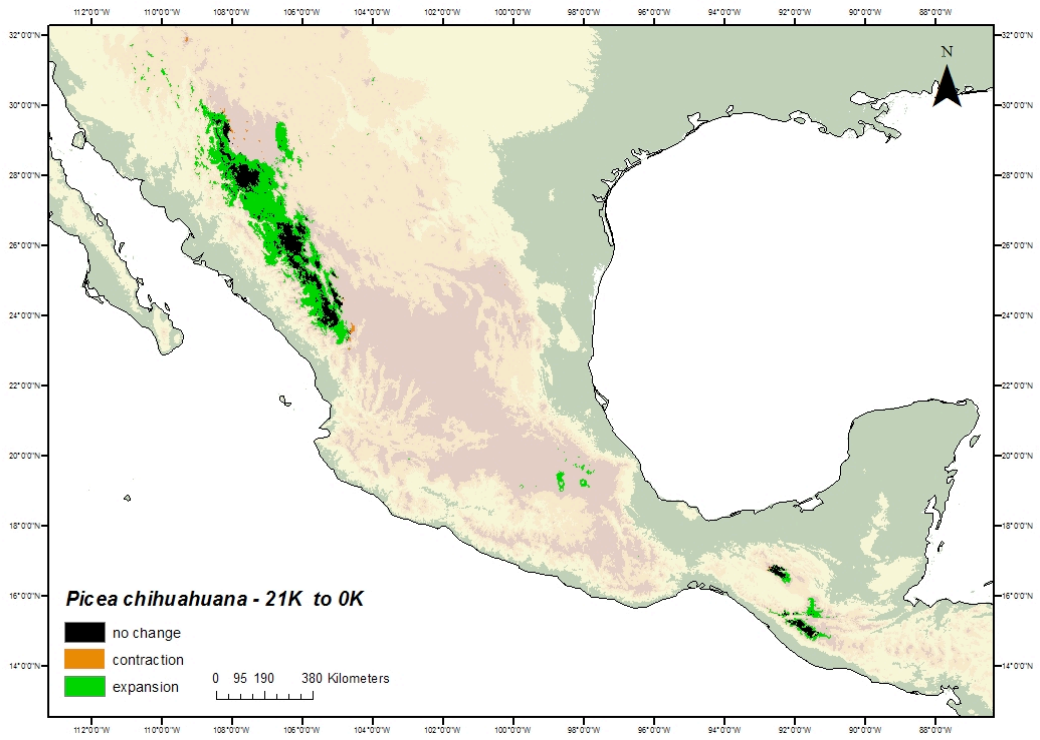

Figure 4.20: *Picea chihuahuana* change map between 21K and 0K

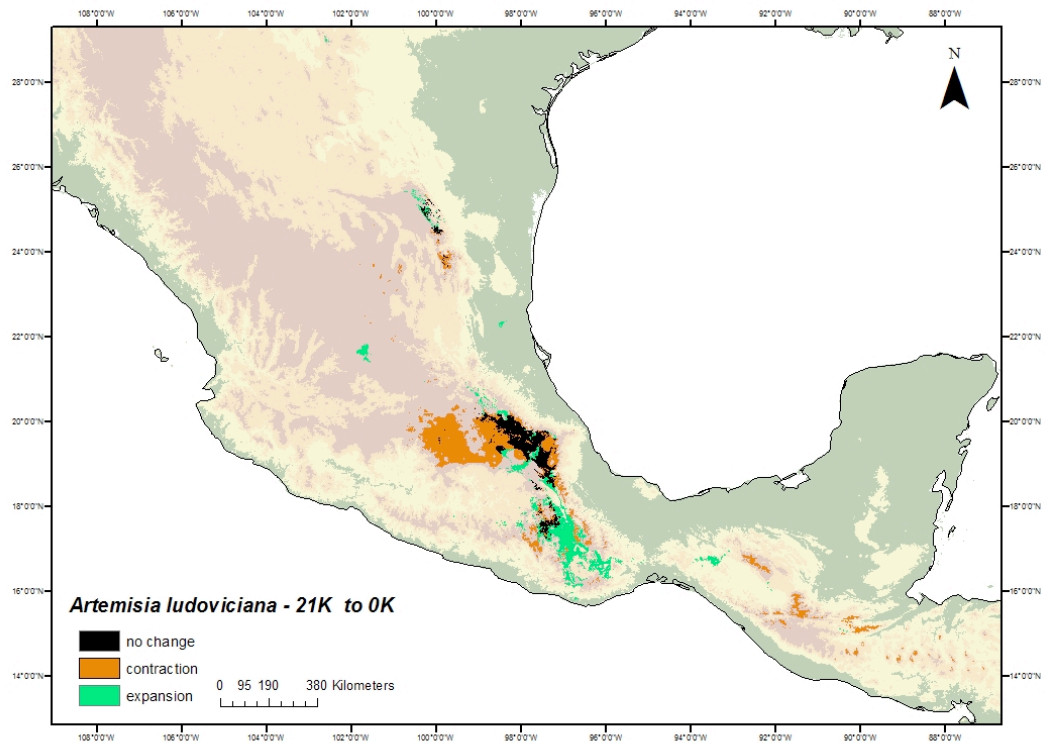

Figure 4.21: *Artemisia ludoviciana* change map between 21K and 0K.

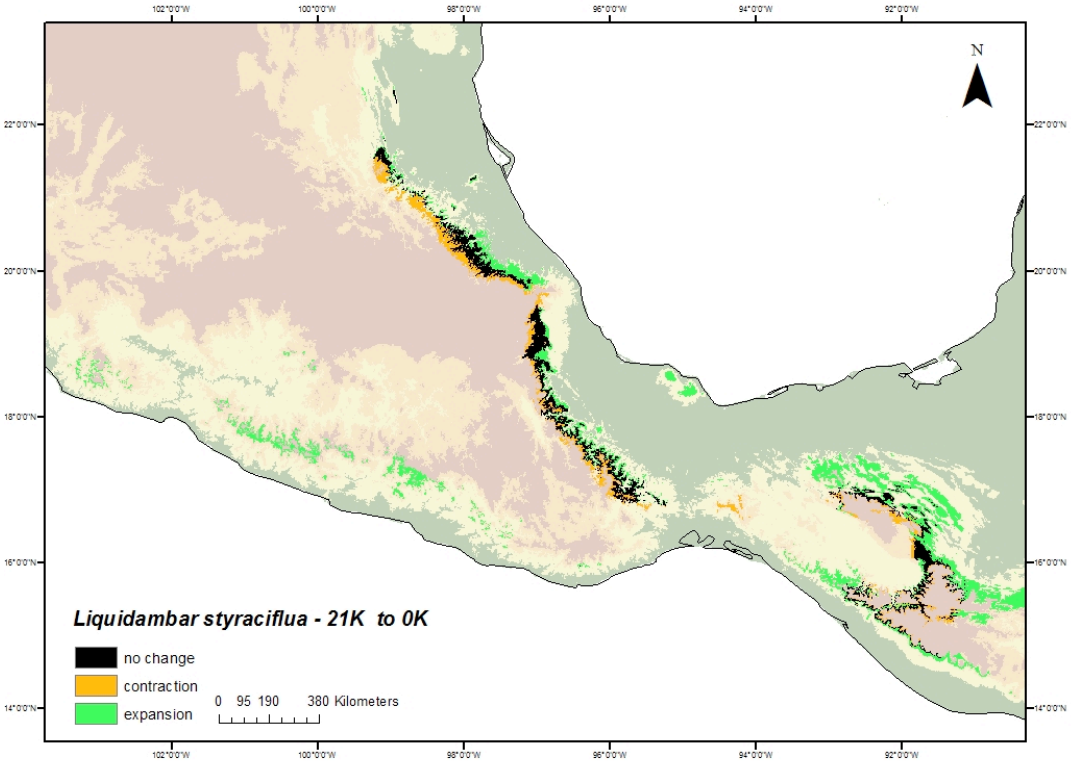

Figure 4.22: *Liquidambar styraciflua* change map between 21K and 0K.

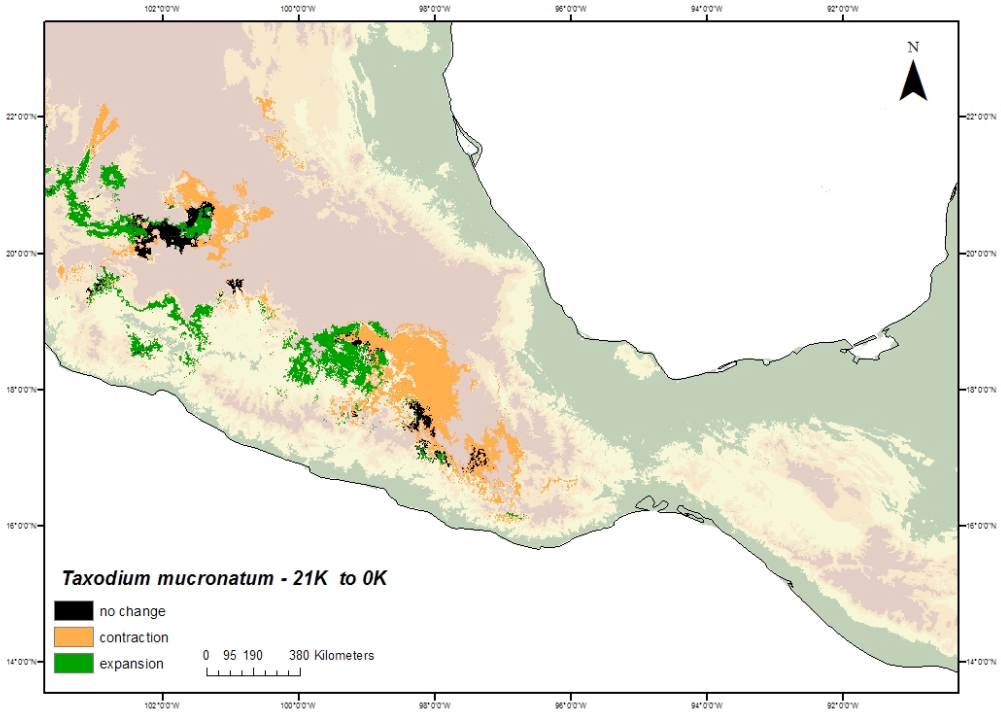

Figure 4.23: *Taxodium mucronatum* change map between 21K and 0K.

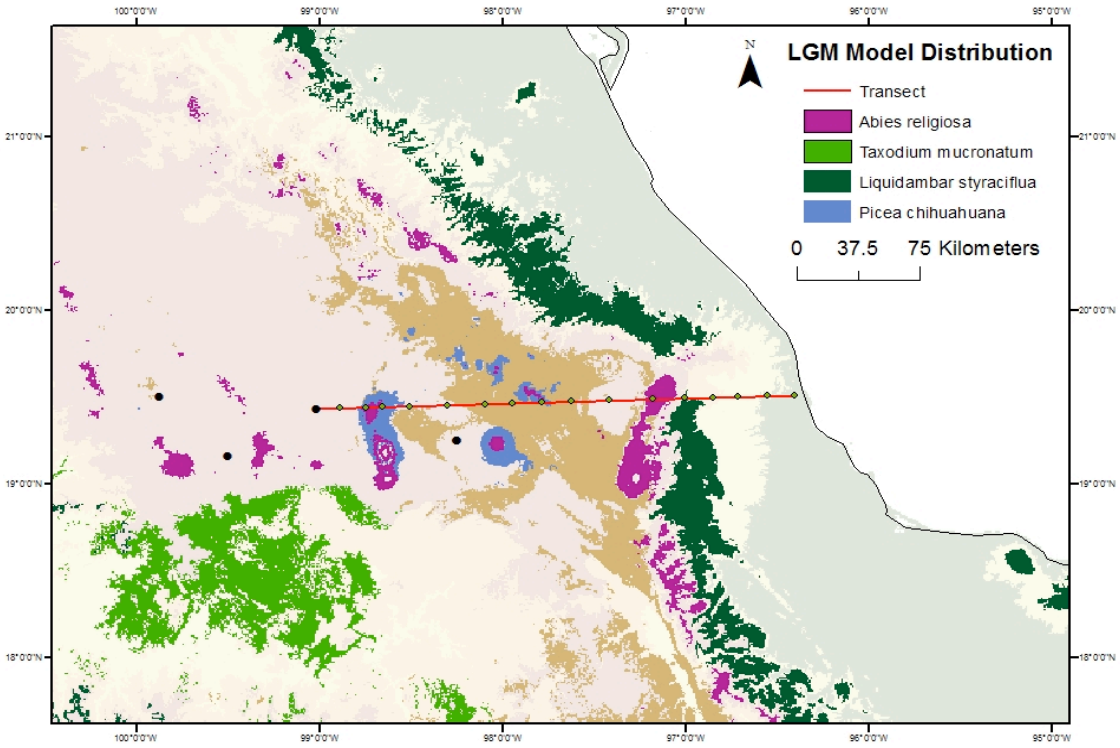

Figure 4.24: MaxEnt results for all species, including a transect from the Valley of Mexico to the coastal plain.

REFERENCES

Brunner, C. (1982) Paleoceanography of surface waters in the Gulf of Mexico during the late Quaternary. *Quaternary Research,* **17**, 105–119.

Byrne, R. (1982) Preliminary pollen analysis of Deep Sea Drilling Project Leg 64, Hole 480, cores 1-11. In: R. Curray and D.G. Moore, Editors, *Initial Reports of the Deep Sea Drilling Project*. 64, U.S. Govt. Printing Office, Washington. 1225–1237 Pt. 2.

Caballero, M., Lozano-García, S., Vázquez-Selem, L., Ortega, B. (2010). Evidencias de cambio climático y ambiental en registros glaciales y en cuencas lacrustes del centro de México durante el último máximo glacial. *Boletin de la Sociedad Geológica Mexicana* **62**, 359-377.

Calvert, W. H. & Brower, L. P. (1986) The location of the monarch butterfly (Danaus plexippus L.) overwintering colonies in Mexico in relation to topography and climate. *Journal of the Lepidoptera Society*, **40**, 164-187.

Chiang, J.C.H. (2010). Extraction of PMIP2 mid-Holocene and LGM anomalies for use in WORLDCLIM. Unpublished raw data.

Deevey, E.S. (1944) Pollen analysis and Mexican archaeology: and attempt to apply the method. *American Antiquity,* **10**, 135–149.

Dyke, A. S., & Prest, V. K. (1987). Late Wisconsinan and Holocene history of the Laurentide ice sheet. *Géographie physique et Quaternaire*, **41,** 237-263.

Farjon, A. (1990) Pinaceae: drawings and descriptions of the genera *Abies, Cedrus, Pseudolarix, Keteleeria, Nothotsuga, Tsuga, Cathaya, Pseudotsuga, Larix,* and *Picea.* Koeltz Scientific Books, Konigstein, Germany.

http://www.gbif.org (See full citation in Appendix 3)

González-Quintero, L. (1986) Análisis polínicos de los sedimentos. In: J.L. Lorenzo and L. Mirambell, Editors, *Tlapacoya: 35,000 años de historia del Lago de Chalco*, pp. 157–166, Instituto Nacional de Antropología e Historia, Mexico City.

Gordon A.G. (1968) Ecology of Picea chihuahuana Martínez. *Ecology*, **49**, 880–896.

Harrison, S. P. A., Kutzbach, J. E., Liu, Z., Bartlein, P. J., Otto-Bliesner, B., Muhs, D., & Thompson, R. S. (2003). Mid-Holocene climates of the Americas: a dynamical response to changed seasonality. *Climate Dynamics*, **20,** 663-688.

Hijmans, R.J., S.E. Cameron, J.L. Parra, P.G. Jones & Jarvis, A. (2005) Very high resolution interpolated climate surfaces for global land areas. International Journal of Climatology, **25**, 1965-1978.

Hoey M.T. & Parks, C.T. (1994) Genetic divergence in *Liquidambar styraciflua*, *L. formosana*, and *L. acalycina* (Hamamelidaceae), *Systematic Botany*, **19**, 308–316.

Huante, P, Rincón, E., Swetnam, T.W. (1991). Dendrochronology of *Abies religiosa* in Michoacan, Mexico. *Tree-Ring Bulletin,* **51,** 15-28.

Kim, S.J., Crowley, T.J., Erickson, D.J., Govindasamy, B., Duffy, P.B., & Lee, B.Y. (2008) High-resolution climate simulation of the last glacial maximum. *Climate Dynamics,* **31,** 1-16.

Ledig FT, Hodgskiss P.D., Krutovskii K.V., Neale D.B. & T. Eguiluz Piedra, (2004) Relationships among the spruces (*Picea, Pinaceae*) of southwestern North America. *Systematic Botany*, **29**, 275–292.

Ledig, T.L, Rehfeldt, G.E., Sáenz-Romero, C. & C. Flores-López (2010) Projections of suitable habitat for rare species under global warming scenarios, *American Journal of Botany,* **97**, 970–987.

Lozano-García, S., Sosa-Nájera, S., Sugiura, Y. & Caballero, M. (2005) 23,000 yr of vegetation history of the Upper Lerma, a tropical high-altitude basin in Central Mexico. *Quaternary Research*, **64**, 70–82.

Lozano García, M. S. & B. Ortega Guerrero (1998) Late Quaternary environmental changes of the central part of the Basin of Mexico; correlation between Texcoco and Chalco basins. *Review of Palaeobotany and Palynology*, **99**, 77–93.

McDonald, J. A. (1993) Phytogeography and history of the alpine-subalpine flora of northeastern Mexico. In: Biological diversity of Mexico: origins and distribution (T. P. Ramamoorthy, R. Bye, A. Lot, and J. Fa, eds.). pp. 681-703, Oxford: Oxford University Press.

Metcalfe, S.E. A. Say, S. Black, R. McCulloch & O' Hara, S.L. (2002) Wet conditions during the last glaciation in the Chihuahuan desert, Alta Babicora Basin, Mexico. *Quaternary Research*, **57**, pp. 91–101.

Montúfar-Lopez, A. (1987). *Estudio polínico de la alta Babícora, Chihuahua*, Departamento de Prehistoria, Instituto Nacional de Antropología e Historia, *Estudios Scientificos,* **38.**

Morris A.B., Ickert-Bond S.M., Brunson D.B., Soltis D.E., & Soltis P.S. (2008) Phylogeographical structure and temporal complexity in American sweetgum (*Liquidambar styraciflua*; Altingiaceae). *Molecular Ecology*, **17** 3889-3900.

Poore, R. Z., Pavich, M. J., & Grissino-Mayer, H. D. (2005). Record of the North American southwest monsoon from Gulf of Mexico sediment cores. *Geology*, **33,** 209-212.

Straka, H. & Ohngemach, D. (1989) Late Quaternary vegetation history of the Mexican highland. *Plant Systematics and Evolution*, **162**, 115-32.

Watts,W.A. & Bradbury, J.P. (1982) Paleoecological studies at Lake Patzcuaro on the west-central Mexican Plateau and at Chalco in the basin of Mexico, *Quaternary Research*, **17**, 56-70.

5. CHAPTER FIVE

SUMMARY

In this dissertation, I present five bioclimatic envelope models for three distinct time periods, the present, the mid-Holocene (6K BP), and the Last Glacial Maximum (21K BP) in Mexico. The goal of my work has been to compare bioclimatic model results with available paleoproxy records, and thereby evaluate late Quaternary climate and vegetation change.

Chapter One offers the reader a brief summary of the ecological and biogeographical literature to show how the study of plant distribution has evolved over the past 300 years. It also covers the basic principles of bioclimatic envelope modeling methods and illustrates a fundamental "disconnect" between practitioners of proxy-based interpretation and those who produce bioclimate envelope models. Finally, I provide a very brief introduction to study area, Mexico.

In Chapter Two, I discuss the study area in more detail, and present detailed summaries of five plant species that have shown particular sensitivity to climate changes in Mexico. The species are *Picea chihuahuana, Abies religiosa, Artemisia ludoviciana, Taxodium mucronatum* and *Liquidambar styraciflua.* The goal of the chapter is to model the present-day distribution in Mexico for these five climatically sensitive species, and to compare the model results to the known distributions of the corresponding species, some of which are available as digital data derived from herbarium specimens. Once the present-day distributions were evaluated, I projected the models into the mid-Holocene and Last Glacial Maximum time periods (Chapters Three and Four).

In terms of the present-day modeling effort, three species (*Picea chihuahuana, Abies religiosa* and *Liquidambar styraciflua)* have particularly narrow climate preferences, making them excellent candidates for the bioclimatic envelope approach. The distributions of *Artemisia ludoviciana* and *Taxodium mucronatum* are more complicated and these species therefore cannot be modeled strictly in terms of their bioclimatic envelopes. The resulting distribution maps for these two species reflect this issue, and illustrate the importance of careful selection of species for modeling applications. Although both *Taxodium mucronatum* and *Artemisia ludoviciana* are sometimes important in the pollen record, their distribution maps are difficult to produce for different reasons. In the case of *Taxodium mucronatum*, incorporating additional non-climate variables into the model may have improved the result (e.g. riparian corridors). However, without having a clear understanding of paleo-geomorphology, it is risky to project such a variable into the past time period. For *Artemisia*, the broad climatic range and broad subspecies distribution through Mexico make it difficult to map accurately.

In Chapter Three, I present results for the mid-Holocene for each of the five species. The models from Chapter Two were projected onto the mid-Holocene climate variable space using the MaxEnt projection feature. As Chapter Two suggested, the models for the three species with narrow climate envelopes, particularly for *Abies religiosa* and *Liquidambar styraciflua,* generated good results that agreed well with the limited pollen records available in Mexico to some extent. However, *Picea's* model gave the unexpected prediction of presence within the TMVB. Only one fossil pollen record

supports such a finding, and more palynological evidence must be uncovered to determine whether or not *Picea* survived in the TMVB during the mid-Holocene or if it disappeared completely by 8500 BP as one pollen record suggests. Finally as anticipated for the cases of *Taxodium mucronatum* and *Artemisia ludoviciana*, I found that the model results were not convincing when compared to the fossil pollen record.

Chapter Four, like Chapter Three, presents results based on the projection of present-day species models into a different time slice. The chapter's focus was the LGM, a time period characterized by extensive northern hemisphere ice sheets and lower greenhouse gas concentrations. Few pollen diagrams cover this time period in Mexico, but the few records that do exist are fairly complete.

In Chapter Four, I present the same five species distributions during the LGM. On comparing the results to the existing proxy records, I found good agreement between the pollen records for *Abies religiosa* and *Picea chihuahuana* and the model results. However, for the remaining species were not in agreement, particularly for the Valley of Mexico. Pollen evidence for *Liquidambar styraciflua, Taxodium mucronatum* in the Valley of Mexico suggested a much wider distribution than is seen in the model results. Reasons range from a limited climate envelope to a non-analogous climate that may have suited the species. The broad climatic range of conditions and multiple species presence are probably responsible for *Artemisia ludoviciana's* wide distribution.

In summary, the findings in this dissertation are important for several reasons: 1) recent computer-based climate envelope models are relevant to paleoecology and can provide insight into past plant species distributions, 2) species with narrow climatic ranges that have significance in the pollen record are well-suited to the envelope modeling method, while equally significant taxa with several subspecies or species and/or a broad climatic range may not meet with success, 3) a careful and critical examination of the pollen record is crucial to interpretation of results using the envelope method, 4) inclusion of the phylogenetic record (when available) is also helpful in interpreting model results, especially because fossil pollen are discernible only to the taxon level, while genetic evidence provides helpful clues about species distribution.

APPENDIX 1: MaxEnt Principles

The basis of the MaxEnt program for geographic distributions is rooted in theoretical statistical mechanics (Phillips 2006, Jaynes 1957). The underlying question that the program attempts to address is, "How does one approximate an unknown probability distribution, and what is the best approximation?" Jaynes' solution to this question was that the best possible approximation (distribution) is one that considers all the possible constraints and has maximum entropy. The idea of a 'probability' distribution is applied widely in physics, and more recently, in ecology and species distribution. The full mathematical explanation for maximum entropy as applied to geographic distributions is in Phillips *et al* (2006). Elith *et al* (2011) provides a more intuitive approach as the principle applies to ecological distributions in space.

The maximum entropy of a distribution is described as a probability distribution that is unknown over a range of values. In a geographic application, the range of values is the landscape. The figure below helps in visualizing the probability distribution over a geographic space.

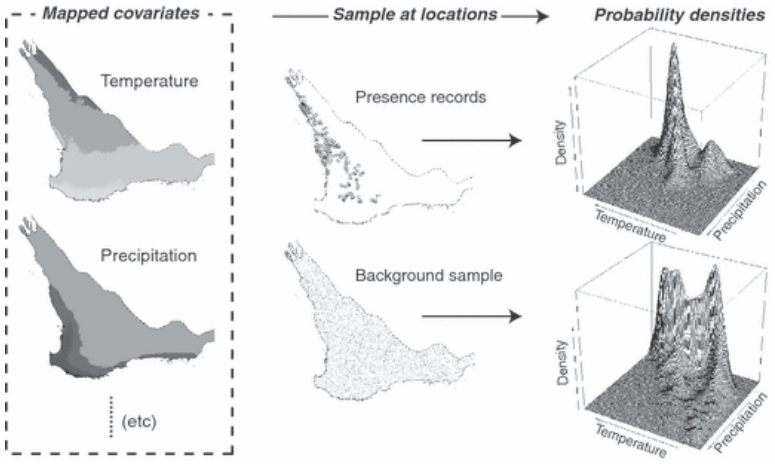

Figure 1: Visualizing MaxEnt; how probability densities relevant to our statistical explanation, may appear, given specific environmental variables. (From Elith *et al* 2011).

MaxEnt's algorithm is particularly well regarded when it comes to using presence-only data. Other species modeling methods such as regression or ordination techniques incorporate both presence and absence data, but such models are limited since absence data are not absolute. Using presence-only data still helps determine unsuitable areas (absence) for a species, simply through the pattern of suggested presence. Because MaxEnt predict a probability, one location may be less likely to contain a species than another location, although both the locations remain possibilities based on the climate envelope. The local landscape characteristics and environmental conditions are crucial factors in interpreting such results.

Applications to Ecology and Biogeography

For applications in ecology and biogeography, the question of what the ideal probability distribution is for a species (or taxon) is handled using a set of environmental variables that best suit the species. These variables constrain the distribution, creating a

bioclimatic “envelope”. In the above section, the optimal probability distribution is one described as that which satisfies maximum entropy under a set of given constraints. However, in terms of a bioclimatic envelope, one might think of the distribution more as one that minimizes relatively entropy within a co-variate space (the variables). Elith *et al* (2011) summarizes several important points about MaxEnt as they relate to applications in biogeography and ecology.

The first concern is that of spatially biased sample points. MaxEnt’s algorithm relies on an unbiased set of species locations, yet most data sets are inherently biased. The bias may be due to incomplete sampling or clustered sampling. Herbaria data, which are commonly used in ecological modeling, are frequently biased since they are usually opportunistic samples. The problem of bias may be addressed in one of two ways, 1) providing background data with biases similar to the species data bias, or 2) using a bias grid that indicates the bias in the survey data. Another possibility arises, which is that of inherently bias reflected in the landscape, such as topography, that is apparent in the survey data.

Another important concern is that of the background landscape’s range of environmental characteristics. The full environmental range for a given species should be present in the background landscape, and regions that have never been surveyed should be excluded from the background so that false positives are not prevalent.

Finally, MaxEnt uses “feature types”, which may be likened to transformations on the predictor variables (co-variates). Elith *et al* (2011) assert that reducing the co-variates to the minimum number based on an ecological understanding of the species may lead to better results, particularly in the case of small samples.

REFERENCES

Elith, J., Phillips, S.J., Hastie, T., Dudík, M., Yung, E.C. & Yates, C.J. (2011) A statistical explanation of MaxEnt for ecologists. *Diversity and Distributions*, 1**7**, 43–57.

Jaynes, E. T. (1957) Information Theory and Statistical Mechanics. II. *Physical Review*, **108**, 171-190.

Phillips, S. J., Anderson, R. P. & R.E. Schapire (2006) Maximum entropy modeling of species geographic distributions. *Ecological Modelling*. **190**, 231-259.

APPENDIX 2: PMIP2 Climate Data General Summary

The Paleoclimate Model Intercomparison Project 2 (PMIP2) is an archive of several climate-modeling efforts around the world (Bracannot, Otto-Bliesner *et al* 2007). The project serves not only as an archive, but also as a data source. Climate data from PMIP2 are readily available to researchers who submit their goals and objectives. PMIP2 focuses on two key time periods, the LGM and the mid-Holocene, primarily because the two time periods are relatively well understood at the global climate scale.

Because several models exist for the same time periods, the question of which model is "right" is foremost. In fact, none of the models is fully "correct". Rather, each model is based on slightly different approaches or algorithms. One can simply assume that the models are in agreement, and take an average of the responses. However, that approach assumes that the models agree. This may not necessarily be the case, so a fairly simple numerical analysis can help narrow how different the models are.

The question of a common response is addressed using a multivariate empirical orthogonal function (EOF) (Chiang, Appendix 5). This linear algebra method is used in many branches of science to help reduce large data sets to a few basic components that explain the maximum variance in the data. In this case, the EOF was applied to the three climate model output data sets (precipitation, sea level pressure and surface air temperature) for both the mid-Holocene and LGM. For the mid-Holocene, nine models were used, and for the LGM, five. In both cases, the hypothesized result is that of a leading EOF with the same sign, and comparable magnitudes across the models.

An advantage to having each EOF loading is that it is possible to test the sensitivity of an ecological model (to climate) by using the maximum and minimum EOF loadings.

EOF Method of Extraction for PMIP2 anomalies

The mathematical procedure to extract EOF's requires 1) a domain (region of interest) and, 2) data fields (mentioned above). The domain in this work was limited primarily to continental Mexico and the surrounding water bodies. Mexico is influenced climatically by the Gulf of Mexico to the east and the Pacific Ocean and associated storm tracks to the west. Mexico's climate is also impacted by North America's climate, particularly during the winter, although the manifestation is realized primarily via the Gulf of Mexico. As already stated, the fields on which the analysis was performed were the sea level pressure, precipitation and surface air temperature from each climate model (traditionally the "time" component) for the LGM and the mid-Holocene.

The mechanics of the EOF procedure were executed in MatLab (Chiang, 2010). A significance test ("North's rule of thumb") was applied to verify that EOF1 is well separated from the EOF2, which indicates EOF1 is reliable as a leading source of variation. In both the mid-Holocene and LGM scenarios, EOF1 was more than 30% separated, making it reliable. The results on the next page are for both the mid-Holocene and LGM EOF analyses.

In both the time slices, the magnitudes and signs of the leading PC (PC1) are comparable and the same, respectively. Thus I have concluded that although the climate models are all slightly different in their construction, they deliver results that are consistent with each other.

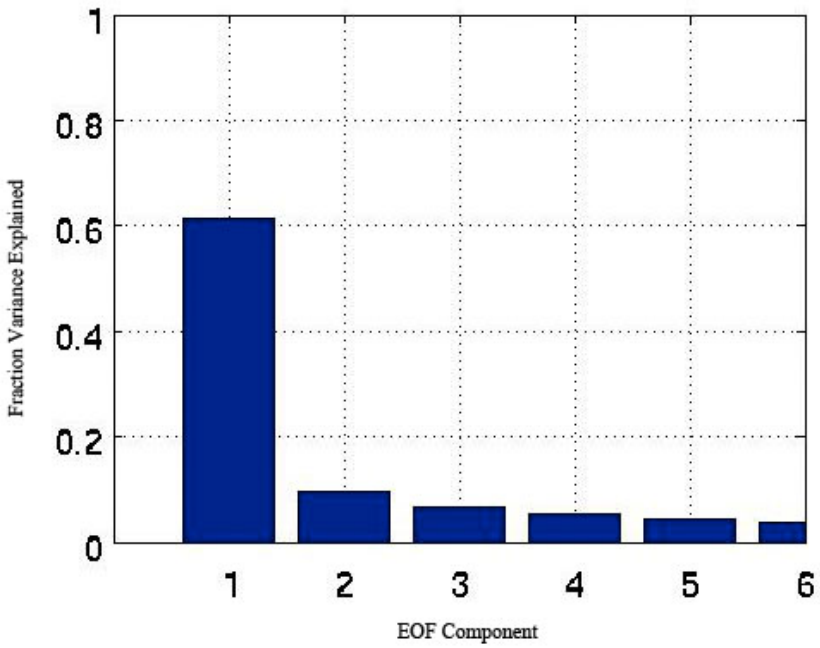

Figure A2-1: The figure above illustrates the calculated EOF's for nine mid-Holocene climate models. The leading EOF is more than 30% larger than the second EOF, fulfilling North's rule of thumb.
(Chiang, J.C.H., 2010).

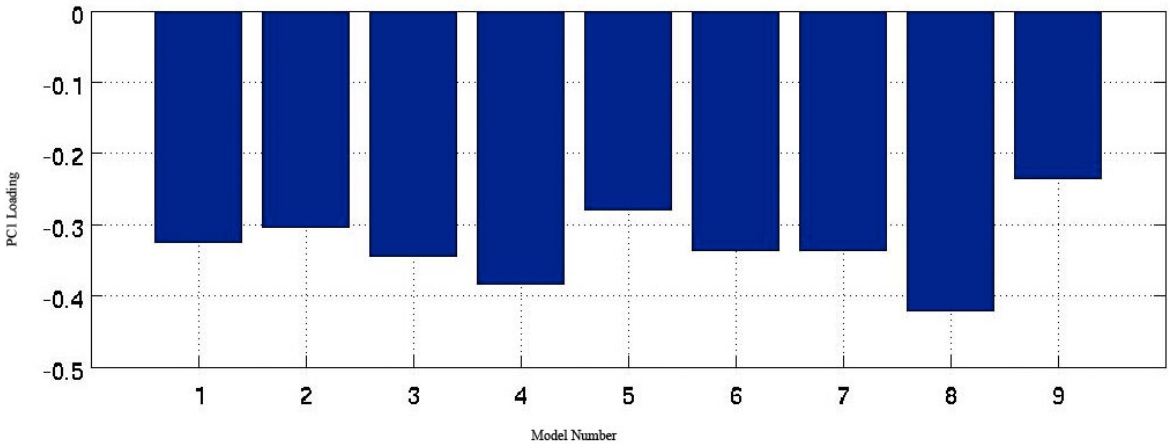

Figure A2-2: The nine model PC1 loadings for the 6K scenario (mid-Holocene). The result shows both same sign responses and similar magnitude responses. This confirms a similar response across all the models. Guide to climate models: 1='CCSM'. 2='ECHAM5', 3='FOAM', 4='GISS', 5='IPSL', 6='MIROC3.2', 7='MRI', 8='UBRIS-HadCM3M2', 9='CSIRO' (Chiang, J.C.H., 2010).

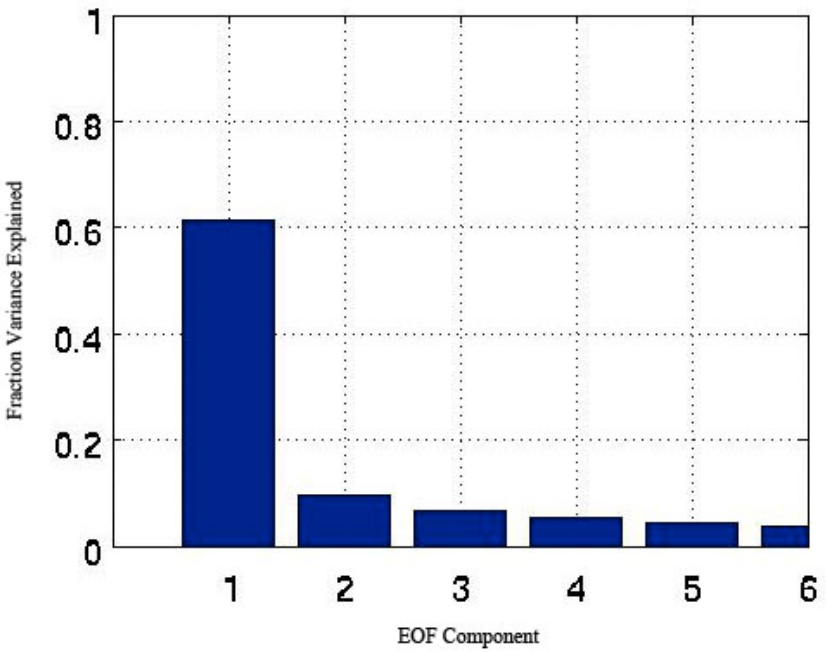

Figure A2-3: The figure above illustrates the calculated EOF's for five LGM climate models. The leading EOF is more than 30% larger than the second EOF, fulfilling North's rule of thumb. (Chiang, J.C.H., 2010).

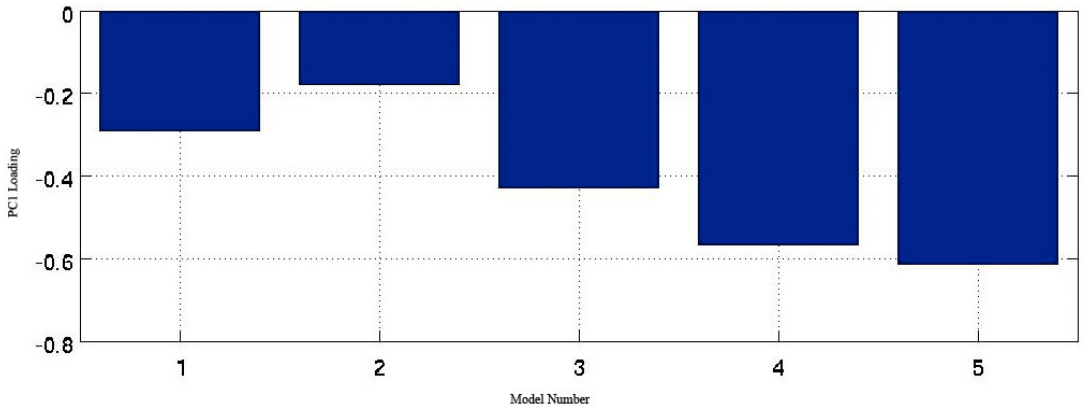

Figure A2-4: The nine model PC1 loadings for the 21K scenario (LGM). The result shows both same sign responses and similar magnitude responses. This confirms a similar response across all the models. Guide to climate models: 1='CCSM', 2='CNRM', 3='HadCM3M2', 4='IPSL', 5='MIROC3.2' (Chiang, J.C.H., 2010).

Conversion to WorldClim format

The final step in using the climate model data for ecological modeling is the conversion to a common format for such applications. The EOF anomalies found here were used to modify the WorldClim climate variables (Hijmans, Cameron, Parra, Jones & Jarvis, 2005) for both time periods. The WorldClim variable format is the collection of "ecological" variables used to construct bioclimatic envelopes. To match the existing WorldClim resolution, the EOF1 anomalies for air temperature and precipitation went through spline interpolation. They were then added to the original WorldClim average monthly mean temperature and precipitation values. Surface air temperature anomalies were also added to the WorldClim average monthly maximum and minimum temperature values. Finally, an ArcInfo script was run to generate the bioclimatic variables for the mid-Holocene and LGM (Hijmans *et al.,* 2005).

While determining the leading EOF for both time periods is helpful in generating a closer approximation of the climate for a given time, the results also help to potentially generate a range of climate scenarios in terms of sensitivity. The maximum and minimum loadings help to construct such a range.

REFERENCES

Chiang, J.C.H. (2010). Extraction of PMIP2 mid-Holocene and LGM anomalies for use in WORLDCLIM. Unpublished raw data.

Hijmans, R.J., S.E. Cameron, J.L. Parra, P.G. Jones & A. Jarvis (2005) Very high resolution interpolated climate surfaces for global land areas. *International Journal of Climatology*, **25** 1965-1978.

APPENDIX 3: Complete herbaria data retrieval

Abies religiosa

(accessed through GBIF data portal, Missouri Botanical Garden, http://data.gbif.org/datasets/resource/621)

(accessed through GBIF data portal, Herbarium de Geo. B. Hinton, Mexico, http://data.gbif.org/datasets/resource/1594)

(accessed through GBIF data portal, MEXU/Flora de Oaxaca, http://data.gbif.org/datasets/resource/8392)

(accessed through GBIF data portal, Herbario del Instituto de Ecología, A.C., Mexico (IE-XAL), http://data.gbif.org/datasets/resource/1597)

(accessed through GBIF data portal, Herbario del Instituto de Ecolog√≠a, A.C., M√©xico (IE-BAJIO), http://data.gbif.org/datasets/resource/1595)

(accessed through GBIF data portal, RBGE Herbarium (E), http://data.gbif.org/datasets/resource/8402)

(accessed through GBIF data portal, Harvard University Herbaria, http://data.gbif.org/datasets/resource/1827)

(accessed through GBIF data portal, Herbario de la Escuela Nacional de Ciencias Biologicas, Mexico (ENCB, IPN), http://data.gbif.org/datasets/resource/1601)

(accessed through GBIF data portal, Banco Nacional de Germoplasma Vegetal, M√©xico (BANGEV, UACH), http://data.gbif.org/datasets/resource/1599)

(accessed through GBIF data portal, RBGE Living Collections, http://data.gbif.org/datasets/resource/9167)

(accessed through GBIF data portal, Estudio Floristico de la Sierra de Pachuca, Hidalgo, Mexico (ENCB, IPN), http://data.gbif.org/datasets/resource/2499)

(accessed through GBIF data portal, Herbario de la Universidad de Arizona, EUA, http://data.gbif.org/datasets/resource/2479)

(accessed through GBIF data portal, UA Herbarium, http://data.gbif.org/datasets/resource/7900)

(accessed through GBIF data portal, Herbarium Berolinense, http://data.gbif.org/datasets/resource/1095)
(accessed through GBIF data portal, Repatriacion de datos del Herbario de Arizona (ARIZ), http://data.gbif.org/datasets/resource/2480)

(accessed through GBIF data portal, Botany Vascular Plant Collection, http://data.gbif.org/datasets/resource/7915)

(accessed through GBIF data portal, Herbarium of The New York Botanical Garden, http://data.gbif.org/datasets/resource/8967)

Picea chihuahuana

(accessed through GBIF data portal, Herbario del Instituto de Ecología, A.C., Mexico (IE-BAJIO), http://data.gbif.org/datasets/resource/1595)

(accessed through GBIF data portal, Herbarium de Geo. B. Hinton, Mexico, http://data.gbif.org/datasets/resource/1594)

(accessed through GBIF data portal, RBGE Living Collections, http://data.gbif.org/datasets/resource/9167)

(accessed through GBIF data portal, Missouri Botanical Garden, http://data.gbif.org/datasets/resource/621)

(accessed through GBIF data portal, Ejemplares tipo de plantas vasculares del Herbario de la Escuela Nacional de Ciencias Biologicas, Mexico (ENCB, IPN), http://data.gbif.org/datasets/resource/2498)

(accessed through GBIF data portal, UA Herbarium, http://data.gbif.org/datasets/resource/7900)

(accessed through GBIF data portal, Repatriacion de datos del Herbario de Arizona (ARIZ), http://data.gbif.org/datasets/resource/2480)

(accessed through GBIF data portal, MEXU/Flora de Oaxaca, http://data.gbif.org/datasets/resource/8392)

(accessed through GBIF data portal, Herbario del Instituto de Ecología, A.C., M√©xico (IE-XAL), http://data.gbif.org/datasets/resource/1597)

(accessed through GBIF data portal, Herbario de la Universidad de Arizona, EUA, http://data.gbif.org/datasets/resource/2479)

(accessed through GBIF data portal, Real Jardin Botanico (Madrid), Vascular Plant Herbarium (MA), http://data.gbif.org/datasets/resource/240)
(accessed through GBIF data portal, RBGE Herbarium (E), http://data.gbif.org/datasets/resource/8402)

(accessed through GBIF data portal, Arboles y Arbustos Nativos para la Restauracion Ecologica y Reforestacion de Mexico (IE-DF,UNAM), http://data.gbif.org/datasets/resource/2484)

(accessed through GBIF data portal, Herbario de la Escuela Nacional de Ciencias Biologicas, Mexico (ENCB, IPN), http://data.gbif.org/datasets/resource/1601)

(accessed through GBIF data portal, Estudio Floristico de la Sierra de Pachuca, Hidalgo,

Mexico (ENCB, IPN), http://data.gbif.org/datasets/resource/2499)

(accessed through GBIF data portal, Herbarium of The New York Botanical Garden, http://data.gbif.org/datasets/resource/8967)

(accessed through GBIF data portal, Phanerogamie, http://data.gbif.org/datasets/resource/1506)

(accessed through GBIF data portal, Royal Botanic Gardens, Kew, http://data.gbif.org/datasets/resource/629)

Artemisia ludoviciana

(accessed through GBIF data portal, Arizona State University Vascular Plant Herbarium, http://data.gbif.org/datasets/resource/676)

(accessed through GBIF data portal, UA Herbarium, http://data.gbif.org/datasets/resource/7900)

(accessed through GBIF data portal, Type herbarium, Gottingen (GOET), http://data.gbif.org/datasets/resource/1494)

(accessed through GBIF data portal, Programa de repatriacion de datos de ejemplares mexicanos, http://data.gbif.org/datasets/resource/2488)

(accessed through GBIF data portal, Agentes Bioactivos de Plantas Deserticas de Latinoamerica (ICBG), http://data.gbif.org/datasets/resource/2485)

(accessed through GBIF data portal, Repatriacion de datos del Herbario de Arizona (ARIZ), http://data.gbif.org/datasets/resource/2480)

(accessed through GBIF data portal, Vascular Plant Collection - University of Washington Herbarium (WTU), http://data.gbif.org/datasets/resource/126)

(accessed through GBIF data portal, Harvard University Herbaria, http://data.gbif.org/datasets/resource/1827)

(accessed through GBIF data portal, USU-UTC Specimen Database, http://data.gbif.org/datasets/resource/1508)

(accessed through GBIF data portal, Missouri Botanical Garden, http://data.gbif.org/datasets/resource/12084)

(accessed through GBIF data portal, Herbario del Instituto de Ecología, A.C., Mexico (IE-BAJIO), http://data.gbif.org/datasets/resource/1595)

(accessed through GBIF data portal, Herbario del Instituto de Ecología, A.C., Mexico (IE-XAL), http://data.gbif.org/datasets/resource/1597)

(accessed through GBIF data portal, NMNH Botany Collections,

http://data.gbif.org/datasets/resource/1874)

(accessed through GBIF data portal, Herbarium of The New York Botanical Garden, http://data.gbif.org/datasets/resource/8967)

(accessed through GBIF data portal, Royal Botanic Gardens, Kew, http://data.gbif.org/datasets/resource/629)

(accessed through GBIF data portal, Herbario XAL del Instituto de Ecología, A.C., Mexico (IE-XAL), http://data.gbif.org/datasets/resource/10980)

(accessed through GBIF data portal, Herbario del CIBNOR, http://data.gbif.org/datasets/resource/11124)

(accessed through GBIF data portal, Herbario IEB del Instituto de Ecología, A.C., Mexico (IE-BAJIO), http://data.gbif.org/datasets/resource/11106)

(accessed through GBIF data portal, RBGE Herbarium (E), http://data.gbif.org/datasets/resource/8402)

(accessed through GBIF data portal, MEXU/Asteraceae, http://data.gbif.org/datasets/resource/787)

(accessed through GBIF data portal, Flora Util del Municipio de la Huerta, Jalisco, http://data.gbif.org/datasets/resource/13099)

(accessed through GBIF data portal, Herbario de la Escuela Nacional de Ciencias Biologicas, Mexico (ENCB, IPN), http://data.gbif.org/datasets/resource/1601)

(accessed through GBIF data portal, Plantas exoticas del centro de Mexico y obtencion de imagenes para una flora virtual de malezas, http://data.gbif.org/datasets/resource/13282)

(accessed through GBIF data portal, Analisis de la heterogeneidad ambiental y conectividad de las areas naturales del sur del Valle de Mexico_1, http://data.gbif.org/datasets/resource/13256)
(accessed through GBIF data portal, CONN GBIF data, http://data.gbif.org/datasets/resource/7857)

(accessed through GBIF data portal, Diversidad y riqueza vegetal de los substratos rocosos del centro del estado de Veracruz, http://data.gbif.org/datasets/resource/13188)

(accessed through GBIF data portal, Estudio Florostico de la Sierra de Pachuca, Hidalgo, Mexico (ENCB, IPN), http://data.gbif.org/datasets/resource/2499)

(accessed through GBIF data portal, MEXU/Coleccion de Plantas Acuaticas, http://data.gbif.org/datasets/resource/8047)

(accessed through GBIF data portal, Inventario floristico y base de datos de la Reserva Ecologica Sierra de San Juan, Nayarit, Mexico, http://data.gbif.org/datasets/resource/13333)

(accessed through GBIF data portal, Base de datos del Herbario de la Unidad Academica de Agronomia de la Universidad Autonoma de Zacatecas, http://data.gbif.org/datasets/resource/13201)

(accessed through GBIF data portal, Coleccion cientifica del Museo de Historia Natural Alfredo Duges, http://data.gbif.org/datasets/resource/13368)

(accessed through GBIF data portal, Base de datos sobre la flora de Durango, http://data.gbif.org/datasets/resource/13360)

(accessed through GBIF data portal, Floristica de areas protegidas en el estado de Durango, http://data.gbif.org/datasets/resource/13359)

(accessed through GBIF data portal, Herbario de la Universidad de Arizona, EUA, http://data.gbif.org/datasets/resource/2479)

(accessed through GBIF data portal, Herbarium de Geo. B. Hinton, Mexico, http://data.gbif.org/datasets/resource/1594)

(accessed through GBIF data portal, Actualizacion de la base de datos del Herbario de la Universidad de Sonora (USON), http://data.gbif.org/datasets/resource/13101)

(accessed through GBIF data portal, Flora del Parque Nacional Cumbres de Monterrey, Nuevo Leon, Mexico, http://data.gbif.org/datasets/resource/13171)

(accessed through GBIF data portal, Floristica de la reserva de la biosfera de Mapas, http://data.gbif.org/datasets/resource/13178)

(accessed through GBIF data portal, Flora de las Barrancas del Cobre, http://data.gbif.org/datasets/resource/13250)
(accessed through GBIF data portal, Diversidad vegetal en un gradiente en la Sierra Madre Occidental: flora y vegetacion de la Region de San Javier y Yacora, Sonora, http://data.gbif.org/datasets/resource/13119)

(accessed through GBIF data portal, Utah Valley State College Herbarium, http://data.gbif.org/datasets/resource/1013)

Liquidambar styraciflua
(accessed through GBIF data portal, Missouri Botanical Garden, http://data.gbif.org/datasets/resource/621)

(accessed through GBIF data portal, Arboles y Arbustos Nativos para la Restauracion Ecologica y Reforestacion de Mexico (IE-DF,UNAM), http://data.gbif.org/datasets/resource/2484)

(accessed through GBIF data portal, Arboles de la Penisula de Yucatan, Flora del Distrito de Tehuantepec, Oaxaca y Familia Asteraceae en Mexico (IBUNAM),

http://data.gbif.org/datasets/resource/2491)

(accessed through GBIF data portal, Herbario del Instituto de Ecología, A.C., Mexico (IE-BAJIO), http://data.gbif.org/datasets/resource/1595)

(accessed through GBIF data portal, Real Jardin Botanico (Madrid), Vascular Plant Herbarium (MA), http://data.gbif.org/datasets/resource/240)

(accessed through GBIF data portal, Paleobiology Database, http://data.gbif.org/datasets/resource/563)

(accessed through GBIF data portal, Banco Nacional de Germoplasma Vegetal, Mexico (BANGEV, UACH), http://data.gbif.org/datasets/resource/1599)

(accessed through GBIF data portal, Herbario de la Universidad de Arizona, EUA, http://data.gbif.org/datasets/resource/2479)

(accessed through GBIF data portal, Herbarium de Geo. B. Hinton, Mexico, http://data.gbif.org/datasets/resource/1594)

(accessed through GBIF data portal, UA Herbarium, http://data.gbif.org/datasets/resource/7900)

(accessed through GBIF data portal, Repatriacion de datos del Herbario de Arizona (ARIZ), http://data.gbif.org/datasets/resource/2480)

Taxodium mucronatum

(accessed through GBIF data portal, Missouri Botanical Garden, http://data.gbif.org/datasets/resource/621)

(accessed through GBIF data portal, Herbario del Instituto de Ecología, A.C., Mexico (IE-BAJIO), http://data.gbif.org/datasets/resource/1595)

(accessed through GBIF data portal, MEXU/Coleccion de Plantas Acuaticas, http://data.gbif.org/datasets/resource/8047)

(accessed through GBIF data portal, UA Herbarium, http://data.gbif.org/datasets/resource/7900)

(accessed through GBIF data portal, Repatriacion de datos del Herbario de Arizona (ARIZ), http://data.gbif.org/datasets/resource/2480)

(accessed through GBIF data portal, RBGE Herbarium (E), http://data.gbif.org/datasets/resource/8402)

(accessed through GBIF data portal, MEXU/Flora de Oaxaca, http://data.gbif.org/datasets/resource/8392)

(accessed through GBIF data portal, Herbario de la Universidad de Arizona, EUA, http://data.gbif.org/datasets/resource/2479)

(accessed through GBIF data portal, Agentes Bioactivos de Plantas Deserticas de Latinoamerica (ICBG), http://data.gbif.org/datasets/resource/2485)

(accessed through GBIF data portal, Herbario de la Escuela Nacional de Ciencias Biologicas, Mexico (ENCB, IPN), http://data.gbif.org/datasets/resource/1601)
(accessed through GBIF data portal, RBGE Living Collections, http://data.gbif.org/datasets/resource/9167)

(accessed through GBIF data portal, Herbarium, http://data.gbif.org/datasets/resource/7984)

(accessed through GBIF data portal, Herbarium de Geo. B. Hinton, Mexico, http://data.gbif.org/datasets/resource/1594)

APPENDIX 4: MaxEnt settings

Abies religiosa: model parameters
Command line to repeat this species model: java density.MaxEnt nowarnings noprefixes -E "" -E Abies_religiosa outputdirectory=V:\APR4_abies projectionlayers=Z:\Chiang21K_USGSvars samplesfile=Z:\gbif\csvTaxa\AdjustedTaxa\Abiesreligiosa.csv environmentallayers=Z:\Climate0K_USGSvars\ascii randomseed replicates=10 fadebyclamping -N aspect -N bio_10 -N bio_10 -N bio_11 -N bio_13 -N bio_14 -N bio_15 -N bio_15 -N bio_16 -N bio_17 -N bio_18 -N bio_18 -N bio_19 -N bio_3 -N bio_4 -N bio_5 -N bio_6 -N bio_9 -N elev -N mexelev -N prec_1 -N prec_7 -N tmean_1 -N tmean_7

Picea chihuahuana: model parameters
Command line to repeat this species model: java density.MaxEnt nowarnings noprefixes -E "" -E Picea outputdirectory=V:\21K_RETRIES\PICEA projectionlayers=Z:\Chiang21K_USGSvars samplesfile=Z:\gbif\csvTaxa\AdjustedTaxa\piceaAdj.csv environmentallayers=Z:\Climate0K_USGSvars\ascii randomseed replicates=10 fadebyclamping -N aspect -N bio_1 -N bio_10 -N bio_11 -N bio_12 -N bio_13 -N bio_14 -N bio_15 -N bio_15 -N bio_17 -N bio_18 -N bio_19 -N bio_2 -N bio_3 -N bio_4 -N bio_5 -N bio_6 -N bio_7 -N bio_9 -N elev -N mexelev -N prec_1 -N prec_7 -N tmean_1 -N tmean_7

Artemisia ludoviciana: model parameters
Command line to repeat this species model: java density.MaxEnt nowarnings noprefixes -E "" -E Artemisia outputdirectory=V:\6KTaxa\Artemisia projectionlayers=Z:\Climate6K_USGSvars samplesfile=Z:\gbif\csvTaxa\AdjustedTaxa\artemisiaAdjCSV.csv environmentallayers=Z:\Climate0K_USGSvars\ascii randomseed replicates=10 fadebyclamping -N aspect -N bio_1 -N bio_10 -N bio_12 -N bio_13 -N bio_14 -N bio_15 -N bio_16 -N bio_17 -N bio_18 -N bio_18 -N bio_19 -N bio_3 -N bio_4 -N bio_5 -N bio_6 -N bio_6 -N bio_7 -N bio_9 -N elev -N mexelev -N prec_1 -N prec_7 -N tmean_1 -N tmean_7

Liquidambar styraciflua: model parameters
Command line to repeat this species model: java density.MaxEnt nowarnings noprefixes -E "" -E Liquidambar responsecurves outputdirectory=V:\MAY19LIQUIDAMBAR projectionlayers=Z:\Chiang21K_USGSvars samplesfile=Z:\gbif\csvTaxa\AdjustedTaxa\liquidambarAdjCSV.csv environmentallayers=Z:\Climate0K_USGSvars\ascii randomseed replicates=10 fadebyclamping noextrapolate -N aspect -N bio_1 -N bio_10 -N bio_10 -N bio_11 -N bio_13 -N bio_14 -N bio_15 -N bio_16 -N bio_17 -N bio_18 -N bio_18 -N bio_19 -N bio_2 -N bio_3 -N bio_4 -N bio_6 -N bio_7 -N bio_9 -N elev -N mexelev -N prec_1 -N prec_7 -N tmean_1 -N tmean_7

Taxodium mucronatum: model parameters
Command line to repeat this species model: java density.MaxEnt nowarnings noprefixes -E "" -E Taxodium outputdirectory=V:\MAY19TAXODIUM projectionlayers=Z:\Chiang21K_USGSvars samplesfile=Z:\gbif\csvTaxa\AdjustedTaxa\taxodiumAdjCSV.csv environmentallayers=Z:\Climate0K_USGSvars\ascii randomseed replicates=10 fadebyclamping noextrapolate -N aspect -N bio_1 -N bio_10 -N bio_10 -N bio_12 -N bio_13 -N bio_14 -N bio_15 -N bio_16 -N bio_17 -N bio_18 -N bio_19 -N bio_2 -N bio_3 -N bio_4 -N bio_5 -N bio_6 -N bio_7 -N bio_9 -N elev -N mexelev -N prec_1 -N prec_7 -N tmean_1 -N tmean_7

APPENDIX 5: EOF Extraction

Extraction of PMIP2 mid-Holocene and LGM anomalies for use in WORLDCLIM

Abstract

I document the procedure used to extract mid-Holocene and Last Glacial Maximum (LGM) monthly mean climate anomalies from the Paleoclimate Model Intercomparison Project 2 (PMIP2) archive for use in WORLDCLIM. A multivariate Empirical Orthogonal Function (EOF) method applied to the PMIP2 monthly mean climate anomalies is used to extract the dominant climate response for the said time period across the PMIP2 model simulations. The EOF extraction is done regionally. The extracted climate response is then added to the WORLDCLIM base climate to produce a high-resolution 'bioclimatology' of the mid-Holocene or LGM.

1.Motivation

WORLDCLIM ([*Hijmans et al.*, 2005], http://www.WorldClim.org/) is a high-resolution climate data product used by ecologists for ecosystem modeling, and based on interpolation of instrumental climate data over the modern period. A set of derived quantities useful to ecosystem modeling – called 'bioclimatic variables' – is computed from the high-resolution climate data. Similar maps of climate-model-estimated past climates are useful for mapping past ecosystems, but unavailable at the time when this project was started. The Paleoclimate Model Intercomparison Project 2 (PMIP2; Braconnot *et al.*, 2007) coordinates and archives simulations of past climates done by various modeling groups around the world, and using state-of-the-art coupled climate models. Two distinct time periods of climate interest are targeted: mid-Holocene (6,000 BP) and Last Glacial Maximum (21,000 BP). The mid-Holocene climate is marked by continental configurations and greenhouse gas levels similar to present-day, but with marked changes in the precessional component of earth's orbit around the Sun that led to more Northern Hemisphere summertime insolation, and less Southern Hemisphere summertime insolation. Massive continental ice sheets over North America and Eurasia characterize The Last Glacial Maximum (LGM) climate, and greenhouse gas concentrations at levels below present-day.

Extraction of climate anomalies from these simulations is technically straightforward, but a question arises as to which model simulations are the 'best' ones to use. No one knows which model simulates the past climate correctly, if indeed there are any. This comment applies especially to regional climates: our track record of simulating consistent changes

in regional climate under climate change scenarios is not great[1]. There is a general sense of which coupled models are more capable, but this is a subjective measure, and only comes about when comparing simulations to present-day climate. Could it be that the 'better' models get it right since they are tuned better for present-day climate?

A more objective method is to simply treat each model's simulation as one possible realization, and simply average over all realizations to get a representative answer – a composite mean. A problem with such an approach is the assumption of a common response across all the models. Imagine, however, if there was not such a response – each model does its own thing. Then the composite anomaly – which will be nonzero since the sample size is small – will be physically meaningless.

We can objectively extract a common response, if there is one, by applying a multivariate empirical orthogonal function (EOF) analysis (e.g. Wilks pp 477-479) on carefully chosen fields of interest, and to a region of interest. EOF analysis is a commonly used data analysis method that computes new basis functions as linear combinations of the original ones. This is done in such a way as to explain the maximum possible fraction of variance in the original data. In other words, the first new basis function or EOF 'mode' explains the most possible variance of the original data; the next EOF explains the most variance in the residual data; and so on and so forth. If there is a common climate response across all models to a given climate forcing, the hope is that it will be extracted as a leading, if not the leading EOF mode, the variance explained will be large, and the corresponding principal component loading will be mostly be of the same sign, indicating that most models have the response in the same directional sense. There are merits in to this approach. First, if there is no common response, then it should be immediately apparent in the analysis. The variance explained by the EOF representing the common response gives an idea of just how representative the response is[2]. The magnitude of the principal component loadings – each representing how much that pattern projects onto each model simulation – gives an indication of the range of sensitivity that the various climate models have for that particular response. The region taken for the EOF analysis can be chosen in such a way as to be climatically meaningful: so for example, it would make sense to do this analysis for the entire tropical Pacific and not just a part of it, since our understanding of the climate physics of that region – in particular the Bjerknes feedback – dictates that we do so. We can choose the climate fields to analyze that are the most important determinants of the climate in that region: so again taking the tropical Pacific as an example, the fields to consider are sea surface temperature (SST), rainfall, and surface winds.

2.Application

We give the example of applying the method to South American climate during the mid-Holocene, outlining the steps taken. The specific target is the Atlantic rainforest region. The procedure for the other regions (e.g. Mexico, Australia) is similar.

---

[1] Two examples worth mentioning is the response of Sahel rainfall, and the tropical Pacific, in IPCC global warming scenarios.

[2] Though it should be pointed out that, given the limited sample size, it may not be possible to assess the stability of the EOF (using, say, rule N).

2.1Choice of region, and fields for the multivariate EOF

We chose a domain that encompasses the entire tropical South America from 40°S-15°N, and 275°E-330°E. This choice is not obvious, since we are focusing on the Atlantic rainforest region. However, my assessment is that climate changes over the Atlantic rainforest is part of the larger change over the Amazon, hence the EOF analysis should contain the entire Amazon region. WORLDCLIM uses four climate measures to construct the secondary bioclimatic variables, namely monthly mean precipitation, average surface air temperature, and minimum and maximum surface air temperature. Consequently, we decided to use the model's monthly mean precipitation and temperature as part of the multivariate EOF. Unfortunately, not all PMIP2 models reported minimum and maximum temperature, so those were omitted (also, minimum and maximum temperature changes are highly correlated to average temperature changes, so inclusion of that information may inappropriately weight the EOF too much towards temperature). We also included sea level pressure in the EOF as a measure of the dynamical response of the model's climate, even though this variable is not part of WORLDCLIM.

For each model, we computed the monthly climatological anomaly fields by subtracting the mid-Holocene climatological climate fields from those corresponding to the present-day simulation. Hence for each fields (e.g. precipitation), we have 12 months worth of monthly climatological anomalies.

2.2EOF procedure

The data matrix for the EOF included use both the individual gridpoint ***and*** individual month as 'stations'; in other words, for gridpoint at location (i,j), the January months constitute one station, February as another, etc. This was done in order to extract the seasonal resemblance across the models. The traditional dimension of time is taken up by the model type. In this instance, the maximum dimension of the datatset is the number of models used, a very small number usually. The models used are listed in table 1. Prior to taking the multivariate EOF, I i) interpolated each model's output to the spatial grid resolution of the CCSM3 model (T42), using bilinear interpolation; ii) normalized the data by the square root of the cosine of latitude to account for the latitudinally-varying surface area represented by the gridpoint; and iii) normalized each field by dividing by the standard deviation of all of that field's data gridpoints (combining both space and month). This latter procedure ensures that no one field dominates the EOF.

We computed the EOF by applying a singular value decomposition (SVD) on the resulting data matrix. If F represents the data matrix, the SVD procedure decomposes the matrix into three components

$$F = \sqrt{n-1}VSE^T \qquad [1]$$

where n is the number of models, the matrix V contains the principal components, E contains the eigenvectors, and S the singular values. Both V and E are orthonormal. The standard EOF decomposition can be obtained simply by letting $U = \sqrt{n-1}VS$, and therefore

where in this case the principal component matrix U is orthogonal.

Results of the multivariate EOF analysis are shown in figure 1. EOF1 dominates the variance (64% of the total), and the corresponding principal component (PC) loadings are all of the same sign and comparable magnitude – in other words, all PMIP models exhibit behavior as represented by EOF1, albeit with varying strength. I interpret this to be the common response to mid-Holocene forcing exhibited by all models. They vary somewhat in the strength of this response (discussed below).

EOF2 explains just over 13% of the total variance. Application of North's "Rule of thumb" [*North et al.*, 1982] indicates that EOF1 is well separated from EOF2 (they should be separated by at least 30% of the variance explained, which they are), and thus robust to perturbations.

Aspects of EOF1 are shown in figures 3-4. The way EOF1 is presented is such that it represents the average projection of EOF1 across the models i.e. if we expand the climate anomaly for each model in terms of the EOF basis functions where f_i is the anomaly for model i, e_j is the j'th EOF, and a_{ij} is the corresponding expansion coefficient, then we present EOF 1 like so:

$$f_i = \Sigma_{j=1}^{n} a_{ij} e_j$$

Before plotting, we also multiply back in the square root of the cosine of latitude, as well as the standard deviation of that field's data points (i.e. the reverse of what was done to prepare the data matrix F for decomposition). Thus, the magnitude of EOF1 as plotted physically represents the average of how all the models respond in that fashion. From here on, all EOF results are plotted in this way. Note that the principal component (PC) loadings offer a simple way to estimate the possible range in the model response to the EOF1: we can simply take the model with the lowest loading, and the highest loading, as an estimate of the potential range given the various model sensitivities. So using PC1 in figure 1b as an example, the PC1 loading for model 2 represents the low end, whereas that for model 8 the high end. In terms of actual climate anomalies, and with reference to equation [4]:

$$EOF1_{low} = \frac{a_{21}}{\frac{1}{n}\sum_{i=1}^{n} a_{i1} e_1} EOF1 = a_{21} e_1$$

2.3Results for South America

The EOF1 results appear physically reasonable, given the nature of the precessional orbital forcing characterizing the mid-Holocene. Figure 2 shows the top-of-atmosphere insolation anomalies (versus present-day) seen during 6,000BP. Over the southern tropics, insolation decreases significantly during December through May, and increases from May through November. As a consequence, one might expect temperatures to decrease and increase accordingly over the Amazon, and perhaps with some lag. This appears to be the case. Figure 3 shows that the Amazon surface air temperatures cooled from Jan-Jun by up to 1.2K, and warmed from July through Dec by up to 1.5K (figure 3a). Sea level pressure responds in concert with the temperatures, higher during the cold anomalies, and lower during the warm period (figure 3b). Precipitation also responded

accordingly: lower during the cold anomalies (by up to 1mm/d), and higher in the warm anomaly seasons (by up to 0.5mm/d).
Figure 4 shows the spatial pattern of anomalies during the key seasons of boreal spring (MAM) and fall (SON). The entire South American continent is colder during MAM, and precipitation drops across most of tropical South America. There is a localized increase in rainfall over NE Brazil, associated with the increase in the Atlantic ITCZ rainfall. Sea level pressure (not shown in figure 4) is a high anomaly centered over the Amazon, and extending towards the southern subtropics. In SON, the pattern is roughly reversed, except that that there is a reduction in rainfall in the northern extremities of South America, again associated with corresponding changes to the Atlantic ITCZ. The corresponding sea level pressure anomaly (not shown) is a low centered over the southern tropics (around 22°S), but extending northwards all the way up the Amazon basin. In short, the EOF1 results appear to be physically reasonable.

3.Application to WORLDCLIM

I now outline how the EOF result is incorporated into WORLDCLIM. Briefly put, I add the anomalies from the EOF to the present-day WORLDCLIM input meteorological fields, and regenerate the bioclim fields.
More specifically, the following steps are taken:

1. **Extraction of the regional present-day input meteorological fields** (monthly min temp, mean temp, max temp, and precipitation) from the standard WORLDCLIM data. The area extracted should be a subset of the region defined by the EOF.
2. **Interpolation and addition of the EOF1 anomalies to the WORLDCLIM input variables**. First, the EOF1 anomalies in precipitation and mean temperature are interpolated to the resolution of the WORLDCLIM input fields. These anomalies are then added to the present-day climatological mean WORLDCLIM precipitation and mean temperature variables, respectively. As for min and max temperature, since the EOF1 does not have min or max temperature, the mean temperature anomalies from the EOF1 are also added to the min and max temperature fields of the WORLDCLIM as an approximation. A MATLAB subroutine – Interp_and_writetoASC.m – is used for this step.
3. **Regeneration of the bioclim variables.** The modified input fields from step 2 are to generate new bioclim fields.

Acknowledgements
The PMIP2 output was provided by several international modeling groups, and collected and archived by the Laboratoire des Sciences du Climat et de l'Environnement. The PMIP2/MOTIF Data Archive is supported by CEA, CNRS, the EU project MOTIF (EVK2-CT-2002-00153) and the Programme National d'Etude de la Dynamique du Climat (PNEDC). More information is available on http://pmip2.lsce.ipsl.fr/ and http://motif.lsce.ipsl.fr/.

Model	Atmospheric model resolution	# years of 6Kbp model output	# years of LGM model output
1. Community Climate System Model 3 (CCSM3)	T42 (approx 2.8° lat by 2.8° lon)	50	50
2. ECHAM5/MPI-OM1	T63 (approx 1.875° lat by 1.875° lon)	100	
3. Fast Ocean-Atmosphere Model (FOAM)	R15 (approx 4.5° lat by 7.5° lon)	100	
4. Goddard Institute for Space Sciences (GISS) model E	4° lat by 5° lon	50	
5. IPSL – CM4 - V1 - MR	2.5° lat by 3.75° lon	100	100
6. MIROC 3.2 (medres)	T42 (approx 2.8° lat by 2.8° lon)	100	100
7. Meteorological Research Institute (MRI) – CGCM2.3.4fa	T42 (approx 2.8° lat by 2.8° lon)	100	
8. Hadley Center Model 3 (HadCM3) with MOSES2 land surface scheme (simulations run at the University of Bristol)	2.5° lat by 3.75° lon	100	100
9. CSIRO Mk3 coupled model	3.2°lat by 5.625°lon	1000	
10. CNRM coupled model	T42 (approx 2.8° lat by 2.8° lon)		100

Table 1*: PMIP2 model simulations used in this study. See [Braconnot et al., 2007] for a general reference, and the PMIP2 website (http://pmip2.lsce.ipsl.fr/) for details of the models and experiments. Note that all simulations used here are ones that do NOT include mid-Holocene nor LGM land vegetation changes.*

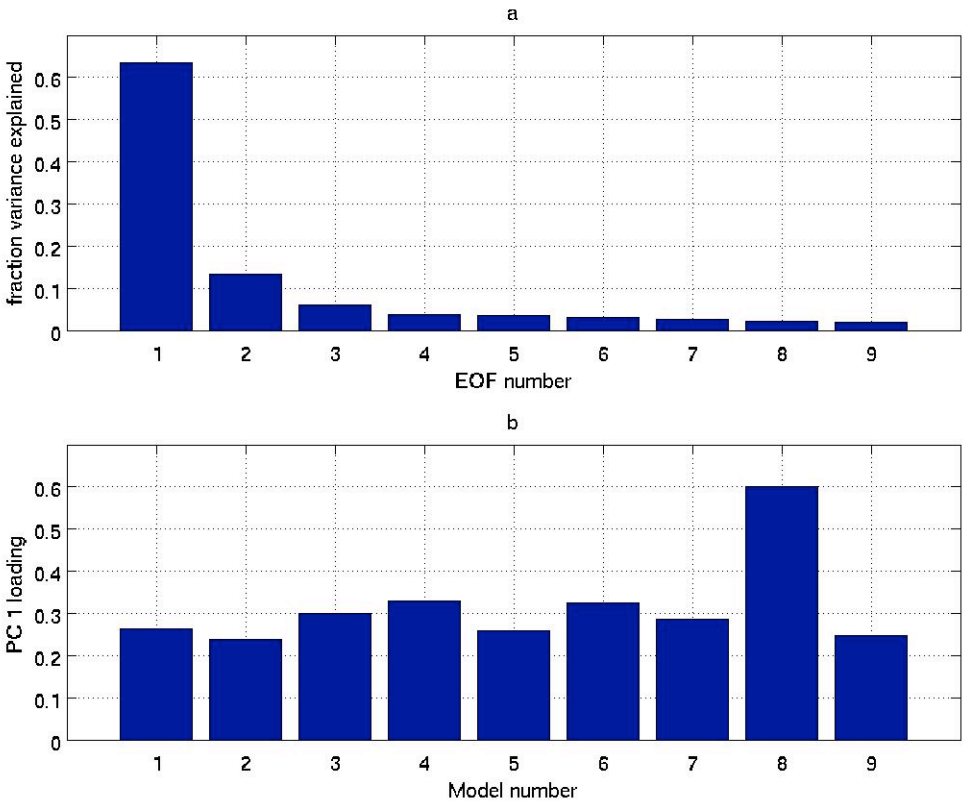

Figure 1. *Results of the multivariate EOF for South America. (a) Fractional variance explained by the EOF modes. EOF 1 dominates the variance, and is well separated from EOF2. (b) Principal component loadings for mode 1. The model number corresponds to those in table 1.*

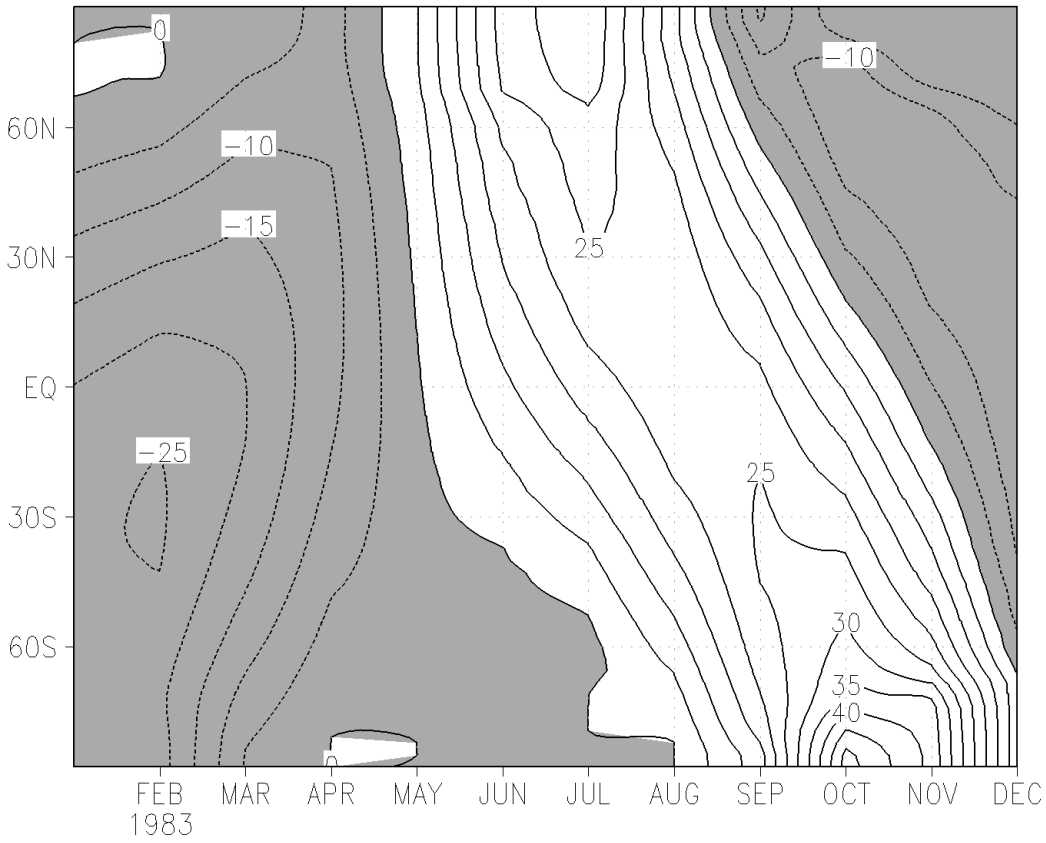

Figure 2. Top-of-atmosphere (TOA) insolation anomalies during 6,000BP, compared to present-day. Units are in W/m^2, and positive values are towards the earth. Over the southern tropics, insolation decreases over December through May, and increases from May through November.

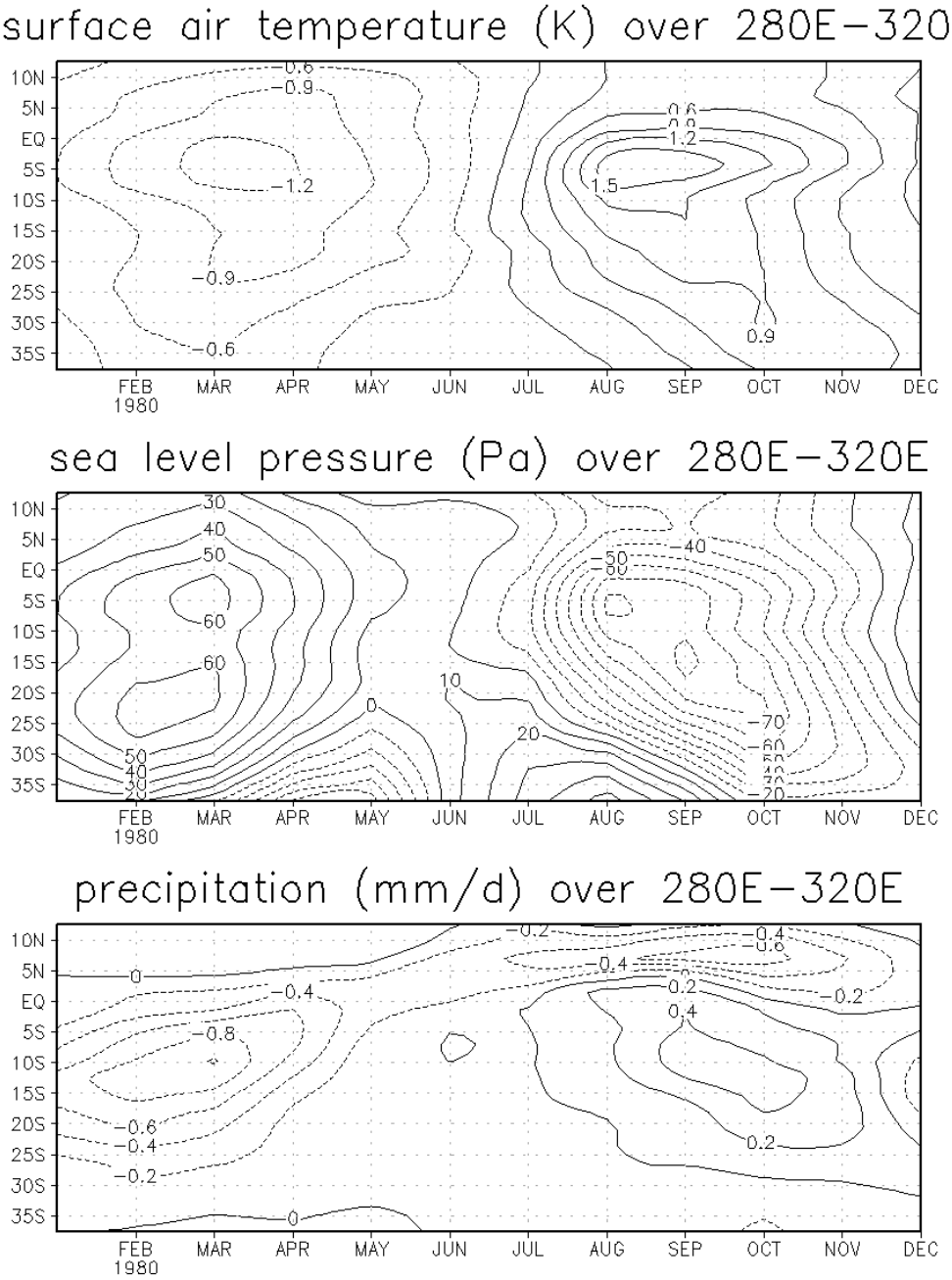

Figure 3. *EOF1 averaged over 280-320°E for (a) surface air temperature, (b) sea level pressure, and (c) precipitation. Units as shown.*

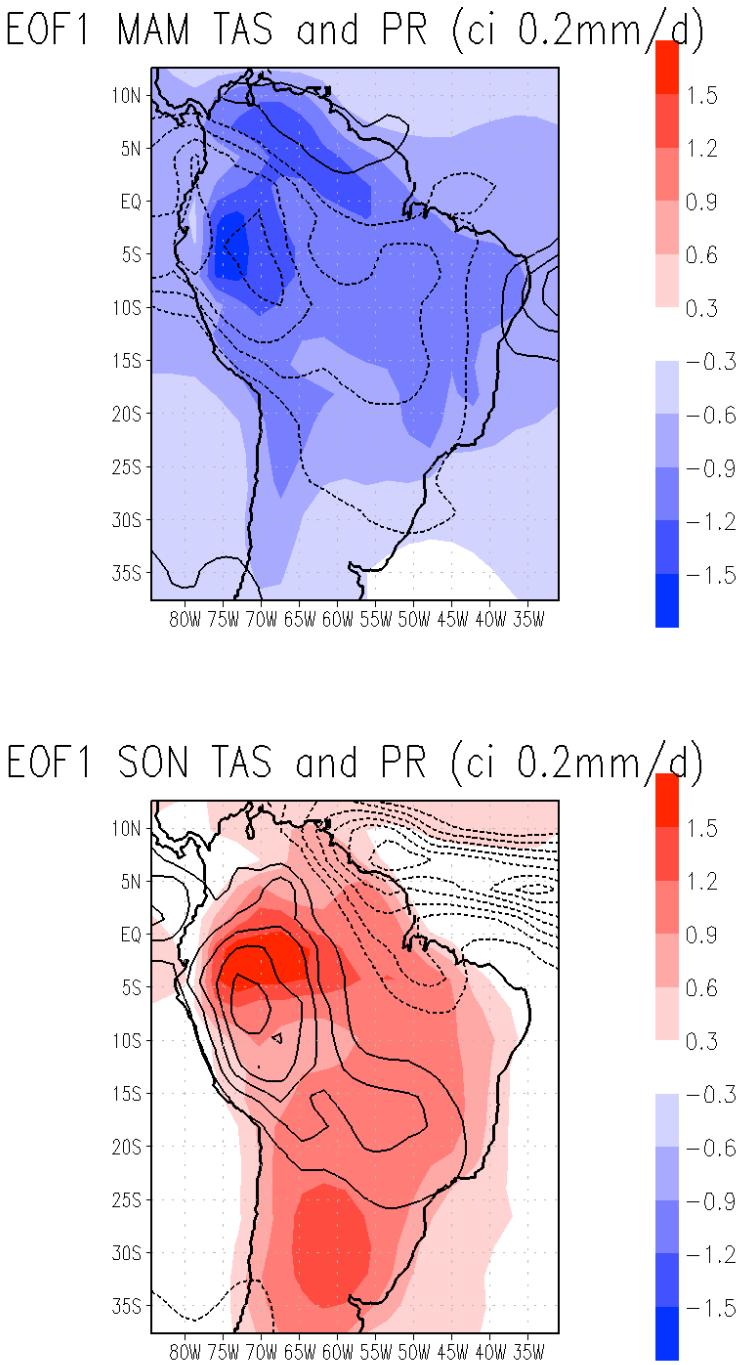

Figure 4. *EOF 1 surface air temperature (colors, units of the color scale in K) and precipitation (contours, contour interval 0.2mm/d, negative values dashed, and zero contour not shown) over (a) MAM and (b) SON.*

References

Braconnot, P., et al. (2007)**,** Results of PMIP2 coupled simulations of the Mid-Holocene and Last Glacial Maximum - Part 1: experiments and large-scale features, Climate of the Past**, 3**, 261-277.

Hijmans, R. J., S. E. Cameron, J. L. Parra, P. G. Jones, and A. Jarvis (2005), Very high resolution interpolated climate surfaces for global land areas, IJC, **25**, 1965-1978.

North, G. R., T. L. Bell, R. F. Cahalan, and F. J. Moeng (1982), Sampling errors in the estimation of empirical orthogonal functions, MWR, **110**, 699-706.

Wilks, D. S. Statistical Methods in the Atmospheric Sciences, 2nd Edition. Academic Press (2006), 627p.